DURABILITY PERFORMANCE OF CEMENTITIOUSLY STABILIZED LAYERS

By

ZHIPENG SU

A thesis submitted in partial fulfillment of

the requirements for the degree of

MASTER OF SCIENCE

(CIVIL AND ENVIRONMENTAL ENGINEERING)

at the

UNIVERSITY OF WISCONSIN-MADISON

2012

DURABILITY PERFORMANCE OF CEMENTITIOUSLY STABILIZED LAYERS

Zhipeng SU — Student Name

9064772784 — Campus ID Number

Approved:

_____ **5-18-12**	_____ **5-18-12**
signature date	signature date
James M. Tinjum, PE	Tuncer B. Edil, PE
Assistant Professor	Professor

ABSTRACT

DURABILITY PERFORMANCE OF CEMENTITIOUSLY STABILIZED LAYERS

By Zhipeng SU

Under the supervision of Professors James M. Tinjum and Tuncer B. Edil at the University of Wisconsin-Madison

The ability to retain stability and integrity over years of exposure to the destructive forces of weathering is one of the most important aspects of cementitiously stabilized layers (CSL) in pavement design. However, the changes of the CSL properties over time and their distress models have not been adequately addressed in the Mechanistic-Empirical Pavement Design Guide (MEPDG). The objectives of this study were to identify mechanical properties changes of CSLs which are undergoing exposure to weathering, such as freeze-thaw (F-T) and wet-dry (W-D) cycling, and also to validate and develop durability performance models. Unconfined compressive strength (UCS) and vacuum saturation were also examined for correlation with the durability performance of the CSLs. Ultrasonic pulse velocity measurement was conducted as a non-destructive test to monitor the effect of F-T and W-D cycling on base and subgrade soils with cement, fly ash, and lime stabilization.

Laboratory durability tests involved F-T cycling, W-D cycling, and vacuum saturation on nine cementitiously stabilized mixtures (CSM). P-wave velocity

measurement after each F-T and W-D cycle and UCS at the end of F-T and W-D cycling were conducted. F-T cycling was an aggressive test, which resulted in degradation in the constrained modulus (D) (up to 71%) and UCS (up to 69%) of all CSMs. The F-T durability performance of the mixtures was greatly affected by the binder content, binder type, and also soil type. Reduction in normalized constrained modulus after the first F-T cycle indicated the frost susceptibility of CSM. Some mixtures showed high resistance to degradation during the first F-T cycle (constrained modulus reduction <10%), including silt-lime-fly ash, sand-cement, gravel-cement, gravel-fly ash, and sand-fly ash. Mixtures with higher initial UCS had less reduction in constrained modulus after the first F-T cycle and less reduction after the W-D cycling as well. Cement-stabilized soils were more durable to F-T cycling with generally higher residual constrained modulus and UCS. Class C fly ash was less effective than lime-fly ash (Class F) with respect to improvement in the durability, strength, and stiffness of silt. Binder content influenced F-T durability significantly; the greater the cement content, the stronger the F-T durability.

An exponential modulus decay model is proposed to account for the effect of F-T cycling. A regression constant, k, can be used as a quantitative index of F-T susceptibility to characterize the performance of CSM. The smaller the k value, the more susceptible the mixtures were to F-T cycling. The effect of initial constrained modulus and UCS on the k value was investigated: mixtures with higher initial constrained modulus or UCS had smaller k, with the exception of clay-cement and gravel-cement mixtures. The F-T susceptibility was divided into

four categories: “high”, “moderate”, “low”, and “negligible” based on several criteria.

W-D cycling was not as detrimental as F-T cycling to CSM except for clay-lime and sand-fly ash mixtures. Some CSM had continuing cementation in cement mixtures and pozzolanic reactions in fly ash or lime mixtures, reflected in the enhancement in constrained modulus and UCS after the first W-D cycle. Cement-stabilized soils were the most durable to W-D cycling, having the largest residual constrained modulus and UCS among all CSM except gravel, for which fly ash was more effective. The combinations of silt with cement or lime-fly ash significantly improved the stiffness and W-D durability, but not with Class C fly ash.

A basic W-D durability model involving a reduction factor (f_R) for D is proposed for CSM subjected to W-D cycling. A larger f_R means more reduction in D when subject to W-D cycling. Generally, f_R for stabilized fine-grained soil (silt and clay) are larger than that for stabilized coarse-grained soil (sand and gravel), except for gravel-cement with 3% cement content. Generally, f_R increases with increasing void ratio for CSM.

The vacuum saturation procedure fully saturated the specimens. The vacuum-saturated specimens generally had lower UCS compared to that of unsaturated specimens. Although the correlation between residual UCS after F-T cycling versus UCS after vacuum saturation was not very strong, the vacuum saturation test can still serve as a fast way to predict the sensitivity to F-T of CSM when the complete F-T cycling test is not available.

Effect of curing progress, moisture content, and compaction characteristics on the P-wave velocity for CSM was investigated as an extension of this study. In general, the P-wave velocity or constrained modulus of the mixtures increased with curing time. The increase in P-wave velocity and constrained modulus from the first to seventh curing days was more pronounced than the increase from the seventh to twenty-eighth curing days for cement-stabilized soil. A slow pozzolanic reaction in lime and fly ash stabilization was also detectable with the ultrasonic wave testing. Unsaturated specimens with higher P-wave velocity had a much smaller increase in P-wave velocity after saturation. The saturation-stiffening effect on the P-wave velocity tended to be larger for soft CSM specimens with low P-wave velocity. The trend between UCS versus dry density or compaction water content was the same as the trend of the P-wave velocity versus dry density. Therefore, the specimens with higher P-wave velocity possessed higher strength (i.e., UCS) for each CSM mixture. For stabilized fine-grained soils, there was a peak in P-wave velocity coinciding with the maximum dry density, whereas for stabilized sand or granular base materials, this trend was not present.

The P-wave velocity and constrained modulus were strongly correlated to the UCS and elastic modulus (e.g., E_0 and E_{50}). The strength of CSM increased with increasing P-wave velocity. The predicted UCS was less proportional using prediction model determined from P-wave velocity than constrained modulus. The prediction model was also verified by the unsaturated UCS. Linear relationships between V_P and E_0, V_P and E_{50}, D and E_0, and D and E_{50} were observed. Constrained modulus correlated best with E_0, with R^2 =0.71.

In this study, the durability performance of CSM was studied and a distress model corresponding to freeze-thaw cycling and wet-dry cycling was proposed. Vacuum saturation techniques were used to correlate to F-T cycling. The characteristics of ultrasonic P-wave in CSM were investigated.

ACKNOWLEDGEMENT

I would like to thank my advisors, Professors Tuncer Edil and James Tinjum for their guidance, time and confidence during these two years. Thank you to Professor Dante Fratta for serving on my committee and giving instruction on my research. And thanks to our project partners at Washington State University, Professor Haifang Wen, Professor Balasingam Muhunthan, and Jingan Wang. Thanks for the contributions from Dr. Ahmet Gokce, Jeff Casmer and Tirupan Mandal for this research project. Thanks to Xiaodong “Buff” Wang and William Lang for their help on the laboratory setup. I also appreciate Andrew Keene for his help and input for the research. I would also like to thank to all of my friends in the GLE group and especially for: Ali Soleimanbeigi, Jongwan Eun, Xiaodong Ma, Jeff Casmer, Jiannan Chen and Kuo Tian. And lastly, I want to thank my girlfriend, Sijue Tan and my family back home in China for their love, unconditional support and encouragement along the way.

TABLE OF CONTENTS

LIST OF TABLES

LISTS OF FIGURES

SECTION 1 INTRODUCTION

According to Federal Highway Administration's (FHWA) Office of Highway Policy Information, road centerline miles in the U.S. have only increased by` about 10% between 1960 and 2002; however, U.S. registered vehicles increased by over 300% and vehicle miles traveled (VMT) increased by more than 380% over this same time. To relieve congestion and pressure on a stressed transportation system, the U.S. government expends $117 billion annually for maintenance and reconstruction and builds approximately 13,000 miles of new roads per year. Soil stabilization began gaining acceptance during the 1960s and '70s due to general shortages of aggregates and petroleum resources. Soil stabilization is a continuing popular trend as global demand for raw materials, fuel, and infrastructure has increased.

Soil stabilization occurs during the early stages of pavement construction. Pavement design is based on the premise each layer in pavement system will achieve a nominal structure level. To increase rutting resistance and avoid excessive cracking of the pavement, stabilization of the subgrade and the subbase and base layers may be required. Stabilization is the process of blending and mixing cementitious materials, such as portland cement and fly ash, with subgrade soil or subbase/base aggregate to improve the engineering properties of the soil. The addition of such binders transforms unbound material layers to

bound layers, which are referred to as chemically or cementitiously stabilized layers (CSL).

A considerable amount of research has been devoted to the stabilization of soils, aggregates, and recycled pavement materials; however, there is a significant lack of research relating the properties of CSL to pavement performance. The AASHTO Interim Mechanistic-Empirical Pavement Design Guide Manual of Practice (MEPDG) provides a methodology for the analysis and performance prediction of pavements incorporating such layers. However, the change in CSL properties over time and their distress models have not been adequately addressed in MEPDG (Wen et al. 2010).

The objective of this study is to identify property changes of CSL that undergo exposure to weathering, such as freeze-thaw and wet-dry cycling, and also to validate and develop freeze-thaw durability performance models. Unconfined compressive strength (UCS) and vacuum saturation were performed for correlation with the durability performance of CSL. A laboratory based, dynamic, and non-destructive testing method using ultrasonic pulse velocity was developed for application to cementitiously stabilized materials. Ultrasonic pulse velocity measurements were conducted to evaluate the effect of freeze-thaw cycling and wet-dry cycling on base and subgrade soil with cement, fly ash, and lime stabilization. This thesis describes the findings of this study and is part of a broader investigation of CSL for NCHRP Project 04-36, *Characterization of Cementitiously Stabilized Layers for Use in Pavement Design and Analysis.*

SECTION 2 BACKGROUND

2.1. STABILIZATION OF ROADWAY BASE/SUBGRADE

Subgrade or subbase/base stabilization is the process of blending and mixing additives to host materials to improve the engineering properties of roadway substructure. The process may include the blending of soil or aggregate to achieve a desired gradation or the mixing of commercially available additives that may alter the gradation, texture, or plasticity, or act as a binder for cementation of the soils (Department of Army, Navy, and Air Force 1994). Washington State University conducted a survey in 2009 in which 28 State Departments of Transportation (DOT) were reported to use stabilization for subgrade, subbase, or base materials. The most popular additives were portland cement, lime, and Class C fly ash. Pavement performance is highly related to the properties of the CSL, including stiffness, strength, durability, fatigue, shrinkage, and erodibility resistance (Wen et al. 2010).

2.1.1. CEMENT

Portland cement is widely used in soil stabilization. Cement reacts with water and bonds with soil particles to generate a stronger and stiffer layer through cementation and hydration. This process can significantly improve the strength, stiffness, and durability of the host material. According to the Portland Cement Association (PCA) guideline (1992), the 7-day UCS of soil-cement falls between

2.1 and 5.5 MPa with cement content 3% to 10%. Numerous studies have shown that cement-treated base functions as a superior load-spreading layer in the pavement system (Walker 1995; Prusinski and Bhattacharya 2007; Lim and Zollinger 2003). Cement-stabilized pavement bases have been commonly used in areas that lack quality aggregates sources and in areas subject to heavy loads. (Mohammad et al. 2007)

An experimental study on the development of strength and modulus of elasticity of cement-treated aggregate base (CTAB) was undertaken by Lim and Zollinger (2003). In this study, conventional crushed limestone base and recycled concrete materials were used in the testing program. The development of strength and modulus of CTAB mixtures were mostly governed by the applied cement content regardless of other mixing variables (e.g., water content and soil type). A relationship between the compressive strength and modulus of elasticity was proposed for CTAB materials. Mohammad et al. (2007) incorporated fiber in cement-treated soil mixtures and evaluated improvements through laboratory tests, such as indirect tensile strength (ITS) and strain, UCS, and indirect tensile resilient modulus. The study showed that the inclusion of the fiber reinforcement significantly increased the ITS and indirect tensile toughness index, but not UCS performance.

Walker (1995) studied the influence of soil characteristics and cement content on the strength, durability and shrinkage characteristics of stabilized soil blocks. In this study, river sand was combined with different clay content and then

stabilized with various cement contents. Average saturated compressive strength decreased with a reduction in cement content and increasing plasticity index. Similar to saturated compressive strength, performance was improved by increased cement content and reduced clay content during wet-dry cycling. Prusinski and Bhattacharya (2007) investigated the stabilizing mechanisms of cement and its effect on engineering properties and durability of the stabilized clays. The research indicated that a small amount of cement content in clay reduced the plasticity and shrinkage properties and improved the compressive strength significantly.

2.1.2. LIME

According to the National Lime Association (2005), lime treatment of soil is a proven method for improving the engineering properties of lime-treated soil. Lime stabilization can be used to dry wet soils quickly, thus minimizing weather-related construction delays. Lime is also widely used in soil modification to temporarily strengthen working platforms. Lime stabilization creates long-lasting changes in soil characteristics, which also provide structural benefits. Lime is widely used as a binder in clayey soil to create strong, but flexible, permanent structural layers in pavement systems.

Strength gain a widely reported phenomenon in a soil or aggregate through treated with lime. Thompson et al. (1970) defined reactive lime-soil mixtures as

one with a 350 kPa change in UCS after a 48-hour period of cure (at 45°C). Based on this definition, lime-soil mixtures can range from non-reactive to highly reactive with strength gains of over 10 MPa. Eades and Grim (1963) studied the cured UCS of lime-treated soils with six distinct mineralogies. Their data demonstrated strength increases due to lime stabilization of 200% to 1,000%. Doty and Alexander (1978) found the 7-day curing strength at 38°C to be roughly equivalent to the 28-day curing strength at 23°C.

Along with the pozzolanic reaction strengthening the soil, a stiffening process in the soil-lime mixtures occurs simultaneously. As illustrated by Little (1996), typical resilient modulus increase due to lime treatment is in the range of 800% to 1,500%. Puppala et al. (1996) also found that resilient modulus of soil-lime mixtures increased 30% to 50% after the lime stabilization with a short 3-d curing period. Swanson and Thompson (1967) performed flexural beam fatigue testing on soil-lime mixtures. The study found that the fatigue life increases along with the maturity of the soil-lime mixtures since the magnitude of stress repetitions in pavements are relatively constant during its design life. Moore and Kennedy (1971) found that a repeatedly loaded IDT test can be effectively used in fatigue testing. The fatigue life was found to increase with the curing of soil-lime mixtures due to the decrease in stress ratio.

2.1.3. FLY ASH

Fly ash is a byproduct of coal combustion and consisting of fine particles that rise with the flue gases. In the U.S., about 119 million tonnes of fly ash are produced annually by 460 coal-fired power plants. A 2008 industry survey estimated that 43% of this ash is beneficially reused. Fly ash is most commonly used as a high-performance substitute for portland cement or as clinker for portland cement production. Geotechnical applications include soil stabilization, road base, structural fill, embankments, and mine reclamation (ACAA 2011).

The primary reason fly ash is used in soil stabilization applications is to improve the compressive and shearing strength of soil. Iowa State University (2005) conducted a study on the effects of self-cementing fly ash on the engineering properties of several Iowa soils. 20% fly ash content increased the CBR (California bearing ratio) up to 75% for compacted gravel specimens. Rapid strength gain of soil-fly ash mixtures occurred during the first 7d to 28d of curing, and a less pronounced increase continued with time due to long-term pozzolanic reactions. Camargo (2008) investigated the UCS and resilient modulus of recycled pavement materials (RPM) and road surface gravel (RSG) stabilized with fly ash. The UCS, CBR, and summary resilient modulus (SRM) of RPM and RSG stabilized with fly ash increased with increasing fly ash content and curing time. A strong relationship was found for SRM and UCS of RPM and RSG stabilized with fly ash, which suggests that the resilient modulus of soil-fly ash mixes can be estimated from UCS test.

Edil et al. (2006) conducted a laboratory study to evaluate the improvement in mechanical properties of soft, fine-grained subgrade soil stabilized with fly ash. The CBR of soil-fly ash mixtures were observed to generally increase with fly ash content and decreased with increasing compaction water content. There was no increase in resilient modulus with soil stabilized with 10% fly ash; however, the resilient modulus increased by 30% when the fly ash content was 18% and strength gain higher in wetter and more plastic fine-grained soil. The resilient modulus grew modestly between 7 and 14 days and an additional increase of 20 to 40% between 14 and 56 days.

Fly ash reduces the potential of a plastic soil to undergo volumetric expansion by a physical cementing mechanism, by which Fly ash controls shrink-swell by cementing the soil grains together. Phanikumar and Sharma (2007) found that addition of fly ash to expansive soils reduced their swelling. Free swell index (FSI) decreased on addition of fly ash, as evidenced by the tests done on two highly swelling clays in the study. Swell potential and swelling pressure also decreased significantly with decreasing fly ash content. For the type of fly ash and expansive clays used, 20% fly ash content reduced FSI, swell potential, and swelling pressure as determined by the free swell method by about 50%.

2.2. DURABILITY

Durability, which is defined as the ability of a material to retain stability and integrity over years of exposure to the destructive forces of weathering (Dempsey and Thompson 1968), is an important property of construction materials. The ability of a CSL to maintain desired properties over the life of a pavement is an important consideration. Variations in climatic conditions have been recognized by pavement engineers as a major factor affecting pavement performance. Stabilized material deteriorates as a result of environmental attack, such as freeze-thaw (F-T) and wet-dry (W-D) cycling. Laboratory studies have indicated that F-T cycling significantly reduced the UCS and flexural strength of CSL (Khoury and Zaman 2005; Dempsey 1973). A field study showed that, after seven years of service, the UCS of CSL was less than 10% of the original strength in the middle of the traffic lane (Wen and Ramme 2008). The loss of strength in the middle of the traffic lane indicates that the deterioration of CSL strength is primarily from environmental conditions instead of traffic loading. In addition, reduction of stiffness and strength causes higher deflection of the surface layer, which results tension fatigue cracking at the bottom of the surface layer. However, the effect of moisture (W-D) or temperature (F-T) on layer stiffness is not considered in rigid nor flexible design in MEPDG analysis which the stiffness of the CSL are assumed to be constant over design life.

2.2.1. FREEZE-THAW AND WET-DRY DURABILITY

Environmental features, namely freeze–thaw and wet–dry cycling, are considered to be one of the most destructive actions that can help to damage the structure of stabilized soil such as pavement or embankment structures (PCA 1992; NLA 2005; Wen and Ramme 2008; Khoury and Zaman 2007). The W-D durability of soils primarily depends on the pore structure and tensile strength of the material. Other parameters, such as inter particle friction and cohesion may also influence the mechanical properties relative to W-D cycling. As water moves in and out of pore network of the specimen during W-D cycling, the pore walls experience capillary pressure and may collapse. Another concern is the detrimental influence of frost action in the roadbed in northern or cold climates. Water migration occurs in soil along with ice crystals formation if temperature is below 0°C or in winter. Moisture migrates from unfrozen soil towards the freezing front due to soil suction pressures produced by the freezing action. The formation of ice lenses produces a vertical pressure and heaves the surface which was called frost heave. Larger ice lenses result from an open freeze-thaw system with an external source of water and lower in a closed system without an external source of water (Rosa 2006). As thawing proceeds downward from the surface in the spring, the ice lenses thaw and contribute water to the soil. The water cannot drain out of the soil fast enough and thus the subgrade becomes substantially weaker (less stiff) and tends to lose bearing capacity.

During the last few decades, increased emphasis has been placed by transportation agencies and researchers to better understand the behavior of stabilized aggregate bases and stabilized subgrade soils under F-T and W-D

cycling. ASTM D559, *"Standard Test Methods for Wetting and Drying Compacted Soil-Cement Mixtures,"* and ASTM D560, "*Standard Test Methods for Freezing and Thawing Compacted Soil-Cement Mixtures,"* describe the procedures for determining the mass losses, water content changes, and volume changes produced by repeated W-D and F-T cycling of hardened soil-cement specimens.

The W-D durability of CSM is affected by many factors; e.g., the plasticity of soil, types, and amounts of stabilizers, mixing and compaction methods, curing conditions, etc. Bhattacharja and Bhatty (2003) studied the W-D cycling effect on portland cement- and lime-stabilized soils following ASTM D559. The cement-stabilized soils exhibited superior W-D performance to those stabilized with hydrated lime which had faster weight loss during W-D cycling. High PI soil or with low dosages of binder experienced more severely during W-D cycling. Furthermore, Parsons and Milburn (2002) found that different mix combination performed significantly different. The soils treated with cement performed better on sulfate bearing lean clays and lime treated soil performed better than cement and fly ash amendments to fat clays. Cement performed well on the samples with less clay content, while fly ash performed well only on the silty sand.

Freeze-thaw cycling was conducted on a series of soil/additive mixtures in accordance with ASTM D560 by Parsons and Milburn (2002). Weight loss in the soil specimens ranged from 2 to 41% after 12 F-T cycles. Cement-treated soils experienced the least soil loss, with reductions in mass of 2 to 7%. The lime-treated samples had the greatest losses, particularly for the lean clay. Fly ash-

treated soils had intermediate losses that ranged from 7 to 19%. Kootstra (2009) investigated the durability performance of Recycled pavement materials (RPM) and road surface gravel (RSG) stabilized with cement and cement klin dust (CKD) following ASTM D560 too. All durability tests with cement resulted in less than 5% mass loss after 12 cycles, with the 3% cement specimen having the largest percent mass loss, and the 7% cement specimen having the lowest. There was no significant difference between the mass loss from W-D and F-T cycles for the RPM; however, RSG had approximately 2-3% higher mass loss from the F-T cycling. For both RPM and RSG, specimens blended with cement were much more durable than specimens blended with CKD.

ASTM test procedures have been widely used by many researchers, although new and different evaluation methods are continually explored. Evaluation of durability based on weight loss is reported as overly severe and it does not simulate the field condition (Khoury and Zaman 2007). Weight loss measurements were not suitable for unbound pavement aggregates since the ASTM procedure is developed for soil-cement. Brushing is subjective and not repeatable due to the susceptibility of brushing technique to operator variability, and loss of single large aggregates. PCA mix design procedure recommends using 7-day UCS and durability tests (ASTM D559 and ASTM D560) to determine the cement content of soil-cement. Since this design procedure takes a long time and tend to be expensive, PCA developed a relationship between 7-day UCS and durability based on more than 1,700 sets of tests. The UCS versus durability relationship provided a short-cut mix design method that requires only a moisture-

density test, sieve analysis, and a 7-day UCS test. The results show that 87% of the cement mixtures survived the durability test with 7-day UCS of 4.14 MPa and 97% for 7-day UCS of 5.17 MPa. This design guide presents empirical proof of higher binder content correlating to improved durability performance. Department of Army, Navy, and Air Force (1994) also considers durability performance as a criteria for establishing admixture content for subgrade stabilization.

Khoury and Zaman (2002) investigated the effect of W-D cycling on low-quality aggregates stabilized with Class C coal fly ash (CFA). Resilient modulus (M_r), UCS, and elastic modulus were used to evaluate improvement in properties. Two different curing ages of soil-fly ash specimens (3-d and 28-d) were investigated. The M_r values of the 28-d-cured specimens increased as W-D cycles increased up to 12, beyond which a reduction was observed. For the 3-d-cured specimens, M_r increased 55% with 30 W-D cycles compared to M_r without any W-D cycles. However, W-D cycling was detrimental to the 28-d-cured specimens of which M_r showed a 5% reduction subjected to 30 cycles compared to M_r without any W-D cycles.

The strength of CSM subject to W-D cycling increases in many cases due to long-term hydration. Bin-Shafique et al. (2010) studied the effect of the W-D cycling using saline water on fly ash-stabilized clay since it was believed that W-D cycling using tap water had insignificant effect on CSM. The W-D cycling with tap water have essentially no significant effect on plasticity, unconfined compressive strength, and vertical swell potential of the stabilized soils. W-D cycling with saline

water reduced the plasticity, but did not have any effect on strength. A slight decrease of the vertical swelling was also observed after W-D cycling using saline water.

F-T cycling is more detrimental to CSM than W-D cycling. Parsons and Milburn (2002) reported strength loss after 12 F-T cycling in CSM. The fly ash and cement samples showed loss in strength compared to the specimens without any F-T cycling but remained stronger than native, unsoaked samples compacted at optimum water content. Bin-Shafique et al. (2010) found that the F-T cycling did not change the plasticity of the stabilized soils. However, the UCS decreased about 20% for stabilized soft soils and about 40% for stabilized expansive soils. Even after losing strength due to F-T cycling, the strength of stabilized soils was still at least three times higher than that of the unstabilized soils. The vertical swelling increased approximately 1% for stabilized expansive soils with 10% and 20% fly ash content, and increased approximately 2-3% for unstabilized soil and stabilized soil with 5% fly ash content due to F-T cycling. The vertical swelling increased rapidly for first four to five cycles and then increased very slowly.

The F-T cycling effects on resilient modulus and UCS of soils stabilized with different fly ash types were investigated by Rosa (2006). In most case, the M_r decreased up to 50% and 28.5% in average with the increasing of F-T cycling for the fly ash-stabilized soils. Additionally, RPMs-fly ash mixtures showed a M_r reduction after F-T cycling as the percentage of fines increased. A reduction in UCS after F-T cycles up to 70% was also obtained in a general trend. Similar to

M_r, the performance were affected by number of F-T cycles, host soils size distribution, *Cao* content and fly ash types. The effect of F-T cycling on the M_r of aggregates stabilized with cement kiln dust (CKD), Class C fly ash (CFA), and fluidized bed ash (FBA) was also investigated by Khoury and Zaman (2007). 15% CKD, 10% CFA and 10% FBA were stabilized with the aggregates and cured in a moist room for 28 days. M_r was tested on these aggregates after 0, 8, 16 and 30 F-T cycles. The M_r value of 10% CFA stabilized aggregate decreased by approximately 40, 73 and 81%; 80% reduction in 10% FBA- stabilized aggregate specimens for 30 cycle of F-T cycling. For another aggregate, resilient modulus was observed decreasing with the F-T cycles up to 30. Additionally, it was also found that the deterioration of F-T cycles varied on different type of stabilized agents. The CKD stabilized specimens had severely damage in comparison to CFA and FBA stabilized aggregates under exposure to F-T cycling.

2.2.2. VACUUM SATURATION

ASTM C 593, “Standard Specification for Fly Ash and Other Pozzolans for Use with Lime” provides evaluation of durability when fly ash or other Pozzolans are used with lime. The test evaluates the relative performance of cement and lime-stabilized soils. The UCS of specimens after vacuum saturation were found to correlate well with residual UCS of specimens after F-T cycling .Vacuum saturation can potentially be a fast and inexpensive way to assess the durability performance of CSM (Dempsey and Thompson 1973; Guthrie et al. 2008).

Dempsey and Thompson (1973) conducted research on the feasibility of vacuum saturation procedures as a rapid method for predicting the durability of stabilized soils including soil-cement, lime-fly ash, and lime-soil mixtures. UCS and moisture contents were used to evaluate the durability performance of the stabilized soils. The relationship between vacuum saturation strengths and 5 and 10 F-T cycles strengths were highly correlated for cement and lime-fly ash materials, with a linear relationship between vacuum saturation strength and F-T strength. In addition, the dry density of the stabilized soils affected the UCS performance of the F-T and vacuum saturation.

Bhattacharja and Bhatty (2003) found that UCS for soil stabilized with portland cement and lime experienced a significant strength loss after the vacuum saturation testing. The cement-stabilized soils after vacuum saturation had a much higher strength than those of the lime-stabilized soils. The 7-day UCS of clay treated with 6% cement reduced from 1.31 MPa to 0.48 MPa; with 6% lime, the UCS went from 0.75 MPa to 0.41 MPa. A similar trend was also found on other clay soils with low plasticity. The 7-day UCS of low plasticity soil treated with 6% cement reduced from 2.93 MPa to 0.86 MPa; with 6% lime, went from 0.83 MPa to 0.34 MPa. Specimens cured for 91 days showed a higher UCS value after the vacuum saturation compared with the UCS of specimens cured for just 7 days. The portland cement-stabilized specimens were more durable than lime-stabilized specimens subjected F-T cycling.

Guthrie et al. (2008) found that there existed a strong correlation between UCS after F-T cycling and UCS after the vacuum saturation test and weak correlations between the final the dielectric value after tube suction testing and all other response variables. The F-T cycling and vacuum saturation were conducted on the fly ash, cement and lime-fly ash soil mixtures followed ASTM D 560 (replacing mass losses measurement with UCS) and ASTM C 593. The lowest additives concentration had the poorest performance both with vacuum saturation and F-T cycling. Vacuum saturation was found to be a more severe test than the F-T cycling. UCS correlations between vacuum saturation and F-T cycling were found to be linear, with R^2 0.70.

2.3. ULTRASONIC PULSE VELOCITY TESTS ON SOILS

Dynamic testing refers to non-destructive testing soils under small strain (< 10^{-4}%) which is typically performed by resonant column and pulse transmission methods in laboratory. Ultrasonic pulse velocity testing is a nondestructive testing technique, which sends sound waves ranging in frequency from 20 kHz to 1 GHz through the specimen. By measuring travel time through the specimen, the p-wave or shear wave velocity and related dynamic properties of the material are determined. During the past decade, ultrasonic pulse velocity has been widely used as a simple and quick measurement for quality control and defects detection in civil infrastructure. The method is simple and quick and attractive for application to soils.

Stephenson (1978) developed the ultrasonic test system for testing soil specimens to determine their design parameters in construction. Young's modulus, shear modulus, Poisson's ratio and damping were determined. The specimen size affected the velocity measurement. For a given band of saturation, the compression (V_p) and shear wave velocity (V_s) tended to decrease with an increase of void ratio, with the rate of decrease of V_s slower than V_p. For a constant void ratio, wave velocities generally increased with the degree of saturation.

Leong et al. (2003) evaluated an ultrasonic test system in determining compression and shear wave velocities. Aluminum, mild steel, stainless steel, nylon, granite, residual soil, and kaolin specimens were tested to establish reliable procedures for determination of the wave travel time. The study investigated the effect of the acoustic coupling agent, signal processing techniques, and the effect of length over diameter (L/D) and length over wave length (L/λ) on the P-wave and shear wave velocities. Increasing confining pressure increased the wave velocities and reduced attenuation. Additionally, a general trend of a decreasing Poisson's ratio with increasing void ratio was observed.

Yesiller et al. (2001) evaluated the feasibility of applying ultrasonic pulse velocity testing method on stabilized materials. Their p-wave measurement system consisted of a 50-kHz p-wave transducer, receiver, and a data acquisition system. The first arrival time was calculated as the difference between the time of application of the pulse by the transmitting transducer and the arrival time of the

signal at the receiver. Tests were conducted on lime, cement, and fly ash-stabilized clays with high plasticity. The ultrasonic pulse velocity testing method was applied to monitor the strength growth of the specimens along the curing time. P-wave velocities increased with curing time generally; the p-wave increased more in the first 7 days than the rest of the curing age. Cement mixtures had larger increasing rates during curing and higher velocities. Additionally, the effect of compaction moisture content on the p-wave velocity was also investigated. For clay-cement and compacted clay specimens, the variation in p-wave velocities with compaction moisture content followed the same trend as the variation in dry density with compaction moisture content. The maximum p-wave velocity was measured in specimens compacted at optimum moisture content. However, this trend wasn't observed in the fly ash-stabilized clay. Good correlations were observed between velocity and strength for fly ash-stabilized soil. The P-wave velocity increased with increasing modulus of the mixture. P-wave velocity was directly correlated to the stiffness of the stabilized mixtures. The velocity was not as closely correlated to strength.

Due to the high attenuation of ultrasonic waves in soil specimens, the research on subgrade/base soil or aggregate using ultrasonic pulse velocity test method is limited. However, many researchers have conducted other soil dynamic testing method on subgrade/base soil/aggregate by applying free-free resonant column (FFRC) techniques (Hilbrich and Scullion 2007). Moduli obtained with seismic measurements are low-strain high-strain-rate values. Vehicular traffic causes high strain deformation at low strain rates. One of the main concerns of

the pavement community throughout the years has been how seismic modulus methods can be successfully used in pavement design. A common test used for characterizing substructure materials is the resilient modulus test. However, there are many types of unconventional materials (i.e., stabilized materials, recycled materials, large particle continuums) where resilient modulus testing may not be appropriate or feasible. Determination of the resilient modulus using traditional laboratory test procedures is expensive and unavailable in many places.

Some studies confirmed constrained modulus correlated well with resilient modulus. Nazarian et al. (2005) conducted a comprehensive research on the development of appropriate FFRC instrumentation, excitation and acquisition techniques, data analysis, and correlation to M_r on subgrade/base materials. The seismic modulus obtained from FFRC is about 51% of the M_r though both field and laboratory testing. Hilbrich and Scullion (2007) proved the FFRC test method can serve as a rapid and cheap alternative for laboratory determination of M_r. Limestone and sandy soil stabilized with cement and RAP and base materials stabilized with asphalt were tested for seismic modulus using the FFRC test method, followed by traditional M_r testing. From the results obtained, the M_r is approximately 71% of the modulus obtained in the seismic modulus testing. Linear relationship between the constrained modulus and resilient modulus was also found by Schuettpelz et al. (2010) for a wide range of granular materials.

Besides these laboratory seismic modulus researches, many non-destructive field testing using p-wave velocity measurement had been attempted

recently. Unlike other field tests, seismic modulus test is more practical and more desirable because they are rapid to perform, and because they test a volume of material non-destructively which means testing in its natural state of stress and undisturbed. A standard specification of applying seismic modulus testing techniques to determine design moduli of pavement base materials were established in the TxDoT research project 1735 (Nazarian et al. 2005). The materials were tested both *in situ* and in laboratory for FFRC test and resilient modulus. Williams and Nazarian (2007) conducted tests to justify the potential use of seismic modulus testing method to conduct QA/QC of base and subgrade layers. A procedure for relating high strain modulus, M_r, and low strain modulus, seismic modulus was provided. The results showed good correlation between M_r and seismic modulus both in cohesive soil and granular soil. The finding was enhanced by two specific site including one clayed subgrade and another for a granular base material.

SECTION 3 MATERIALS AND METHODS

3.1. SOILS

3.1.1. SOURCES

The host materials selected for this study represent materials classified as gravel, sand, silt, and clay based on the Unified Soil Classification System (USCS). The gravel was procured from a quarry in Jefferson County, Wisconsin, and owned by Evenson Construction Company. Wisconsin DOT testing indicated the gravel at this quarry does not meet specifications for use as a base course without stabilization. Sand was procured locally from Capital Sand and Gravel in Cross Plains, Wisconsin. Commercially, the product is known as ‘torpedo’ sand. The silt and clay were obtained from the Dane County Public Works Landfill on USH 12 in Madison, Wisconsin. Silt was brought to the landfill during construction excavation for a project on the University of Wisconsin-Madison campus, while the clay was part of a remnant stockpile from the landfill’s clay liner construction (Casmer 2011). Figure 3.1 depicts the four kinds of soils used.

3.1.2. INDEX PROPERTIES OF TEST MATERIALS

Index properties, and compaction properties and classifications of the test soils are summarized in Table 3.1. The soils classify as gravel (GM), sand (SP), silt (ML), and clay (CL) according to USCS (ASTM D2487). Except clay, the other

host materials are non-plastic (NP). The clay had a liquid limit (LL) of 39 and a plastic limit (PL) of 19.

Particle size distributions for the four soils are shown in Figure 3.2. Compaction curves corresponding to standard Proctor effort were determined following ASTM D 698, except for gravel which ASTM D1557 (Method B: modified compactive effort) was used. Gravel is insensitive to water content, as the compaction curves shown in Figure 3.3; while the bell-shaped curves of the silt and clay clearly indicate their maximum dry unit weights. The curve for sand shows optimum moisture content between 10 and 12%. Optimum water contents and maximum dry unit weights are summarized in Table 3.2.

3.2. BINDERS

Four different binders were used in this study: cement, Class C fly ash, Class F fly ash, and lime. The mix combinations and mix design results were determined at Washington State University (Wen et al. 2011). A total of nine mix combinations were compacted to maximum density at optimum moisture content for three different binder contents. The specimens were cured for 7 days following appropriate curing method and then subjected to unconfined compression strength (UCS) testing. The minimum binder content to achieve a specified strength was selected for each mix combination.

Type I Portland cement was used to stabilize each of the host materials for this study. The cement was manufactured by Lafarge and purchased from a local supplier in 21.3-kg bags. Three different cement contents were used to determine the binder contents. The minimum cement content that resulted in an UCS larger than 2.1 MPa after 7 day curing was selected for that soil based on ASTM D 1633 (PCA, 1992). The mix design results indicated that 3% cement content is suitable for stabilizing gravel, 6% for sand, 8% for silt, and 12% for clay.

Class C fly ash was obtained from the Oak Creek Power Plant in Oak Creek, Wisconsin. The power plant pulverizes coal prior to combustion to produce electricity using four boiler units. Fly ash is removed from the system with electrostatic precipitators. Three Class C fly ash contents (10%, 13% and 16%) were used as trial contents for silt, sand, and gravel. The FHWA recommends at least 2.8 MPa for the 7-day unconfined compressive strength based on ASTM D 1633 (FHWA 2003). The sand-fly ash specimen was the only mixtures to fulfill this criterion with 13% fly ash by weight. 13% fly ash is recommended for stabilizing silt and gravel, because this content has been used successfully in the past studies and is consistent with the content used by agencies, such as Oklahoma DOT, Wisconsin DOT and Minnesota DOT (Wen et al. 2011).

High calcium hydrated lime was obtained from a local supplier in 22.7-kg bags, which was manufactured by Western Lime Corporation. Class F fly ash was processed from the Elm Road Generating Station at the Oak Creek power plant. Lime and lime-class F fly ash were used to stabilized clay and silt, respectively.

National Lime Association (NLA) standards recommend that lime-stabilized soils have a UCS of at least 0.5 MPa after 7-day curing at 40°C based on ASTM D 5102 (NLA 2006). 6% lime by weight in clay led to the UCS exceeding 70 psi specified by the NLA. Since the silt and lime mix for this study is not appropriate according to NLA standards, lime-class F fly ash was used to stabilize with the silt instead. MEPDG recommend soil-lime-fly ash specimens have a 7-day UCS of at least 1.4 MPa based on ASTM C 593 (ARA Inc. 2004). 4% lime and 12% class F fly ash by weight met the recommendation.

The final mix design, the maximum dry density, and optimum moisture content for all stabilized mixtures are presented in Table 3.3. Detailed information of the mix design can be found in Appendix A.

3.3. TEST PROCEDURES

3.3.1. SPECIMENS PREPARATION

For durability tests, a standard proctor-size mold (diameter of 102 mm and a height of 152 mm), in conjunction with the appropriate hammer weight, drop height, and compaction effort, was mainly used for preparation of the durability test specimens. Specimens were prepared as follows:

(1) Moisture content of soil is measured and then was blended with the required percentage by weight of binders until the mixture had uniform color according to Table 3.3.

(2) The soil-fly ash mixture was moistened with water to the target water content and blended until uniform; the mixtures were compacted immediately except for clay-lime which was tightly covered and allowed to mellow 24 hour before compaction.

(3) The specimens were compacted in three equal layers in the standard proctor size mold to achieve the maximum dry unit weight. The surface between layers was scarified to a depth of 0.6 mm (¼ in.) to ensure a good bond.

(4) The specimens were taken to corresponding curing facilities depending on the binder types.

Different curing procedures were applied to different mixtures depending on the binder. Cement-stabilized mixtures (gravel, sand, silt, and clay) were cured in the moist room (100% relative humidity, 21°C) for 28 days (ASTM D 558). Fly ash-stabilized mixtures (sand, silt, and gravel), clay-lime and silt-lime-Class F fly ash were sealed with plastic wrap and cured for 7 days in an oven set to 40°C (ASTM C 593).

3.3.2. WET–DRY AND FREEZE-THAW CYCLING TESTS PROCEDURES

ASTM D559, “Standard Test Methods for Wetting and Drying Compacted Soil-Cement Mixtures,” and ASTM D560, “Standard Test Methods for Freezing and Thawing Compacted Soil-Cement Mixtures,” describe the procedures for

determining the soil-cement losses, water content changes, and volume changes produced by repeated wetting and drying and freezing and thawing of hardened soil-cement specimens. The procedure followed in this study was adopted from ASTM D559 and ASTM D 560 in terms of number of cycles, cyclic durations and temperature profiles, whereas property measurements were modified to fit the purpose of the durability model validation. P-wave velocity was determined at the end of each cycle.

For W-D cycling, the specimens are submerged into potable water at room temperature for a period of 5 hours at the end of curing. At this stage, modulus and physical properties of each specimen are measured representing zero cycle records. Then the specimens are placed in an oven at 71°C for 42 hours. At the end of drying phase, the specimens are removed from the oven and submerged into water for 5 hours. Again the required properties of the specimens are measured. This procedure constitutes one cycle (48 hours) of drying and wetting. The W-D procedure is designed to continue testing each specimen until it reaches some defined termination criteria. Figure 3.4 shows the specimen subject to W-D cycling.

For F-T cycling, modulus and physical properties of each specimen are measured, which represents zero cycle records at the end of curing time. Then, the specimens are placed on the top of a water absorbing pad in the freezing apparatus with temperatures lower than -23°C for 24 hours. Following the freezing stage, the specimens are placed in the moist room having a temperature

of 21°C and a relative humidity of 100% for 23 hours. Then, the measurement of seismic modulus is taken at the end of each cycle. Similar to W-D durability test, F-T procedure is designed to continue until the specimen reaches defined termination criteria. Figure 3.5 present the specimen at thawing and freezing condition.

The criteria for test termination are defined as one of the following situations:

- The freeze–thaw and wet- dry cycling reach 12 cycles as the ASTM D 559 and D 560 required.
- The surface deteriorates severely until stable readings from Pundit Plus equipment cannot be made. (“Stable reading” means the time on the Pundit Plus screen changes within 3%)

Unconfined compressive strength test (UCS) (ASTM D5102 without 4 hours soaking) were performed on the specimens once the F-T and W-D cycling were completed and compared to the UCS of specimens without any durability tests.

3.3.3. VACUUM SATURATION TEST PROCEDURE

Vacuum saturation strength test was carried out according to ASTM C593, “Standard Specification for Fly Ash and Other Pozzolans for Use with Lime for Soil Stabilization.” A vacuum system which was capable of maintaining a vacuum

of 61 cm Hg (81 kPa) was assembled as shown in Figure 3.6. Then the specimens were placed in the vacuum chamber. The air chamber was evacuated to a pressure of 61 cm Hg. Vacuum pressure was increased over a period of not less than 45 s and the vacuum pressure was held for 30 min to remove air from the voids in the specimens. After the 30-min de-airing period, the vacuum chamber was flooded with water at room temperature to a depth sufficient to cover the specimens. Then, the vacuum was removed and the specimens were soaked for 1 hour at atmospheric pressure.

At the end of the soaking period, the specimens were removed from the water and were allowed to drain for approximately 2 min. Then, the unconfined compressive strengths (ASTM D1633) of the vacuum saturated specimens were performed as soon as possible. Unconfined compression strength test following ASTM D1633 were also performed on the control specimens without 4 hours soaking period, which represent the state before vacuum saturation.

3.3.4. ULTRASONIC PULSE VELOCITY TEST

All pulse velocity measurements determined in this study utilized a PUNDIT-plus Ultrasonic Velocity Test System produced by CNSFARNELL. The device consists of a transducer and a receiver and connected to an electronic timing device for measuring the time interval between the initiation of a pulse generated at the transmitting transducer and its arrival at the receiver. The travel

time through the specimen can be read from the PUNDIT-Plus digital display screen.

The PUNDIT-plus Ultrasonic Velocity Test System used in this study operated at a frequency of 54 kHz. ASTM C597, “Standard Test Method for Pulse Velocity through Concrete”, was followed in this study. Instead of testing concrete beam specimens, cylindrical soil specimens were tested in the direct transmission arrangement in which the transducers are contacted to the ends of the specimens. A water-based jelly (K-Y by Target) was used as the coupling agent to ensure fully contact of the transducers and the surfaces. Travel time and the exact length of the specimens were recorded for the calculation of the pulse velocity. A schematic of the test system and the PUNDIT-plus equipment were shown at Figure 3.7 and Figure 3.8.

SECTION 4 DURABILITY TESTS RESULTS AND ANALYSIS

4.1. FREEZE-THAW CYCLING EFFECT

4.1.1. CONSTRAINED MODULUS CHANGE

An objective of this research was to study how the mechanical properties of cementitiously stabilized layers (CSL) in pavement change when undergoing exposure to weathering, such as freeze-thaw (F-T) and wet-dry (W-D) cycling. Typical methods for evaluating the durability include weight loss measurement (ASTM D 559 and ASTM D560), resilient modulus change (Rosa 2006; Khoury and Zaman 2007), and unconfined compressive strength (UCS) change (Dempsey and Thompson 1972; Parsons 2002) during F-T and W-D cycling test. Ultrasonic pulse velocity testing was used as a non-destructive method to monitor the change of constrained modulus for CSL during each F-T and W-D cycle. The main advantage of applying non-destructive seismic modulus testing instead of other physical laboratory tests (resilient modulus, triaxial compression test or unconfined compression test) is the ability to detect mechanical property (constrained modulus) changes on the same specimen during F-T or W-D cycling. Seismic modulus testing is a relatively inexpensive and provides quick assessment of material properties compared to other laboratory testing methods. Researchers have validated the use of seismic modulus testing methods to characterize the mechanistic properties of subgrade/base materials (Hilbrich and Scullion 2007; Nazarian et al. 2005; Williams and Nazarian 2007; Sawangsuriya et al. 2003; Sawangsuriya et al. 2009; Schuettpelz et al. 2010). The ultrasonic

wave testing is a form of seismic modulus testing. The constrained modulus, D, is calculated as

$$D = \rho V_p^2 \quad (4.1)$$

where compression wave (P-wave) velocity, V_p, is calculated by dividing the length of the specimen by the corresponding travel time of wave through the specimen and ρ is the bulk density of the specimen. For the purpose of this study, residual constrained modulus is defined as the constrained modulus of the thawed specimen measured after the last F-T and W-D cycle. Normalized constrained modulus is the modulus after each F-T cycle using constrained modulus at 0 cycles (initial constrained modulus) for normalization.

4.1.1.1. GENERAL EFFECT OF FREEZE-THAW CYCLING

At least 3 replicates were prepared for each mixture. Constrained modulus for the thawed condition was measured after each F-T cycle. The test results for cement-stabilized soils along with physical characteristics, e.g., dry unit weight, void ratio, compaction moisture content, and moisture content, are given in Table 4.1. Similarly, specimens were prepared with fly ash and lime as the binder based on the optimum binder contents as determined by the mix design. Table 4.2 summarizes the results for fly ash-stabilized soils and Table 4.3 for lime-stabilized soils subjected to the F-T cycling. The constrained modulus changes with number of F-T cycles for all mixtures, as presented in Figure 4.3 for cement-stabilized soils, Figure 4.4 for fly ash-stabilized soils, and Figure 4.5 for lime-stabilized soil.

In Chapter 3, the termination criteria of the test were defined as either completion of 12 F-T cycles or visual observation of specimen degradation. Fluctuating in the reading from the Pundit is attributed to loosening of soil particles from the surface during F-T cycling (Figure 4.1), which can result in unreliable travel time reading. Durability can be defined as the ability of a mixture to maintain integrity during exposure to weathering, such as F-T and W-D cycles. Based on the test termination criteria, the number of cycles that the specimen can withstand can be considered as an indicator of durability. The remainder of this section is a discussion/analysis of the test results.

The four cement-stabilized materials exhibited varying performance during F-T cycling (Table 4.1 and Figure 4.3). The gravel-cement specimens resisted only 2 F-T cycles despite having the highest initial stiffness; whereas the silt-cement specimens survived 6 or 7 F-T cycles. The sand-cement and clay-cement specimens completed the 12 F-T cycles. The normalized constrained modulus of sand-cement and clay-cement specimens at the end of F-T cycling was higher than gravel-cement and silt-cement specimens, which indicates greater durability. Sand-cement specimens with 6% cement showed no degradation of constrained modulus due to F-T cycling whereas clay-cement specimens showed 49% average reduction in constrained modulus after 12 F-T cycles. The reduction in constrained modulus of gravel-cement specimens was around 72% on average, with low variability. At the end of the F-T cycling, the constrained modulus for silt-cement specimens showed 57% reduction on average, but with high variability (24% to 76%). For all cement-stabilized materials, the reduction in constrained

modulus after F-T cycling ranged from 39% to 72%. The normalized residual constrained modulus of sand-cement was the highest (93%) among the cement-stabilized soils.

Similar to the performance of sand-cement specimens, Class C fly ash-stabilized sand survived 12 F-T cycles without significant surface deterioration (Table 4.2 and Figure 4.4). Among the fly ash-stabilized materials, gravel-fly ash specimens showed the highest residual constrained modulus and UCS. The gravel-fly ash specimens' normalized constrained modulus was reduced by 53%. Silt-fly ash specimens had essentially no resistance to F-T cycling and did not survive more than 4 F-T cycles. Some minor cracking and significant soil particle loss were observed after 1 cycle with 40% reduction in constrained modulus. For fly ash-stabilized soils, constrained modulus reductions ranged from 32% to 77%. Rosa (2006) reported that the resilient modulus initially decreased in response to F-T cycling, and then leveled off after 1 to 5 cycles for granular materials stabilized with fly ash and 1-3 cycles for fine-grained soil-fly ash. The drop in resilient modulus ranged between 7% and 50%, with an average 28.5% for granular soil-fly ash and 23.5% or fine-grained soil-fly ash. Constrained modulus reductions in this study are comparable to the resilient modulus reduction given by Rosa (2006) although there are some differences in the testing procedures employed.

Low resistance to F-T cycling was also observed for silt-lime-fly ash (Class F) and clay-lime specimens (Table 4.3 and Figure 4.5). After 6 cycles, the

normalized constrained modulus of silt-lime-fly ash specimens was reduced by more than 90%. Similar to the silt-lime-fly ash specimens, clay-lime specimens did not maintain integrity through the first F-T cycle. F-T cycling was detrimental to the clay-lime specimens and cracks propagating around the specimens were noticed as shown in Figure 4.2. After the first F-T cycle, minor adhesion of the sensor coupling agent, used between the PUNDIT-Plus transducer/receiver and specimen surface, was enough to dislodge soil particles in both silt-lime-fly ash and clay-lime specimens. The overall constrained modulus reduction in lime-stabilized soils ranged from 76%-93%, with low variability. Lime-stabilized soils had poor durability compared to fly ash and cement-stabilized soils.

Resilient modulus reduction due to F-T cycling has been documented in both laboratory tests and from field data for CSM. For example, for cement kiln dust (CKD)-stabilized base aggregate, Zaman et al. (1999) reported resilient modulus reductions were 54%, 67%, and 65% for four, eight, and twelve cycles, respectively. Khoury and Zaman (2007) also reported continuous resilient modulus reduction (up to 90%) on CKD, fluidized bed ash (FBA), and Class C fly ash (CFA)-stabilized aggregate after 30 F-T cycles. In some field studies, after one to three F-T cycles, the resilient modulus reduction of various unstabilized coarse and fine-grained soils ranged between 20% and 66% (Jong et al. 1998; Lee et al. 1995). Fly ash-stabilized fine-grained subgrade and coarse-grained base course showed little change in field modulus after 1 winter season (Li et al. 2007; Hatipoglu et al. 2008; Li et al. 2008; Wen et al. 2010).

Difficulty arises in comparing constrained modulus reduction results between laboratory tests and field data due to limited research on how F-T cycling affects constrained modulus of CSM. However, it is appropriate to compare the constrained modulus reduction with the resilient modulus reduction during F-T cycling, provided a good correlation exists between them. Some studies confirmed that constrained modulus correlates well with resilient modulus. Nazarian et al. (2005) found the seismic modulus obtained from free-free resonant column (FFRC) testing is about 51% of the resilient modulus determined though both field and laboratory testing. Hilbrich and Scullion (2007) showed that the resilient modulus is approximately 71% of the constrained modulus for cement-stabilized base aggregates. Schuettpelz et al. (2010) showed that the resilient modulus is approximately 70% of the constrained modulus for a wide range of granular materials.

4.1.1.2. EFFECT OF FIRST FREEZE-THAW CYCLE ON MODULUS

Water migration occurs in soil specimens when temperature is below 0°C along with ice crystals formation. Moisture migrates from the unfrozen soil part towards the freezing front due to soil suction pressures produced by freezing action. Higher moisture content increases are observed for an open F-T system with an external source of water as compared to lower increase in a closed system without an external source of water (Rosa 2006). The ASTM D560 test procedure is an intensive F-T cycling test in which there are water-absorbing pads,

which allows for external source of water beneath the specimen. An external water source allows for larger ice lens formation, thus resulting in more severe frost action. Due to expansion with ice formation, internal pressure generated, thus resulting in weaker soil structure through the continuous F-T cycling.

Typically, frost-susceptible soil structure is weakened by the frost action after the first few F-T cycles. Simonsen et al. (2002) reported resilient modulus reduction between 20-60% on unstabilized coarse- and fine-grained soils after the first F-T cycle. Lee et al. (1995) also reported a resilient modulus reduction between 30% and 50% on a compacted fine-grained soil after the first F-T cycle, the subsequent two F-T cycles showed less significant change. This result was confirmed by Rosa (2006) from research involving fly ash-stabilized soils where most of the resilient modulus reduction occurred during one to three F-T cycles.

Reduction in normalized constrained modulus after the first F-T cycle indicates frost susceptibility of CSMs tested in this study, however, with varying degrees, as shown in Figure 4.6 (a). To understand the overall effect of the first F-T cycle, the ratio of constrained modulus reduction after the first F-T cycle to the total constrained modulus reduction is graphed in Figure 4.6 (b). For example, clay-lime specimens had the largest constrained modulus reduction (66%) after the first F-T cycle. Specimens showed high resistance to degradation after the first F-T cycle (constrained modulus reduction<10%), including silt-lime-fly ash, sand-cement, gravel-cement, gravel-fly ash, and sand-fly ash. The soil-cement mix procedure recognized that the higher initial UCS/strength the higher F-T

durability (PCA 1992). This general trend also was also proved in our study as shown in Figure 4.7 (a) & (b): mixtures with higher initial UCS had less reduction after the first F-T cycle and less total reduction in constrained modulus.

4.1.1.3. EFFECT OF BINDER TYPE ON MODULUS

Criteria and soil classifications for frost susceptible soils usually reflect susceptibility to softening on thawing as well as to heaving (ACPA 2008). Frost susceptibility increases with increasing fines content for subgrade soils, thus granular material is generally considered as non-frost susceptible. There is a wide diversity in frost susceptibility determination methods. In Wisconsin and Minnesota, base and subbase materials are considered frost susceptible if the amount passing the No. 200 sieve exceeds 5% and 10%, respectively. The gravel, silt, and clay used in this study are frost susceptible since the fines content are larger than 14%. The U.S. Army Corps of Engineers recommends conducting two F-T cycles on soils to determine frost-heaving and thaw-weakening susceptibility. The capillarity and permeability of soils can be used to assign frost susceptibility of subgrade soils as shown in Figure 4.8 (ACPA 2008). Based on this criterion, the materials used in this study, i.e., silty gravel (GM) is characterized as moderately frost susceptible soil, lean silt (ML) as severely frost susceptible, lean clay (CL) as moderately to severely frost susceptible, and poorly graded sand (SP) non-frost susceptible.

Section 4.1.2 documented that soil stabilized with different binders behaves differently. The number of F-T cycles, normalized constrained modulus, normalized UCS, and reduction in constrained modulus after first F-T cycle are various indicators of the F-T durability. Compared to other mixtures, cementitiously stabilized sand showed superior F-T durability which is expected since the sand contains the least fine contents (0.1%) and non-frost susceptible. Sand-cement and sand-fly ash specimens completed twelve F-T cycles, and the first cycle reduction in constrained modulus was the least as shown in Figure 4.9 (b).

The low quality silty gravel contains 14.1% fines which results in weaker F-T durability. Although the residual constrained modulus still remains relatively high for gravel-cement (6.9 GPa) and gravel-fly ash(3.4 GPa), the F-T cycling degrades the stiffness a lot; the normalized constrained modulus of the gravel-fly ash specimens was 43% after completing 4 F-T cycles, whereas the normalized constrained modulus of the gravel-cement specimens was 28% after 2 F-T cycles.

Fly ash- and fly ash-lime-stabilized silt and clay also had weak F-T durability, as shown in Figure 4.10 (a). Silt-fly ash specimens did not maintain the integrity after the first cycle, with the residual constrained modulus dropping to 2.2 GPa (60%). The residual constrained modulus of silt-lime-fly ash specimens was 0.7GPa (10%) after six F-T cycles. The residual constrained modulus of silt-cement specimens was much larger (7.0 GPa) after seven F-T cycles. The strong

F-T durability of silt-cement can attribute to the high cement content (8%) which results in much larger initial constrained modulus and UCS.

Similar to silt-cement, high cement content (12%) in clay-cement produce a strong resistance to F-T cycling. The clay-cement specimens finished twelve F-T cycles with 3.8 GPa in residual constrained modulus, whereas clay-lime specimens showed no resistance to F-T cycling and did not maintain integrity, as shown in Figure 4.10 (b) and Figure 4.2.

Generally, cement-stabilized soils were more durable to F-T cycling than other CSMs based on the residual constrained modulus in this study. Class C fly ash was less effective than lime-fly ash (Class F) to improve the durability, strength, and stiffness of silt (ML). An objective of this study was to investigate the performance of CSMs exposure to weathering and incorporate the results into MEPDG. The F-T durability of CSM is not the concern of this study and not enough tests have been conducted to verify the conclusion. The conclusion that cement-stabilized soils had stronger durability may be biased since they possess the highest initial strength and stiffness. Additionally, conclusion can’t be drawn since single binder content was evaluated in the study which has been reported to influence F-T durability significantly (Rosa 2006; Parsons and Milburn 2002; Khoury and Zaman 2007; Dempsey and Thompson 1973; Guthrie et al. 2008).

4.1.1.4. EFFECT OF BINDER CONTENT ON MODULUS

F-T durability of the two different cement contents used to stabilize gravel and sand in this study is examined. Normalized constrained modulus change vs. increasing number of F-T cycling for gravel stabilized with 3% and 4% cement are presented in Figure 4.3 (a). Gravel-cement (4%) specimens finished twelve F-T cycles, and normalized residual constrained modulus was 68%. However, gravel-cement (3%) specimens displayed significant degradation after 2 F-T cycles and one of the specimens broke after two cycles. Visual observation also supported the lower F-T durability of gravel-cement (3%), which started losing particles after the first F-T cycle. The average first cycle constrained modulus reduction for the gravel-cement with 3% and 4% cement content specimens was 43% and 6%, respectively. Trend in F-T durability were significantly different in the sand-cement specimens (6% and 8% cement) as shown Figure 4.3 (c). The sand-cement specimens with cement content of 8% had no degradation in constrained modulus with F-T cycling. The modulus reductions were only 3% and 7% after the first cycle for 6% cement and 8% cement-stabilized sand, respectively.

These findings are consistent with the PCA soil-cement design guide (PCA 1992). Soil-cement mix design is mainly based on 7-day UCS and durability tests (ASTM D559 and ASTM D560). PCA conducted a series of tests which showed that that 87% of the cement-stabilized specimens complete the durability test with 7-day UCS value of 4.14 MPa and 97% for 7-day UCS value of 5.17 MPa. Resistance against F-T and W-D cycling increases with increasing UCS. The greater the cement content, the stronger is the anticipated durability. Appendix A (mix design results) provides the 7-day UCS of gravel-cement and sand-cement

specimens with various cement contents. The average 7-day UCS value is 6.20 MPa for 8% cement-stabilized sand specimens and 2.76 MPa for 6% cement-stabilized sand specimens. The average 7-day UCS for 3% and 4% cement-stabilized gravel is 3.45 MPa and 4.83 MPa (estimated from 3% and 5% cement content), respectively. Generally, higher binder content results in higher UCS of and thus stronger F-T durability.

(With the limitation of this study, the binder content effect of fly ash and lime on the durability performance will not be discussed.)

4.1.2. UNCONFINED COMPRESSIVE STRENGTH (UCS) CHANGE

Numerous laboratory studies have documented that F-T cycling degrades the UCS and flexural strength of CSM (Khoury and Zaman 2005; Zaman et al. 1999; Dempsey and Thompson 1973). A field study showed that, after seven years of service, the UCS of a CSM was less than 10% of its original strength in the middle of the traffic lane (Wen and Ramme 2008). The loss of strength in the middle of the traffic lane indicates that the deterioration of CSM strength is primarily from climatic conditions instead of traffic loads.

The UCS and the normalized UCS (i.e., the ratio of initial UCS to residual UCS after F-T cycling) are summarized in Table 4.1 for cement-stabilized soils, in Table 4.2 for fly ash-stabilized soils, and in Table 4.3 for lime-stabilized soils. The initial UCS for all CSMs (end of curing) were reported by Casmer (2011). UCS

was obtained by averaging at least three replicates. Detailed information for the initial UCS of CSM is presented in Appendix B.

4.1.2.1. GENERAL EFFECT OF FREEZE-THAW CYCLING ON UCS

The four cement-stabilized materials exhibited initial UCS ranging from 3.68 MPa to 4.7 MPa. All of the cement-stabilized soils showed reduction in UCS after F-T cycling. The average residual UCS are 3.05 MPa (66%), 2.52 MPa (63%), 1.99 MPa (55%), and 1.78 MPa (49%) for gravel-cement, sand-cement, silt-cement and clay-cement specimens, respectively. The residual UCS of cement-stabilized soils decreased as the fine contents of the host soils increased. However, this conclusion is subject to change as the number of F-T cycles varied and binder content changed.

The initial UCS of fly ash-stabilized soils are 2.65 MPa, 1.98 MPa and 0.63 MPa for sand-fly ash, gravel-fly ash, silt-fly ash specimens, respectively. The silt-fly ash specimens did not constitute a strong combination which withstood one F-T cycles to lose integrity and having the lowest initial and residual strength among the fly ash-stabilized soils. Rosa (2006) reported a strength (UCS) reduction up to 70% in a wide variety of fly ash-stabilized soils and higher reductions of strength were observed in fly ash-stabilized coarse-grained soils.

Similar to the constrained modulus degradation, the average normalized residual UCS decreased 55% to 0.84 MPa for the silt-lime-fly ash specimens after

6 F-T cycles (one of them lasted only two cycles). Except for silt-fly ash, the clay-lime specimens are the most frost susceptible mixtures, which had the lowest average residual UCS 0.39 MPa.

Residual UCS after F-T cycling ranged from 17% to 84% for cement-stabilized soils, 29% to 63% for Class C fly ash-stabilized soils, and 35% to 48% for lime-stabilized soils. Although all of the CSMs lost strength after F-T cycling, they are still much stronger than the native soils without stabilization, which is also reported by many researchers (Bin-Shafique et al. 2010; Rosa 2006; Parsons and Milburn 2002; Little 1996) and accepted by many agencies (PCA 1992; NLA 2001; ACAA 2011). Parsons and Milburn (2002) reported that the fly ash-stabilized clay had 170% and 370% the strength of the native soil and cement-stabilized soil had 230% to 570% strength of the native soils after 12 F-T cycles.

Cement improved the soil strength most effectively and cement-stabilized soil also possessed the highest residual UCS after F-T cycling. Lime-fly ash (Class F) was more effective in stabilizing the silt used in this study, in compared to Class C fly ash in terms of strength and residual strength. Dempsey and Thompson (1973) reported that the residual UCS were 0.06 MPa, 2.70 MPa, 2.00 MPa and 0.23 MPa after 10 F-T cycles for clay-cement, clay-lime, silt-cement and silt-lime specimens, respectively. Parsons and Milburn (2002) also reported similar performance that the cement treated soil has the strongest F-T durability, then fly ash and then lime-treated soil specimens through soil weight loss measurements and residual UCS. However, conclusions made in this study are

subject to change as the binder type, binder content, and soil type having significant impact on the results.

4.2. WET-DRY CYCLING EFFECT

Similar to F-T cycling, the durability of cementitiously stabilized materials under W-D cycling was systematically evaluated. W-D cycling is considered to be one of the most destructive actions to pavement structure (Wen et al. 2011). However, the effect of W-D cycling on the behavior of CSM received little attention. W-D durability of soils primarily depends on the pore structure and tensile strength of the material (Bhattacharja and Bhatty 2003). Other parameters, such as inter particle friction and cohesion may also influence the mechanical properties relative to W-D cycling. As water moves in and out of the pore network of the specimen during wetting and dying, the pore walls experience capillary pressure. ASTM D559 has been widely followed by many researchers to evaluate the W-D durability through weight change measurement (Bhattacharja and Bhatty 2003; Parsons and Milburn 2002). However, stiffness and strength are more representative than weight change data to study the W-D cycling effect (Khoury and Zaman 2005; Zaman et al. 1999). Instead of monitoring the weight change, constrained modulus after each W-D cycle and UCS after the W-D cycling were evaluated in this study. Ultrasonic wave testing is a relatively inexpensive, nondestructive and quick assessment of material properties (constrained modulus)

compared to the other laboratory mechanical testing methods (e.g., resilient modulus and triaxial compression test).

4.2.1. CONSTRAINED MODULUS CHANGE

4.2.1.1. GENERAL EFFECT OF WET-DRY CYCLING ON MODULUS

The results of W-D cycling are presented in Table 4.4 for cement-stabilized materials, Table 4.5 for fly ash-stabilized materials, and Table 4.6 for lime-stabilized materials. Furthermore, detailed results of the normalized constrained modulus changes along each W-D cycle are presented in Figure 4.12 for cement-stabilized materials, Figure 4.13 for fly ash-stabilized materials, and Figure 4.14 for lime-stabilized materials.

All of the cement mixtures completed 12 W-D cycles displayed strong W-D durability. Unlike F-T cycling, visual observation of specimens revealed no cracks and no significant soil particle loss among the cement-stabilized specimens during W-D cycling. The average reduction in constrained modulus was 36% for sand-cement which is the lowest, 49% for silt-cement, 62% for clay-cement, and 66% for gravel-cement specimens after W-D cycling.

The residual constrained modulus after W-D cycling for Class C fly ash-stabilized soils ranged from 1.9 GPa to 5.4 GPa. The constrained modulus reduction in the Class C fly ash-stabilized soils ranged from 14% to 80%. Gravel-fly ash specimens had the lowest W-D durability due to the largest constrained

modulus reduction (65% in average) after 12 W-D cycles. Silt-fly ash had weak W-D durability which had the lowest average residual constrained modulus (2.5 GPa) after 7 W-D cycles.

Silt-lime-fly ash specimens and the clay-lime specimens showed strong W-D durability with completion of 12 and 10 W-D cycles, respectively. W-D cycling is not as detrimental as F-T cycling to these mixtures. The average residual constrained modulus were 3.0 GPa and 0.7 GPa after W-D cycling for silt-lime-fly ash and clay-lime specimens, respectively. The clay-lime specimens also lost some particles during W-D cycling as shown in Figure 4.11.

Few studies have applied seismic modulus on CSMs subjected to W-D cycling. However, some researchers (Khoury and Zaman 2005; Bin-Shafique et al. 2009; Bhattacharja and Bhatty 2003) evaluated the W-D cycling through alternate methods, e.g. weight loss measurement, resilient modulus change, and UCS changes. Zaman et al. (1999) reported reductions in resilient modulus for various W-D cycles for stabilized aggregate. The UCS changes of fly ash-stabilized fine-grained soil during W-D cycling were also documented by Bin-Shafique et al. (2009). Bhattacharja and Bhatty (2003) found that the cement-stabilized soil had less weight loss than lime-stabilized soil, and higher binder content resulted in less weight loss.

4.2.1.2. EFFECT OF FIRST WET-DRY CYCLE ON MODULUS

Most of the constrained modulus reduction happened during the first W-D cycle as shown in Figure 4.12, Figure 4.13, and Figure 4.14. The constrained modulus reduced significantly after one W-D cycle and then leveled off for the remaining W-D cycles with large fluctuations. Constrained modulus reductions after the first W-D cycle are presented in Figure 4.15 (a). The constrained modulus reduction after the first W-D cycle ranged from 17% to 58%. The clay-lime and the gravel-cement (3%) specimens have the largest reduction, i.e., on average 58%, after the first W-D cycle. The gravel-fly ash and the sand-fly ash specimens had the minimum reductions among all the mixtures, i.e., 10% and 17%, respectively.

The ratio of first W-D cycle reduction to the total reduction in constrained modulus after W-D cycling is shown in Figure 4.15 (b). The trend is different than the first W-D cycle reduction in constrained modulus as shown in Figure 4.15 (a). The ratio are larger than 70% except sand-fly ash (37%) and gravel-fly ash (44%), which illustrates that the first W-D cycle is very critical to CSMs. Mixtures (e.g., silt-fly ash, sand-cement, silt-lime-fly ash, and gravel-cement) with ratio larger than 100% prove that specimens become stiffer after the first W-D cycle. For example, silt-fly ash specimens had 23% total reduction after 7 W-D cycles and 42% after first W-D cycle, which means 19% stiffness was gained during 2^{nd} to 7^{th} W-D cycles. These results demonstrate that these CSMs had continuing cementation in cement mixtures and pozzolanic reactions in fly ash or lime mixtures, which are known to be long-term reaction and last for years (Bin-Shafique et al. 2010; Little 1996; Khoury and Zaman 2002). Additionally, high

temperature (drying phase) and external moisture (wetting phase) during W-D cycling provide the essential conditions for cementation/pozzolanic reaction. Khoury and Zaman (2002) also found that the mean resilient modulus of 3-day-cured and 28-day-cured stabilized aggregate specimens increased as W-D cycles increased and the increase was especially prevalent at lower W-D cycles.

4.2.1.3. EFFECT OF BINDER TYPE ON MODULUS

The initial constrained modulus of gravel-cement is 2.8 times than that of gravel fly ash; however, the ratio reduced to 1.2 after W-D cycling. Gravel-fly ash behaved predominately better than gravel-cement during W-D cycling with much less constrained modulus reduction as shown in Figure 4.16 (a). W-D cycling is not as detrimental as F-T cycling to stabilized-gravel mixtures based on the residual constrained modulus and visual observation. Strong W-D durability is also found in the stabilized sand as presented in Figure 4.16 (b). The average normalized residual constrained modulus are 69% and 55% for the sand-cement and the sand-fly ash specimens, respectively. Besides, the sand-cement specimens were much stiffer than sand-fly ash specimens with higher initial and residual constrained modulus.

Similar to F-T cycling, the silt-fly ash specimens were the weakest during the W-D cycling which only withstood 7 W-D cycles and had the lowest residual constrained modulus as shown in Figure 4.17 (a). The strongest W-D durability

was found in the cement-stabilized silt. The combination of silt with cement or lime-fly ash significantly improved the stiffness and W-D durability but not with Class C fly ash. The cement-stabilized clay also had stronger W-D durability than clay-lime as shown in Figure 4.17 (b).

Based on the results, cement-stabilized soils are the most durable to W-D cycling except on gravel of which fly ash is more effective to improve the W-D durability. The finding is consistent with the research by Bhattacharja and Bhatty (2003) and Parsons and Milburn (2002). Unlike F-T cycling, W-D is less detrimental and most of the stiffness reduction happens during the first W-D cycle. However, the conclusion is subject to change since only one single binder content was evaluated in this study. Binder content was reported to have strong impact on the W-D durability (Khoury and Zaman, 2002, 2007; Bhattacharja and Bhatty 2003), which is discussed in next section.

4.2.1.4. EFFECT OF BINDER CONTENT ON MODULUS

Two binder contents were used to stabilize sand and gravel. The W-D cycling results on gravel-cement and sand-cement specimens are presented in Figure 4.12 (a) & (c). As discussed in last section, both of the mixtures exhibited strong W-D durability without any significant degradation after 12 W-D cycling.

Cement content has a strong impact on the W-D durability: 4% cement-stabilized gravel had less constrained modulus reduction during the W-D cycling

than 3% cement-stabilized gravel (see Figure 4.12 (a)). The average residual constrained modulus after twelve W-D cycles were 9.5 GPa and 21.5 GPa for 3% and the 4% cement-stabilized gravel specimens, respectively. An additional percentage of cement in gravel produced much higher stiffness and W-D and F-T durability. Similar findings were found in sand-cement mixtures too. The cement-stabilized sand with 6% and 8% cement had almost the same constrained modulus reduction after the first W-D cycle. However, the average normalized constrained modulus was higher for the 8% cement-stabilized sand.

Generally, the W-D durability increased with the increasing amount of the cement content in both sand and gravel. The results conformed to the findings of various agencies and researchers (PCA 1992), which found that higher strength (higher binder content) result in stronger durability; Bhattacharja and Bhatty (2003) and Zhang et al. (2008) found that soil stabilized with higher cement content have less weight loss during W-D cycling. Bin-Shafique et al. (2009) reported that higher fly ash content in fine-grained soils had higher initial and residual UCS after W-D cycling.

(With the limitation of this study, the binder content effect of fly ash and lime on the durability performance will not be discussed.)

4.2.2. UNCONFINED COMPRESSION STRENGTH (UCS) CHANGE

4.2.2.1. GENERAL EFFECT OF WET-DRY CYCLING ON UCS

After W-D cycling, all of the specimens were subjected to the UCS test following corresponding ASTM standards. The initial and residual UCS are presented in Table 4.4 for the cement-stabilized mixtures, in Table 4.5 for the fly ash-stabilized mixtures, and in Table 4.6 for the lime-stabilized mixtures.

In this study and at the binder content evaluated, cement is the most effective binder in enhancing the W-D durability in most cases. The cement-stabilized soils had the highest initial and residual UCS except in comparison to gravel-fly ash specimens. Generally, W-D cycling is not detrimental as F-T cycling to CSM since the residual UCS after W-D cycling are higher for some mixtures. The residual UCS of the cement-stabilized soils ranged from 3.6 MPa to 8.7 MPa. Except for sand-cement specimens, the average residual UCS of cement-stabilized specimens were higher than their initial UCS. Higher UCS after the W-D cycling was also observed on silt-fly ash, gravel-fly ash and clay-lime specimens (normalized residual UCS are larger than 100%). The exact reasons for the strength enhancement were not investigated. However, normalized residual UCS larger than 100% indicates that there were cementitious/pozzolanic reactions during W-D cycling. W-D cycling takes at least 24 days to complete with high temperature (drying phase) and external moisture (wetting phase), which apparently provide the essential conditions for cementation/pozzolanic reaction. The W-D cycling degraded the strength of sand-cement and sand-fly ash significantly with reduction in normalized residual UCS of 35% to 59%.

Strength enhancement during W-D cycling also documented by some studies: Khoury and Zaman (2005) reported that the UCS increase as the number of W-D cycles increased up to 30 cycles for Class C fly ash-stabilized aggregates. The strength of fly ash-stabilized fine-grained soil increased after W-D cycling due to long-term cement hydration (Bin-Shafique et al. 2009).

4.3. VACUUM SATURATION TEST RESULTS

Vacuum saturation testing is accepted as a rapid assessment of moisture susceptibility of soils by some researchers (Dempsey and Thompson 1973; Bhattacharja and Bhatty 2003; Gurhrie et al. 2008). Good correlation between the residual UCS after vacuum saturation and F-T cycling was documented by these researchers. Vacuum saturation is considered to be a severe test, which will reduce the strength of specimens with rapid air removal and water infiltration (Bhattacharja and Bhatty 2003). Bin-Shafique et al. (2009) found that the strength of fly ash-stabilized soils is a function of moisture content, and the strength decreases with increasing moisture content (similar to natural soil). Additionally, the high vacuum pressure induces more water to be retained in the specimen, which will generate positive pore water pressure when subjected to compression, thus resulting in lower strength.

4.3.1. MOISTURE CONTENT CHANGE

Moisture content change during vacuum saturation was investigated in this study. The moisture content of specimens is expected to increase during the vacuum saturation. The high-vacuum pressure (75.8 kPa) forces more water into the specimens with corresponding increase in moisture content. Dempsey and Thompson (1973) found the vacuum saturation procedure used in this study can fully saturate specimens. The physical properties of specimens (e.g. initial void ratio, initial dry unit weight and moisture content) before and after vacuum saturation are presented in

Table 4.7. For example, the void ratio of stabilized gravel specimens ranged from 0.20 to 0.23. The average increase in moisture content was 2.2% and 1.6% after vacuum saturation for gravel-cement and gravel-fly ash, respectively.

Good correlation exists between void ratio or dry unit weight and the moisture content after the vacuum saturation. Linear relationships are found between them with a coefficient of determination (R^2) of 0.94 as presented in Figure 4.18. The 100% and 80% saturation lines which is calculated from the dry unit weight and void ratio are also plotted (Figure 4.18). The linear relationship between dry unit weight and moisture content has potential use in estimation of the degree of saturation. The degree of saturation is slightly higher than 100%, which may result from the extra water retained on surface of the specimens or inaccuracies of dimension measurement. Nonetheless, the relationship presented

in Figure 4.18 demonstrates that the vacuum saturation procedure used in this study can fully saturate specimens.

4.3.2. UNCONFINED COMPRESSION STRENGTH RESULTS

As discussed above, vacuum saturation testing increases the moisture content significantly and even can fully saturate the specimens. The UCS of the specimens before and after vacuum saturation were evaluated in triplicates, representing unsaturated and saturated conditions. Standard UCS (Appendix B by Casmer 2011) calls for a 4-hours soaking period prior to UCS testing except for clay-lime specimens. Unsaturated UCS and saturated UCS are obtained before (end of curing) and after vacuum saturation. The saturated UCS, unsaturated UCS, and standard UCS are used for the interpretation of the vacuum saturation results.

Table 4.7 summarizes the binder content, test moisture content, and dry unit weight of the specimens. Table 4.8 presents the average UCS (e.g., standard UCS, unsaturated UCS, and UCS after F-T cycling) and the normalized UCS which is normalized by standard UCS for the CSMs. The specimens were fabricated at identical composition and moisture contents for the UCS test. The moisture content was calculated from weight measurements.

The average UCS are 4.40 MPa, 4.40 MPa and 5.25 MPa for vacuum saturated, standard and unsaturated gravel-cement specimens. Unsaturated

specimens had the lowest moisture content and highest UCS. Compared to the normalized UCS of unsaturated gravel-cement specimens (119%), the vacuum saturation can reduce the average UCS to 100% with 0.85 MPa reduction, whereas the F-T cycling reduce the average UCS to 69% with 2.20 MPa reduction. The results are comparable to Dempsey and Thompson (1973) and Guthrie et al. (2008). Gravel (A-1-a) was investigated by Dempsey and Thompson (1973) for vacuum saturation. 4% cement-stabilized gravel had 19% reduction with 1.10 MPa drop on UCS. Guthrie et al. (2008) also conducted vacuum saturation on cement-stabilized aggregate and found cement-stabilized aggregate had average 21% reduction with 0.53 MPa drop on UCS after vacuum saturation.

Based on the test results, the cement-stabilized gravel and silt had less strength reduction (2% to 16%) after vacuum saturation. Fly ash and lime mixtures were more vulnerable to vacuum saturation, with strength reduction ranging from 24% to 56%. Weaker strength of the lime mixtures after vacuum saturation was also found by Dempsey and Thompson (1973). Lime mixtures had lower residual strength than lime-fly ash and cement mixtures. Figure 4.19 presents the relationship between the unsaturated UCS versus saturated UCS (after vacuum saturation). All of the data point fall below the 1:1 ratio line, which means the average unsaturated UCS is larger than the vacuum saturated UCS. This phenomenon can be attributed to higher moisture content in vacuum saturated specimen (100% saturated), which reduces the strength. The conclusion is consistent with Bin-Shafique et al. (2009)’s research on the moisture content effect on the compacted soil specimens.

4.3.3. CORRELATION WITH FREEZE-THAW CYCLING

One of the objectives of this study was to determine if correlations exist between the residual strengths after F-T cycling and vacuum saturation test. Strong correlation between UCS after F-T cycling and UCS after vacuum saturation was documented by Dempsey and Thompson (1973) and Guthrie et al. (2008). Dempsey and Thompson (1973) found that good correlation (R^2 value as high as 0.98) exists between the strength after vacuum saturation and the strength after 5 and 10 F-T cycles. The coefficient of determination (R^2 value) of the same correlation in Guthrie et al. (2008) was found to be 0.70.

Repetitive F-T cycling degrades the strength of soils through generating cracks with ice lens melting and inducing more water into the voids (Rosa 2006), whereas vacuum saturation breaks the pore structure and force more water retained in the soils (Bhattacharja and Bhatty 2003). Figure 4.20 presents a plot of the average UCS after F-T cycling versus UCS after vacuum saturation. The F-T cycling was more detrimental to the CSMs than vacuum saturation as shown in Figure 4.20. The coefficient of determination (R^2 value) associated with this correlation is 0.60. The relative low R^2 in this study may be due to the differences in testing procedure. Different mixtures completed different number of F-T cycles, such as 12 F-T cycles for sand-cement mixtures and 2 F-T cycles for gravel-cement. This variation result in variability when results are analyzed together. Additionally, procedure employed by Guthrie et al. (2008) in which constant strain rate of compression and a 4-hours soaking period was included for all UCS test.

Nonetheless, the vacuum saturation test can still serve as a fast way to predict the F-T durability of CSMs through strength degradation, when the complete F-T cycling test is not available.

SECTION 5 DURABILITY PERFORMANCE MODEL

5.1. FREEZE-THAW CYCLING MODEL

The overall objective of this study is to develop methods to identify property changes of cementitiously stabilized layers (CSL), undergoing exposure to weathering, such as F-T and W-D cycling. To this extent, validating and developing durability performance models is required. The performance of cementitiously stabilized materials (CSM) during F-T and W-D cycling and vacuum saturation are discussed in Chapter 4. In general, F-T cycling is much more detrimental than W-D cycling to CSM. Pavement subgrade or base layers constructed with CSM can cause significant distress when subject to F-T and W-D cycling. The deficiency can shorten the service life of the pavement, resulting in economic loss. A distress model accounting for the effect of F-T cycling on modulus degradation of CSM will assist developing conservative, reasonable and safe design in MEPDG. F-T durability performance model is preferred discussed in this section.

The modulus distress model due to F-T cycling can be considered to be similar to that of concrete F-T cycling distress model as modified by Wen et al. (2010):

$$E(N) = E_0 e^{\frac{k_1 T (\frac{\Delta L}{L})^2 N}{3}} \quad (5.1)$$

where E(N) = modulus after N cycles of F-T,

E_0 = modulus before F-T cycling,

k_1 = regression constant,

T = duration of one F-T cycle,

ΔL = original length of specimen,

L = increase of specimen length after freezing,

N = number of F-T cycles.

Due to weaker bond strength in stabilized soil specimens compared to concrete specimens, the stabilized soil specimens start to lose particles during F-T cycling makes the dimension measurement unreliable during F-T cycling. On the other hand, the constrained modulus (D) along each F-T cycling is available for model development. The basic F-T durability model involving degradation in D for CSM is proposed as follows:

$$\frac{D(N)}{D_0} \times 100\% = e^{-k \cdot N} \quad (5.2)$$

where D(N)= constrained modulus after N F-T cycles,

D_0 = constrained modulus before F-T cycling,

k = regression constant,

N = number of F-T cycles.

The unknown regression constant k is determined by change in D using least squares optimization.

There is wide diversity in characterizing F-T durability of CSMs: such as first or total F-T cycle reduction and number of F-T cycles the specimens is able to withstand. The regression constant k can be used as a quantitative index of F-T durability, i.e., larger k means greater rate of reduction in D during F-T cycling, and thus low F-T durability.

5.1.1. MODEL EVALUATION

Gravel-cement, sand-fly ash, and silt-lime-fly ash were used as examples to illustrate how the exponential decay model fit the F-T cycling results as shown in Figure 5.1 to Figure 5.3. The properties of each mixture (e.g., void ratio, dry unit weight and initial UCS, regression constant k, and R^2 for each specimen) are presented in Table 5.1. The F-T durability is affected by many factors, such as the material properties, binders, environment conditions, and source of water. The exponential decay model does not fit perfectly with the experimental results in some cases, such as the results of sand-fly ash, clay-cement, and sand-cement mixtures. However, the laboratory F-T cycling includes the water absorbing pad beneath the specimens (external source of water), which is more intensive than field condition. Thus, the model overall is conservative in representing the performance of CSM during F-T cycling.

The F-T cycling had a slight effect (<10%) on sand-cement mixtures and the constrained modulus has large scatters. The average k values are the lowest (0.004 and 0.009) for 3% and 4% cement-stabilized sand, which is consistent with our previous qualitative observation. Soils stabilized with less cement content are more frost susceptible (observation similar also for the gravel-cement mixtures). Gravel-cement (4%) had k value of 0.031 in comparison to 0.621 for gravel-cement (3%). An additional percentage of cement improved the F-T durability of gravel. For clay-cement mixtures, which had the highest cement content (12%), the constrained modulus reduced primarily after the first cycle and then leveled off.

The smaller the k value, the stronger the F-T durability of the mixture has. For fly ash-stabilized mixtures, the average k values are 0.074, 0.229 and 0.528 for sand-fly ash, gravel-fly ash, and silt–fly ash specimens. The results also confirm that fly ash is more effective in improving the F-T durability of sand and gravel but not for silt. Silt-lime–fly ash has smaller average k of 0.478 than silt-fly ash mixtures. Clay-lime specimens are the most frost susceptible mixtures, with the largest average k value of 0.850.

5.1.1. EFFECT OF STIFFNESS/STRENGTH ON k

The k value can be considered as the F-T durability index of CSMs. Previous research reported that the F-T durability can be associated with dry unit weight or void ratio (Dempsey and Thompson 1973) and initial UCS (PCA 1992). The relationship between the durability and initial UCS was used for a short-cut mix design for soil-cement mixtures (PCA 1992). It is considered that stiffness or strength of the CSM have a great impact on the F-T durability. PCA's guideline on durability of soil-cement mix design is based on the initial UCS; i.e., 87% of the cement-stabilized specimens complete the durability test with 7-day UCS value of 4.14 MPa and 97% for 7-day UCS value of 5.17 MPa (PCA, 1992).

Figure 5.4 show the relationship between k and initial D of CSM. Generally, specimens with higher initial D have smaller k with the exception of clay-cement and gravel-cement mixtures. The initial UCS effect on k value was also

investigated in this study as shown in Figure 5.5. The results follow the same trend as the trend between initial D with k. Generally, higher initial UCS had lower k (strong F-T durability) with a few exceptions. The mixtures below the line of k=0.100 or to the right of the line UCS=4.60 MPa, finished the targeted 12 F-T cycles and show very high F-T durability.

The frost susceptibility of subgrade soil can be estimated by two hydraulic properties: capillarity and permeability as shown in Figure 4.8 (ACPA's EB204P). A similar attempt is made to define the frost susceptibility or F-T durability of CSM based on initial UCS, k and the number of F-T cycles to stop (N_F). The F-T susceptibility was divided into four categories: negligible, low, moderate, and High. Negligible F-T susceptibility is assigned to the mixtures with k≤0.100, UCS≥4.60 MPa and $N_{F=}$12. Mixtures with k≤0.100, UCS<4.60 MPa and N_F=12 are designated as low F-T susceptibility. High F-T susceptibility was the mixtures/soils that do not resist more than 2 F-T cycles (N_F≤2) and with very low UCS (UCS<1.5 MPa) and high k value (k>0.1). The rest of the mixtures were classified as moderate F-T susceptibility (k>0.1 and UCS ≥1.5 MPa).

There is a wide diversity in the methods assessing frost susceptibility for subgrade soils; almost all of the methods are unique for individual state, provincial, and federal agencies. Based on the laboratory testing procedure used in this study, a criterion is proposed for characterizing the F-T susceptibility of CSM. However, it is based on the specific procedure used in this study, thus it needs to be further verified and subject to change as more tests completed. Furthermore,

the study was limited to single combination (e.g., single binder content for most of the mixtures and single soil type). Further investigation on the F-T susceptibility of CSMs should be conducted to verify and improve the proposed F-T model and criterion for determination of F-T susceptibility.

5.1.2. FUTURE USE Of k

The effect of moisture (W-D cycling) or temperature (F-T cycling) on layer stiffness is not considered in rigid nor flexible design in MEPDG analysis. The MEPDG disregards the long-term degradation of the modulus of elasticity of a CSM layer. This is one of the significant drawbacks in characterizing CSM. The MEPDG software simulates temperature and moisture profiles in the pavement structure and subgrade over the design life of a pavement using the Enhanced Integrated Climatic Model (EICM). To address the degradation due to F-T cycling of CSL, the temperature and moisture distribution in the CSL need to be developed. Another major issue is the implementation of the degradation due to durability of stiffness model into MEPDG software. Combined with development of the EICM for CSL, the modulus distress model proposed in this study need to be incorporated into MEPDG. Furthermore, k can used to as an index to classified the F-T susceptibility of CSM and more tests should performed on the specimens with various combination and composition conducted following this specific procedure.

5.2. WET-DRY CYCLING MODELING

Distresses due to durability are not predicted within the framework of MEPDG for CSM. However, W-D durability for CSMs are of significant importance for predicting material deterioration during W-D cycling, which are reported to be significant in some cases (Section 4.2). The stiffness reduction mostly happen at the first W-D cycles, and the stiffness tend to be constant or have increasing trend (cementation/pozzolanic reaction) after the first W-D cycle. Thus, a reduction factor (f_R) needs to be applied to the stiffness change during W-D cycling to ensure a reliable and safe design of the pavement structure.

The basic W-D durability model involving the consideration of a reduction in D for CSM subjected to W-D cycling is proposed as follows:

$$D(N) = (1 - f_R) \cdot D_0 \quad (5.3)$$

where D(N)= constrained modulus after N W-D cycles,

D_0 = constrained modulus before W-D cycling,

f_R= reduction factor

f_R equals to the larger value between first W-D cycle reduction and total reduction in normalized constrained modulus.

5.2.1. MODEL EVALUATION

Average normalized constrained modulus after first W-D cycle, normalized residual constrained modulus, and reduction factor for the CSMs were plotted in

Figure 5.6. Generally, f_R for stabilized fine-grained soils (silt and clay) are larger than that for stabilized coarse-grained soils (sand and gravel) except for gravel-cement (3%). Larger f_R means more reduction in D when the specimens subject to W-D cycling. f_R range from 0.31 to 0.66, 0.22 to 0.45, and 0.45 to 0.70 for cement-stabilized, fly ash-stabilized, and lime-stabilized soils, respectively.

5.2.2. EFFECT OF VOID RATIO ON f_R

Section 5.1.1 presents the trend that F-T durability increases as the initial UCS increase. F-T and W-D durability particularly relied on the pore structure and tensile strength between the soil particles (Bhattacharja and Bhatty 2003), which believed to correlate closely to UCS as well. However, this trend was not found in W-D cycling test. An example is that the sand-cement (8%) has a larger f_R than sand-cement (6%), whereas the UCS is much higher.

Figure 5.7 presents the correlation between f_R and average void ratio for CSM. Generally, f_R increases with the increase in void ratio for CSMs, which is conformed to the previous observation: the stabilized-fine grained soils had lower f_R. A good linear relationship (R^2=0.72) were also observed on this relationship if not considering gravel-cement (3%). Not enough cement content in gravel-cement (3%) generates the network inside the mixture, which leads to weak W-D durability.

5.2.3. FUTURE USE Of f_R

The long-term degradation of stiffness for CSMs due to weathering is not addressed in MEPDG, which is one of the drawbacks in characterizing CSM. The stiffness degradation model due to F-T cycling is proposed and recommended to implement into MEPDG with EICM. The proposed f_R based on the laboratory testing results is also expected to useful to account for the degradation in stiffness for CSM due to W-D cycling. Similar to F-T cycling, the distress model due to W-D cycling for CSM can be used to modify the input properties of CSM.

SECTION 6 CHARACTERISTICS OF ULTRASONIC WAVE ON CEMENTITIOUSLY STABILIZED MATERIALS

6.1. P-WAVE VELOCITY AND CONSTRAINED MODULUS FOR MONITORING CURING PROCESS

One of the main objectives of using cementitiously stabilized layers is meeting the minimum specified structural quality of the subgrade soil or base aggregate for pavement design. Cementitious stabilization improves the engineering properties (e.g., strength, stiffness, durability, etc.) of pavement subgrade soil or base aggregate through chemical reactions, which are known as hydration and pozzolanic reactions (Mohammad et al. 2007; Thompson 1969; Edil et al. 2006; Khoury and Zaman 2005). Generally, the strength or stiffness of the CSM increases with curing time. Researchers are beginning to use seismic modulus test methods to monitor the maturity of CSM in a non-destructive manner (Pucci 2010 and Yesiller et al. 2001). Since the ultrasonic pulse velocity test is a non-destructive testing method, the measurement of variation of P-wave velocity (V_P) with curing time for CSMs is possible. In this study, cement-stabilized soils were cured in the moist room (100% relative humidity, 21°C) for 28 days, while P-wave velocity measurements were taken at the 1st, 7th, and 28th day of curing. Fly ash- and lime-stabilized soils were cured for 7 days in an oven set to 40°C (104 °F), and P-wave velocity measurements taken after the 1st , 3rd or 4th, and 7th day of curing.

The results for cement-stabilized soils and for fly ash- and lime-stabilized soils are presented in Figure 6.1 and Figure 6.2, respectively. The P-wave velocity or constrained modulus of the CSM mixtures with exception of silt-fly ash increased with curing time. As curing time increases, the mixtures become stiffer through long-term cementitious hydration or pozzolanic reactions, which are reflected in the enhancement of P-wave velocity and thus constrained modulus. The increase in P-wave velocity and constrained modulus from the 1^{st} to 7^{th} curing days was more pronounced than the increase from the 7^{th} to 28^{th} curing days for cement-stabilized soils. Sand-fly ash, gravel-fly ash, silt-lime-fly ash, and clay-lime had large increases in the P-wave velocity and constrained modulus from the 1st to 7th day of curing. A similar trend was observed by Yesiller et al. (2001) for cement- and lime-stabilized soils. Direct comparison of P-wave velocity and constrained modulus between cement and fly ash or lime mixtures was made after 7 days curing (See Figure 6.3): during the first 7 days of curing, the cement-stabilized soils were found to have a larger increase in velocity and constrained modulus than fly ash- or lime-stabilized soils indicating a greater increase in stiffness in general except on sand-cement and sand-fly ash. The little change of P-wave velocity and constrained modulus of silt-fly ash indicate that the fly ash used in this study might not be appropriate to stabilize the silt as different fly ash type reacts distinctly (Edil et al. 2006; Rosa 2006). Besides the slower stiffness/strength gain in clay-lime and silt-fly ash may due to the slow pozzolanic reaction in lime stabilization (Little 1996; Thompson 1969) and fly ash stabilization (Khoury and Zaman 2002).

6.2. EFFECT OF MOISTURE CONTENT

P-wave velocities through the CSMs were evaluated on saturated and unsaturated specimens to understand the effect of the degree of saturation (S_r) on P-wave velocity and are plotted in Figure 6.4. The moisture content corresponding to 100% and 80% degrees of saturation was calculated from void ratio and dry unit weight as reference lines. The trend lines in Figure 6.4 were fitted using squares optimization scheme. The specimens are assumed to be 100% saturated after the vacuum saturation.

Unsaturated specimens with higher P-wave velocity had a much smaller increase in P-wave velocity after saturation (see Figure 6.6). The P-wave velocities of saturated specimens (after vacuum saturation) are generally higher than those of the unsaturated specimens (before vacuum saturation or at the end of curing) as shown in Figure 6.6. The unsaturated specimens with P-wave velocity higher than 2000 m/s had less than 10% increase after saturation. This saturation effect on the P-wave velocity tends to be larger for soft CSM specimens with low P-wave velocity.

Clay-lime (unsaturated V_P <1600 m/s) and silt-lime-fly ash (unsaturated V_P>1600 m/s) specimens were investigated at different S_r corresponding to three different moisture contents: end of curing, 4-hours soaking, and vacuum saturation. Clay-lime specimens were more sensitive to S_r indicated by the P-wave velocity jump from around 1200 m/s to 1600 m/s when saturated which also demonstrated that the P-wave velocity of water is 1600 m/s, whereas the silt-lime-

fly ash had slightly increase in P-wave velocity as the degree of saturation varied (Figure 6.7).

Compression waves propagate through soil, which are three-phase materials consists of solid particles and voids filled with water and/or air. In several studies (Richart et al. 1970; Fratta et al. 2005), the P-wave velocity is defined as

$$V_p = \sqrt{\frac{B_{soil} + \frac{4}{3} G_{soil}}{\rho_{soil}}}$$

where B_{soil} is the soil bulk modulus, G_{soil} is the soil shear modulus, and ρ_{soil} is the bulk density. B_{soil} is a function of B_f (fluid stiffness), B_g (the stiffness of the soil mineral grains), G_{soil}, and porosity. Differences in S_r have no effect on B_g in the vacuum saturation procedure, whereas ρ_{soil}, B_f, and G_{soil} are affected by S_r. The variation of these parameters with degree of saturation is shown in Figure 6.8. As the S_r increases, the B_f and ρ_{soil} increases but the G_{soil} decreases (Fratta et al. 2005; Stokoe and Santamarina 2000), as seen in Figure 6.8 (a) & (b). These three competing variables control the P-wave velocity through CSM. The stiffening effect of the fluid (Figure 6.8(a)) on the soil modulus results in a sharp increase of P-wave velocity when the specimen is saturated (Figure 6.8 (c)). This effect is pronounced in materials with low velocity (e.g., natural soil) (see Figure 6.6). Cementation enhances G_{soil} significantly by increasing the contact area of granular soil particles (Fernandez and Santamarina 2001). The effects of

cementation and degree of saturation on P-wave velocity is illustrated in Figure 6.9.

A straightforward and simple explanation of the phenomenon is the “fastest path theory”, which states that in porous material, the constrained compression wave propagation occurs along the fastest path (Pucci 2010). As sketched in Figure 6.9, the “fastest path” is depicted through the soil particles in an unsaturated condition and through the water in a saturated condition, which is the case for specimens made from material with low P-wave velocity (e.g., clay-lime mixtures and naturally compacted silt, etc.). However, the fastest path will include more of the solid particles and less fluid in the matrix within specimens with larger P-wave velocity (specimens with cementation stiffening effect, e.g. CSMs). Thus, the stiffening effect due to saturation is less pronounced in specimens with larger P-wave velocity (e.g., silt-lime-fly ash and gravel-cement mixtures).

6.3. COMPACTION CHARACTERISTICS AND P-WAVE VELOCITY

CSM specimens were compacted at various moisture contents to investigate the relationship between the P-wave velocity and the dry density and compaction moisture content. P-wave velocity measurements were taken for each compacted test specimen in addition to the measurements of the mass, volume, and moisture content. An UCS test was performed on the specimen at the end of curing to investigate the effect of dry density on strength. Silt-lime-fly ash, silt-

cement, clay-cement, clay-lime sand-cement, sand-fly ash, and gravel-fly ash mixtures were fabricated at four or five different moisture contents or dry densities for this study.

The bell-shaped compaction curve of silt-lime-fly ash, silt-cement, clay-cement, and clay-lime indicate that the compacted dry density is highly sensitive to compaction moisture content (see Figure 6.10 (a) to Figure 6.13 (a)). P-wave velocity measurements were taken for each of the specimens compacted to different moisture contents. Similar trends were observed with the P-wave velocity and the compaction moisture content for each of the mixtures. For silt-lime-fly ash and silt-cement mixtures, the P-wave velocity increased with increasing compaction moisture content up to the optimum dry density and corresponding optimum moisture content then decreased after the optimum, while the compaction moisture content continued to increase. The P-wave velocity of clay-lime and clay-cement also decreased as the compaction moisture content increased (above optimum moisture content). For sand-cement, sand-fly ash, and gravel-fly ash mixtures, the dry density and P-wave velocity were insensitive to compaction moisture content (see Figure 6.14 (a), Figure 6.15 (a) and Figure 6.16 (a)). Similar trends were observed by Nazarrian et al. (2005), where numerous natural clay, sand, and granular base materials were tested at various compaction moisture contents. For clay, there was a peak in P-wave velocity coinciding with the optimum moisture content, whereas for sand and granular base materials, this trend was not present. The trend between UCS versus dry density was the same as the trend of the P-wave velocity versus dry density. Specimens with higher P-

wave velocity possessed higher strength (i.e., UCS) for each CSM mixture. In silt and clay mixtures, the specimens with highest density had the highest UCS and P-wave velocity; while for gravel and sand mixtures, the specimens with lower dry density had relative higher UCS and P-wave velocity. This relationship between strength and P-wave velocity is detailed in the follow section.

Density and moisture content measurements are essential for the Quality Control/Quality Assurance (QC/QA) in pavement systems. The empirical relationships developed in the laboratory between P-wave velocity, UCS, and dry density for CSMs provides insights for use of this non-destructive method in QC/QA. However, to close the gap between the field application of seismic testing on QC/QA and laboratory testing results, more design parameters and constitutive relationships require further development.

6.4. CORRELATION BETWEEN UNCONFINED COMPRESSION STRENGTH (UCS) AND CONSTRAINED MODULUS

The ultrasonic pulse velocity technique is popular as a non-destructive technique to assess the properties of concrete. Although concrete quality is generally assessed by measuring the UCS, there is also a good correlation between UCS and pulse velocity in concrete (Trtnik et al. 2007). Correlations between strength and P-wave velocity of concrete have been proposed and

numerous data sets presented. The most popular formula is from Popovics et al. (2007)

$$UCS = a \cdot e^{b \cdot V_p} \quad (1)$$

where a and b are empirical fitting parameters, and V_p is the P-wave velocity of the concrete specimens.

In this study, the P-wave velocity was observed to have a strong relationship with the UCS of CSM. For CSM, a strong correlation is anticipated between the square root of constrained modulus and UCS. A model that accounts for the density of CSM is proposed as:

$$UCS = a \cdot e^{b \cdot \sqrt{D}} \quad (2)$$

where a and b are empirical fitting parameters, and D is the constrained modulus.

6.4.1. EXPERIMENTAL RESULTS

The UCS and P-wave velocity were obtained from the same specimens that were tested with vacuum saturation (Section 4.3). The P-wave velocity was determined prior to UCS testing with 4-hours soaking period. The relationship between P-wave velocity and UCS of the CSMs tested is presented in Figure 6.17 (a). For each mixture, three or more replicate tests were conducted for comparison of P-wave velocity and saturated UCS. The strength of CSMs increased with increasing P-wave velocity (see Figure 6.17). These findings

demonstrate the feasibility of using Eq.#1 for estimating strength of CSMs from P-wave velocity:

$$UCS = 0.42e^{0.001V_P} \quad (3)$$

In porous materials, wave propagation occurs along the fastest path in the material, which is typically correlates to and is used for predicting the stiffness of the material (Yesiller et al. 2001). Many factors, e.g., soil composition, binder type, binder content, density and moisture content etc., influence the stiffness of CSM. The effect of these factors on the strength and P-wave velocity may not be the same way or to the same extent although higher strengths are generally associated with higher velocities as shown in Eq.#3. Thus, the correlations were not very strong due to the lack of consideration of these additional factors. Eq.#2 accounts for the effects of density on the UCS of CSMs (D is calculated from V_P and density). A better correlation (R^2=0.87) was determined between UCS and constrained modulus as shown in Figure 6.17 (b). The relationship is given as

$$UCS = 0.30e^{0.56\sqrt{D}} \quad (4)$$

6.4.2. VERIFICATION WITH MEASURED UCS

Eq.#3 & #4 were developed to predict the UCS for the saturated specimens from the V_p and D, respectively. The strength of the model is presented by comparing predicted versus measured values for saturated UCS, as shown in Figure 6.18 (a) & (b): the predicted UCS was less proportional using V_p

than the prediction of UCS using D. Additionally, unsaturated UCS and P-wave velocity of six different mixtures of at least four various compaction moisture contents were measured in Section 6.3. The predicted UCS from Eq.#3 vs. unsaturated UCS is plotted in Figure 6.19. The unsaturated UCS tends to be higher than the predicted UCS since Eq.#3 is based on saturated UCS.

6.5. CORRELATION BETWEEN ELASTIC MODULUS AND P-WAVE VELOCITY OR CONSTRAINED MODULUS

The ultrasonic pulse velocity testing method represents the small-strain response of soil specimens non-destructive at relatively low cost and time. The correlation between P-wave velocity and constrained modulus to UCS is discussed in Section 4. The desire is to relate P-wave velocity or constrained modulus to performance indicators, which are preferably used in the mechanistic design, e.g., resilient modulus for subgrade/base materials in pavement construction. Many researchers have shown the feasibility of using seismic methods to characterize the mechanical properties of subgrade/base materials. The seismic modulus was found to be linearly correlated with resilient modulus of compacted soils by Hilbrich and Scullion (2007), Nazarian et al. (2005), Williams and Nazarian (2007) and Schuettpelz et al. (2010). The elastic modulus is one of the primary parameters of CSMs used in pavement design procedures (e.g., AASHTO 2002 Design Guide). Yesiller et al. (2001) reported that P-wave velocity was linearly correlated with Young’s modulus for CSM.

The Young's modulus is the primary design parameter of CSMs in many existing mechanistic pavement design procedures and in the AASHTO 2002 Design Guide. In this study, relationships between the small strain parameters, V_P and D to elastic modulus, i.e., initial tangent modulus, E_0, and secant modulus, E_{50} at 50% of strength were evaluated. E_0 and E_{50} were obtained from a typical stress-strain curve from a UCS test (Figure 6.20). Figure 6.21(a) & (b) presents V_P vs. E_0 and V_P vs. $E_{50,}$ respectively. Two reasonably good relationships between the three parameters are obtained. Figure 6.22 (a) & (b) present D vs. E_0 and D vs. E_{50}. A linear relationship between these parameters was observed. D correlated best with E_0, with R^2 0.71. Given the level of robustness of the measurements of elastic modulus from the UCS test, the correlation seems acceptable. As reflected in Figure 6.22 (a) & (b), E_0 and E_{50} are approximately eight times greater than D. The difference can be attributed to the strain level generated during the two tests. The elastic modulus from UCS testing is obtained from a much larger strain level than the seismic modulus test. However, the correlation has several advantages. The linear relationship between the seismic modulus and Young's modulus was obtained, which has potential for determination of the design modulus of CSM in pavement design. Therefore, use of this method can lead to less reliance on extensive laboratory mechanical tests. A material-specific relationship is desirable between the two moduli for practical use in pavement design procedure. Along with the correlation with UCS, seismic modulus is useful for developing trends in CSM for pavement design when specific laboratory data are not available.

SECTION 7 CONCLUSIONS

The objective of this research was to identify property changes of CSL that undergo exposure to weathering, and to propose stiffness degradation models for implementation into MEPDG. To reach this objective, nine CSMs, including gravel, sand, silt, and clay stabilized with cement, lime, and fly ash, were selected for laboratory durability tests. Ultrasonic pulse velocity testing was conducted to evaluate the effect of F-T cycling and W-D cycling on the stiffness of CSMs. UCS test was conducted at the end of the F-T and W-D cycling. Comparison between the residual UCS after F-T cycling with the UCS after vacuum saturation was investigated. Additionally, the characteristics of ultrasonic waves through CSMs were also evaluated in this study.

7.1. FREEZE-THAW CYCLING EFFECT

7.1.1. CONSTRAINED MODULUS CHANGE

The four cement-stabilized materials exhibited varying performance during F-T cycling: the drop in constrained modulus after F-T cycling ranged from 39% to 72%. The normalized residual constrained modulus of sand-cement was the highest (93%) among the cement-stabilized soils. For fly ash-stabilized soils, constrained modulus reductions ranged from 32% to 77%. Silt-fly ash specimens had essentially no resistance to F-T cycling and did not survive more than 4 F-T

cycles. Low resistance to F-T cycling was also observed for silt-lime-fly ash (Class F) and clay-lime specimens.

Reduction in normalized constrained modulus after the first F-T cycle indicates frost susceptibility of CSM. Some mixtures showed high resistance to degradation during the first F-T cycle (constrained modulus reduction<10%), including silt-lime-fly ash, sand-cement, gravel-cement, gravel-fly ash, and sand-fly ash. Mixtures with higher initial UCS had less reduction in constrained modulus after the first F-T cycle and less reduction after the F-T cycling as well.

Cement-stabilized soils were more durable to F-T cycling, with high residual constrained modulus than most other CSM. Class C fly ash used in this study was less effective than lime-fly ash (Class F) in improving the durability, strength, and stiffness of silt (ML). Binder content was proven to influence F-T durability significantly. Resistance against F-T cycling increases with increasing UCS/strength. The greater the cement content, the stronger the anticipated durability.

7.1.2. UNCONFINED COMPRESSIVE STRENGTH CHANGE DURING FREEZE-THAW CYCLING

All of the CSM showed reduction in UCS after F-T cycling. In general, residual UCS after F-T cycling ranged from 17% to 84% for cement-stabilized soils, 29% to 63% for Class C fly ash-stabilized soils, and 35% to 48% for lime-

stabilized soils. Cement improved the soil strength most effectively and also possessed the highest residual strength after F-T cycling. Lime-fly ash (Class F) is more appropriate to stabilize silt used in this study than Class C fly ash in terms of strength and residual strength. Except silt-fly ash, clay-lime specimens are the most frost susceptible mixtures which had the lowest average residual UCS 0.39 MPa.

7.2. WET-DRY CYCLING EFFECT

7.2.1. CONSTRAINED MODULUS CHANGE DURING WET-DRY CYCLING

The four cement mixtures all completed 12 W-D cycles displayed strong W-D durability. The average reduction in constrained modulus was 36% for sand-cement which is the lowest, 49% for silt-cement, 62% for clay-cement, and 66% for gravel-cement specimens after W-D cycling. The constrained modulus reduction in the Class C fly ash-stabilized soils ranged from 14% to 80%. Gravel-fly ash and silt-fly ash mixtures had very limited W-D durability due to the great constrained modulus reduction. Silt-lime-fly ash specimens and clay-lime specimens showed strong W-D durability with completion of 12 and 10 W-D cycles, respectively.

The constrained modulus reduced significantly after one W-D cycle and then leveled off for the remaining W-D cycles with large fluctuations. The constrained modulus reduction after the first W-D cycle ranged from 17% to 58%.

Some CSMs had continuing cementation in cement mixtures and pozzolanic reactions in fly ash or lime mixtures, reflected in the enhancement in constrained modulus after the first W-D cycles.

Cement-stabilized soils are the most W-D durable among all CSMs except for gravel, of which fly ash is more effective to improve the W-D durability. The combination between silt and cement or lime-fly ash significantly improved the stiffness and W-D durability but not with Class C fly ash.

7.2.2. UNCONFINED COMPRESSIVE STRENGTH CHANGE DURING WET-DRY CYCLING

Among the nine cementitiously stabilized mixtures, the cement-stabilized soils have the highest initial and residual UCS except in comparison to gravel-fly ash specimens. Generally, W-D cycling is not detrimental as F-T cycling to CSMs since the residual UCS after W-D cycling were higher. A complete W-D cycling test takes at least 24 days to finish with high temperature (drying phase) and external moisture (wetting phase), which apparently provide the essential conditions for cementation/pozzolanic reaction. The normalized residual UCS larger than 100% indicates that there were cementitious/pozzolanic reactions during the W-D cycling in some mixtures (e.g., gravel-cement, silt-cement, clay-lime, and silt-fly ash). However, The W-D cycling degraded the strength of sand-

cement and sand-fly ash significantly, with normalized residual UCS of 41% to 65%.

7.3. VACUUM SATURATION

The high vacuum pressure induces more water to be retained in the specimen, which will generate positive pore water pressure when subjected to compression, thus resulting in lower strength. Furthermore, vacuum saturation breaks the pore structure within the soils. Good correlation exists between void ratio or dry unit weight and the moisture content after the vacuum saturation, which proves that the vacuum saturation procedure used in this study can fully saturate the specimens.

Based on the test results, the cement-stabilized gravel and silt had less strength reduction (2% to 16%) after vacuum saturation. Fly ash and lime mixtures were more vulnerable to vacuum saturation, with strength reduction ranging from 24% to 56%. Unsaturated specimens had the lowest moisture content and highest UCS. Although, the correlation between residual UCS after F-T cycling versus UCS after vacuum saturation is not very strong, the vacuum saturation test can still serve as a fast way to predict F-T durability of CSMs when the complete F-T cycling test is not available.

7.4. DURABILITY PERFORMANCE MODEL

7.4.1. FREEZE-THAW CYCLING MODEL

An exponential modulus decay model due to F-T cycling was proposed. The regression constant, k, was used as a quantitative index of F-T durability to characterize CSM. The smaller the k value, the stronger of the F-T durability of the mixtures have. For example, clay-lime specimens are the most frost susceptible mixtures, with the largest average k of 0.850.

The initial constrained modulus and UCS effect on k was investigated: specimens with higher initial constrained modulus and UCS have smaller k with exception for clay-cement and gravel-cement mixtures. Based on the laboratory testing procedure used in this study, a criterion is proposed for characterizing the F-T susceptibility of CSMs through the relationship between k and initial UCS, which was divided into four categories: High, moderate, low, and negligible.

7.4.2. WET-DRY CYCLING MODELING

The basic W-D durability model involving the consideration of a reduction in D for CSM subjected to W-D cycling is proposed. Reduction factor, $f_{R,}$ equals to the larger value between first W-D cycle reduction and total reduction in normalized constrained modulus. Smaller f_R means less reduction in constrained modulus when the specimens subject to W-D cycling. Generally, f_R for stabilized fine-grained soils (silt and clay) are larger than that for stabilized coarse-grained soils (sand and gravel), except for gravel-cement (3%). A linear relationship

(R^2=0.72) was observed in this relationship (not considering gravel-cement, 3%). Generally, f_R decreases with the increase in void ratio for CSM.

7.5. CHARACTERISTICS OF ULTRASONIC WAVE ON CEMENTITIOUSLY STABILIZED MATERIALS

7.5.1. P-WAVE VELOCITY AND CONSTRAINED MODULUS FOR MONITORING CURING PROCESS

In general, the P-wave velocity or constrained modulus of the CSM increased with curing time. The increase in P-wave velocity and constrained modulus from the 1st to 7th curing days was more pronounced than the increase from 7th to 28th curing days for cement-stabilized soils. During the first 7 days of curing, the cement-stabilized soils were found to have a larger increase in velocity and constrained modulus than fly ash- or lime-stabilized soils, indicating a greater increase in stiffness except for sand-cement and sand-fly ash. This phenomenon is due to slow pozzolanic reaction in lime and fly ash stabilization.

7.5.2. EFFECT OF MOISTURE CONTENT

Unsaturated specimens with higher P-wave velocity had a much smaller increase in P-wave velocity after saturation. The saturation stiffening effect on the P-wave velocity tends to be larger for soft CSM specimens with low P-wave velocity which is explained by the “fastest path” theory. Clay-lime specimens were

more sensitive to S_r with P-wave velocity increase from around 1200 m/s to 1600 m/s when saturated, which also demonstrated that the P-wave velocity of water is 1600 m/s.

7.5.3. COMPACTION CHARACTERISTICS AND P-WAVE VELOCITY

For stabilized fine-grained soils, there was a peak in P-wave velocity coinciding with the optimum moisture content, whereas for stabilized sand or granular base materials, this trend was not present. The trend between UCS versus dry density was the same as the trend of the P-wave velocity versus dry density. Specimens with higher P-wave velocity possessed higher strength (i.e., UCS) for various CSMs. The empirical relationships developed in the laboratory between P-wave velocity, UCS, and dry density for CSMs provides insights for use of the non-destructive method in QC/QA.

7.5.4. CORRELATION BETWEEN UNCONFINED COMPRESSION STRENGTH (UCS) AND CONSTRAINED MODULUS

The strength of CSMs increased with increasing P-wave velocity. Equation for predicting UCS from P-wave velocity/constrained modulus was proposed. Density effect on the UCS of CSM was considered in the proposed prediction. The predicted UCS was less proportional using P-wave velocity (R^2=0.70) than

the prediction of UCS using constrained modulus (R^2=0.87). The prediction model was also verified by unsaturated UCS.

7.5.5. CORRELATION BETWEEN ELASTIC MODULUS AND P-WAVE VELOCITY OR CONSTRAINED MODULUS

Linear relationship between V_P vs. E_0 , V_P vs. E_{50}, D vs. E_0, and D vs. E_{50} were observed. D correlated best with E_0, with R^2 0.71. E_0 and E_{50} are approximately eight times greater than D, which has potential for determination of the design modulus of CSM in pavement design. Therefore, use of this method can lead to less reliance on extensive laboratory mechanical tests.

SECTION 8 REFERENCES

AASHTO, (2004), “Distribution of the Recommended Mechanistic-Empirical Pavement Design Guide (NCHRP Project 1-37A),” Memo to Interested Reviewers.

American Concrete Pavement Association, EB204P, “Subgrade and Subbase For Concrete Pavements.”

American Coal Ash Association, (2011), www.acaa-usa.org.

ARA, (2004), “Guide for Mechanistic-Empirical Design of New and Rehabilitated Pavement Structures,” NCHRP Project 1-37A, prepared for National Cooperative Highway Research Program, Washington D.C.

Bhattacharja, S. and Bhatty, J.I., (2003), ”Comparative Performance of Portland Cement and Lime Stabilization of Moderate to High Plasticity Clay Soils,” Research and Development Bulletin RD125, Portland Cement Association.

Bin-Shafique, S., Rahman, K., Yaykiran, M. and Azfar, I., (2010), “The long-term performance of two fly ash stabilized fine-grained soil subbases”, Resources, Conservation and Recycling, Vol. 54, pp 666-672.

Camargo, F., (2008), “Strength and Stiffness of Recycled Base Materials Blended with Fly Ash,” MS Thesis, University of Wisconsin-Madison, Madison, WI.

Casmer, J. D., (2011), “Fatigue Cracking Of Cementitiously Stabilized Pavement Layers Through Large-Scale Model Experiments,” MS Thesis, University of Wisconsin-Madison, Madison, WI.

Chemical & Engineering News (2009), "The Foul Side of 'Clean Coal'," p.44

Dempsey, B. J., and Thompson, M. R., (1972), ‘‘Effects of Freeze-Thaw Parameters on the Durability Of Stabilized Materials.’’ Highway Research Board 379, Washington, D.C.

Dempsey, B. J., and Thompson, M. R., (1973), “Vacuum Saturation Method for Predicting Freeze-Thaw Durability of Stabilized Materials,” In Highway Research Record 442, HRB, National Research Council, Washington, D.C., pp. 44–57.

Department of the Army, the Navy, and the Air Force (1994), “Soil Stabilization for Pavements,” Army TM 5-822-14/Air Force AFJMAN 32-1019.

Eades, J. L., and Grim, R. E., (1960), “Reactions of Hydrated Lime with Pure Clay Minerals in Soil Stabilization,” Highway Research Bulletin 262.

Edil, T., Acosta, H., and Benson, C. H., (2006), “Stabilizing Soft Fine-Grained Soils with Fly Ash,” Journal of Materials in Civil Engineering, 18(2), 283-294.

Federal Highway Administration, (2003), “Ch. 4 Fly Ash in Stabilized Base Course,” Fly Ash Facts for Highway Engineers, Web Site, http:www.fhwa.dot.gov/pavement/recyc ling/ fach04.cfm.

Fernandez, A., And Santamarina J. C., (2000), “Effect Of Cementation On The Small-Strain Parameters Of Sands,” Canadian Geotechnical Journal, 38, 191–199.

Fratta D., Alshibli K.A., Tanner W.M., Roussel L., (2005), “Combined TDR And P-Wave Velocity Measurements For The Determination Of In Situ Soil Density,” Geotechnical Testing Journal, 28(6), 553-563.

Hatipoglu B., Edil T. B. and Benson C. H., (2008), “Evaluation of Base Prepared from Road Surface Gravel Stabilized with Fly Ash,” GeoCongress 2008, New Orleans, LA, American Society of Civil Engineers, CD-ROM.

Hilbrich S. L. and Scullion T.,(2007), “Rapid Alternative for Laboratory Determination of Resilient Modulus Input Values on Stabilized Materials for AASHTO Mechanistic-Empirical Design Guide,” Journal of the Transportation Research Board, No. 2026, pp. 63-69.

Guthrie W. S., Roper M. B., and Eggett D. L., (2008), “Evaluation of Laboratory Durability Tests for Stabilized Aggregate Base Materials,” TRB 2008 Annual Meeting CD-ROM.

Iowa State University, (2005), “Fly Ash Soil Stabilization for Non-Uniform Subgrade Soils,” Volume I: Engineering Properties and Construction Guidelines, IHRB Project TR-461, FHWA Project.

Jong D. T., Bosscher P. J., Benson C. H., (1998), “Field Assessment of Changes in Pavement Moduli Caused by Freezing and Thawing,” Transportation Research Record. 1615, Transportation Research Board, Washington D.C., 41-48.

Khoury, N. N. and Zaman, M. M., (2002), “Environmental Effects On Durability Of Aggregates Stabilized With Cementitious Materials,” Transportation Research Record 1787, pp 13-21.

Khoury, N. N. and Zaman, M. M., (2007), “Environmental Effects On Durability Of Aggregates Stabilized With Cementitious Materials,” Journal of materials in civil engineering, ASCE, Vol. 19, NO.1.

Khoury, N. N. and Zaman M. M., (2005), “Effect of Wet–Dry Cycles on Resilient Modulus of Class C Coal Fly Ash–Stabilized Aggregate Base,” Transportation Research Record 1787, pp 13-21.

Khoury, N. N. and Zaman M. M., (2005), “Flexural Properties of Stabilized-Aggregate Beams Subjected to Freeze-Thaw Cycles,” TRB 2005 Annual Meeting CD-ROM.

Kootstra B. R., (2009), “Large Scale Model Experiments Of Recycled Base Course Materials Stabilized With Cement And Cement Kiln Dust,” MS Thesis, University of Wisconsin-Madison, Madison, WI.

Lee, W., Bohra, N.C., Atlschaeffl, A.G., and White, T.D., (1995), “Resilient Modulus of Cohesive Soils and the Effect of Freeze-Thaw,” Can. Geotech. J., 31, 559-568.

Lim S. and Zollinger D. G., (2003), “Estimation of the Compressive Strength and Modulus of Elasticity of Cement-Treated Aggregate Base Materials,” Transportation Research Record 1837, pp 30-38.

Li L., Benson C. H., Edil T. B. and Hatipoglu B., (2007), “Evaluation of Recycled Asphalt Pavement Material Stabilized with Fly Ash,” GeoDenver2007, American Society of Civil Engineers, CD-ROM.

Li L., Benson C. H., Edil T. B. and Hatipoglu B., (2008), “Sustainable Construction Case History: Fly Ash Stabilization of Recycled Asphalt Pavement Material,” Geotechnical and Geological Engineering, Vol. 26, No. 2, pp. 177-188.

Little, D. N., (1996), “Evaluation of Resilient and Strength Properties of Lime-Stabilized Soils from the Denver, Colorado Area,” Report for the Chemical Lime Company.

Mohammad, L. N., Raghavandra, A. and Huang, B. H., (1981), “Laboratory performance evaluation of cement-stabilized soil base mixtures,” Transportation Research Record 0361, pp 19-28.

Moore, T., K. and Kennedy, T., W., (1971), “Tensile behavior of subbase materials under repetitive loading,” Center for Highway Research, University of Texas at Austin, Austin, TX.

National Lime Association (2001), “Using Lime for Soil Stabilization and Modification.”

National Lime Association (2005), “Lime Treated Soils Save Time & Money,” Web Site, http://www.lime.org.

Nazarian, S., D. Yuan, V. Tandon, and M. Arellano., (2005), “Quality Management of Flexible Pavement Layers with Seismic Methods. Research Report 1735-3. Center for Transportation Infrastructure Systems, The University of Texas at El Paso.

Parsons R., L. and Milburn J., P., (2003), “Engineering Behavior of Stabilized Soils,” Transportation Research Record: Journal of the Transportation Research Board, vol. 1837,2003.

PhaniKumar, B. R., and Sharma, R. S., (2007), “Volume change behavior of fly ash-stabilized clays,” J. Mater. Civ. Eng., 19(1), 67–74.

Portland Cement Association, (1992), “Soil-Cement Laboratory Handbook”.

Prusinski, J.R. and Bhattacharya S., (2007), “Effectiveness of Portland Cement and Lime in Stabilizing Clay Soils,” Transportation Research Record 1652, 1999, pp 215-227.

Puppala, A. J., Mohammad and Allen, A., (1996), “Engineering Behavior of Lime-Treated Louisiana Subgrade Soil,” Transportation Research Record No. 1548.

Pucci, M., J., (2012), “Development of a Multi-Measurement Confined Free-Free Resonant Column Device and Initial Studies,” MS Thesis, University of Texas at Austin, Austin, TX.

Richart, F. E., Hall, J. R., and Wood, R. D., 1970, “Vibrations of Soils and Foundations,” Prentice-Hall. Englewood, NJ.

Rosa, M. G., (2006), “Effect of freeze and thaw cycling on soils stabilized using fly ash,” MS Thesis, University of Wisconsin-Madison, Madison, WI.

Sawangsuriya A., Edil T. B., and Bosscher, P. J., (2003), “Relationship of Soil Stiffness Gauge Modulus to Other Test Moduli,” Journal of Transportation Research Board, No. 1849, Paper No. 03-4089, National Research Council, Washington D. C., pp. 3-10.

Sawangsuriya A., Edil T. B. and Bosscher P. J., (2009), “Modulus-Suction-Moisture Relationship for Compacted Soils in Post-Compaction State, Journal of Geotechnical and Geoenvironmental Engineering, American Society of Civil Engineers, Vol. 135, No. 10, pp. 1390-1403.

Schuettpelz, C. C., Fratta, D., and Edil, T. B., (2010), “Mechanistic corrections for determining the resilient modulus of base course materials based on elastic wave measurements”. Journal of Geotechnical and Geoenvironmental Engineering. Vol. 136, No. 8, pp. 1086-1094.

Simonsen, E., Janoo, V., and Isacsson, U., (2002), “Resilient Properties of Unbound Road Material during Seasonal Frost Conditions,” J. Cold Region Eng., 16, 28-50.

Stephenson, R.,W., (1978), “Ultrasonic Testing for Determining Dynamic Soil Moduli,” Dynamic Geotechnical Testing, ASTM STP 654, American Society For Testing And Materials, pp. 179-195.

Stokoe, K.H., II and Santamarina, J.C., (2000), “Seismic-Wave-Based Testing in Geotechnical Engineering,” International Conference on Geotechnical and Geological Engineering, Invited Paper, GeoEng 2000, Melbourne, Australia, pp. 1490-1536.

Swanson, T. E. and Thompson, M. R., (1967), “Flexural Fatigue Strength of Lime-Soil Mixtures,” Highway Research Record 198, pp 9-18.

Tastan E. O., Edil T. B., Benson C. H. and Aydilek A. H., (2011),"Stabilization of Organic Soils with Fly Ash," Journal of Geotechnical and Geoenvironmental Engineering 137(9): 819-833.

Thompson, M. R., (1969), “Engineering Properties of Lime-Soil Mixtures,” Journal of Materials -ASTM, Vol. 4, No. 4.

Toutanji H., Delatte N., Aggoun S., Duval R. and Danson A., (2004), “Effect of supplementary cementitious materials on the compressive strength and durability of short-term cured concrete. Cement and Concrete Research, 34(2):311–9.

Trtnik G., Kavcic F., and Turk G., (2009), “Prediction Of Concrete Strength Using Ultrasonic Pulse Velocity And Artificial Neural Networks,” Ultrasonics, Vol. 49, pp. 53–60.

Walker, P. J., (1995), “Strength, Durability and Shrinkage Characteristics of Cement Stabilized Soil Blocks,” *Cement and Concrete Composites,* vol. 17, 1995, pp 301-310.

Wen H., Martono W., Edil T. B. and Clyne T. R. and Patton R., (2010), “Field Evaluation of Recycled Pavement Materials at MnROAD,” Paving Materials and Pavement Analysis, GeoShanghai 2010, American Society of Civil Engineers, Shanghai, China, pp. 264-269.

Wen H. and Ramme B., (2008), “A Performance Evaluation of Asphalt Pavement with Recycled Pavement Materials Treated by Self Cementing Fly Ash and Field Verification Using M-E Design Guide: A Case Study,” Paper presented at 2008 ASCE Pavement Conference, Bellevue, WA.

Williams, R. R. and Nazarian, S., (2007), “Correlation of Resilient and seismic modulus test results,” Journal of Materials in Civil Engineering, 19(12): 1026-1032.

Yesiller N., Hanson J.L., Rener A.T. and Usmen M.A., (2001), “Ultrasonic testing for evaluation of stabilized mixtures,” Transport Research Record, 1757, pp. 32–39

Zaman M., Laguros J. G. and Sayah. A., (1992), “Soil Stabilization Using Cement Kiln Dust”. Proceedings 7th International Conference on Expansive Soils, Dallas, Tex., pp. 1–5.

Zaman, M. M., J.-H. Zhu, and J. G. Laguros., (1999) “Durability Effects on Resilient Moduli of Stabilized Aggregate Base”. In Transportation Research Record: Journal of the Transportation Research Board, No. 1687, TRB, National Research Council, Washington, D.C., pp. 29–38.

TABLES

Table 3.1. Index properties for gravel, sand, silt, and clay.

Sample	D_{50} (mm)	C_u	C_c	G_s	ω_{opt} (%)	γ_{dmax} (kN/m^3)	LL (%)	PL (%)	Gravel Content (%)	Sand Content (%)	Fines Content (%)	USCS Symbol	AASHTO Symbol
Gravel	3.500	110.0	1.3	-	7.0	22.0	NP	NP	45.4	40.5	14.1	GM	A-1-a
Sand	0.500	2.8	0.83	2.69	11.0	18.7	NP	NP	2.1	97.8	0.1	SP	A-1-b
Silt	0.010	15.0	6.7	2.72	10.5	19.4	18	NP	3.0	37.0	60.0	ML	A-4
Clay	0.015	33.3	2.1	2.62	16.0	16.9	39	19	2.0	18.0	80.0	CL	A-6

D_{50} = median particle size, C_u = coefficient of uniformity, C_c = coefficient of curvature, G_s = specific gravity, ω_{opt} = optimum water content,
γ_{dmax} = maximum dry unit weight, LL = liquid limit, PL = plastic limit, NP = nonplastic.

Note: Particle size analysis conducted following ASTM D6913, G_s determined by ASTM D854, γ, γ_{dmax} and ω_{opt} determined by ASTM D698 except for gravel determined by ASTM D1557, USCS classification by ASTM D2487, AASHTO classification by ASTM D3282, and Atterberg limits by ASTM D431

Table 3.2. Optimum moisture contents and maximum dry unit weights for native soils

Materials	Optimum Moisture Content (%)	Maximum Dry Unit Weight (kN/m^3)
Gravel	7.0	22.1
Sand	11.0	18.7
Silt	10.5	19.4
Clay	14.5	16.9

Table 3.3. Final mix design, maximum dry density and optimum moisture content of stabilized mixtures

	Clay			Silt			Sand			Gravel		
	Additive content (%)	OMC (%)	MDUW (kN/m^3)	Additive content (%)	OMC (%)	MDUW (kN/m^3)	Additive content (%)	OMC (%)	MDUW (kN/m^3)	Additive content (%)	OMC (%)	MDUW (kN/m^3)
No additive	N/A	19.12	16.88	N/A	10.39	19.44	N/A	7.15	18.13	N/A	7.74	21.77
Cement	12	17.98	16.22	8	11.12	18.84	6	8.67	19.26	3	6.23	22.01
Lime (Lime-Class F fly ash*)	6	19.35	16.47	4/12*	12.44	18.59	x			x		
Fly ash	x			13	10.04	19.05	13	19.05	21.25	13	7.38	21.89

MDUW = Maximum Dry Unit Weight;

Note: *Lime+Class F Fly Ash (Wen et al. 2011).

Table 4.1. Freeze-thaw cycling test results (cement-stabilized soils)

Status			Before F-T cycling (0 Cycle) (End of Curing)						End of F-T cycling (Thawed Condition)				
Mixtures	Binder Content (%)	Specimen No.	DUW (kN/m^3)	Void Ratio	CMC (%)	MC (%)	D (GPa)	Initial UCS[1] (MPa)	Cycles	Residual D (GPa)	Residual UCS (MPa)	Normalized D (%)	Normalized UCS (%)
Gravel-cement	3%	5	21.71	0.22	6.2	6.9	24.3	4.40	2	7.0	3.69	29	84
		6	22.30	0.18	6.2	6.7	25.2		2	7.0	2.89	28	66
		7	21.54	0.22	6.2	7.1	23.5		2 (broken)	5.7	N/A	24	N/A
		8	21.72	0.21	6.2	6.8	24.4		2	7.7	2.6	32	58
Sand-cement	6%	4	19.27	0.37	8.2	9.0	20.4	4.70	12	19.6	2.26	96	61
		5	20.56	0.40	8.2	9.0	20.9		12	19.4	2.78	93	75
		6	22.19	0.37	8.2	9.0	21.0		12	19.2	2.54	91	54
Silt-cement	8%	5	19.23	0.39	11.3	13.4	17.1	4.49	6	4.1	0.77	24	17
		6	18.93	0.41	11.3	15.2	16.1		6	3.8	3.50	24	78
		7	19.15	0.39	11.3	14.1	16.6		7	8.1	1.78	49	40
		8	19.05	0.40	11.3	14.8	16.0		7	12.1	1.93	76	43
Clay-cement	12%	5	16.48	0.54	19.2	19.5	6.1	3.68	12	4.5	1.90	75	52
		6	16.55	0.55	19.2	19.7	8.4		12	3.0	1.98	36	54
		8	17.25	0.52	18.0	18.4	5.5		12	3.9	1.47	71	40

UCS[1] Unconfined compressive strength can be found in Appendix A; DUW= Dry Unit Weight; CMC= Compaction Moisture Content; MC= Moisture Content; Cycles Of F-T test: to loss of specimen integrity; D=constrained modulus; $Normalized\ D = \frac{Residual\ D}{D} \times 100\%$*;* $Normalized\ UCS = \frac{Residual\ UCS}{UCS} \times 100\%$

Table 4.2. Freeze-thaw cycling test results (fly ash-stabilized soils)

Status			Before F-T cycling (0 Cycle) (End of Curing)						End of F-T cycling (Thawed Condition)				
Mixtures	Binder Content (%)	Specimen No.	DUW (kN/m^3)	Void Ratio	CMC (%)	MC (%)	D (GPa)	Initial UCS[1] (MPa)	Cycles	Residual D (GPa)	Residual UCS (MPa)	Normalized D (%)	Normalized UCS (%)
Gravel-fly ash	13%	4	22.88	0.15	6.5	5.8	8.5	1.98	4	5.1	1.17	60	59
		5	22.00	0.20	6.0	5.4	6.8		4	2.9	1.19	43	60
		6	21.80	0.22	6.0	5.4	8.9		4	2.3	1.16	26	59
Silt-fly ash	13%	5	19.40	0.375	9.5	9.1	3.9	0.63	1	2.5	0.39	63	63
		6	19.68	0.356	9.5	8.9	4.0		1	1.9	0.36	48	57
		7	19.05	0.401	9.5	8.8	3.4		1	2.3	0.37	68	58
Sand - fly ash	13%	10	19.99	0.314	6.8	6.20	9.0	2.65	12	2.1	0.77	23	29
		11	20.66	0.271	6.8	5.78	10.1		12	4.0	0.84	40	32
		12	20.24	0.297	6.8	7.10	9.1		12	2.8	0.86	31	32

UCS[1] Unconfined compressive strength can be found in Appendix A; DUW= Dry Unit Weight; CMC= Compaction Moisture Content; MC= Moisture Content; Cycles Of F-T test: to loss of specimen integrity; D=constrained modulus; $Normalized\ D = \frac{Residual\ D}{D} \times 100\%$; $Normalized\ UCS = \frac{Residual\ UCS}{UCS} \times 100\%$

Table 4.3. Freeze-thaw cycling test results (lime-stabilized soils)

Status			Before F-T cycling (0 Cycle) (End of Curing)						End of F-T cycling (Thawed Condition)				
Mixtures	Binder Content (%)	Specimen No.	DUW (kN/m^3)	Void Ratio	CMC (%)	MC (%)	D (GPa)	Initial UCS[1] (MPa)	Cycles	Residual D (GPa)	Residual UCS (MPa)	Normalized D (%)	Normalized UCS (%)
Silt-lime-fly ash* (Class F)	4%, 12%*	4	18.26	0.46	12.7	11.0	5.5	1.87	3	0.8	0.77	15	41
		5	19.99	0.50	12.7	12.2	8.7		6	0.6	0.90	7	48
		6	20.21	0.49	12.7	12.5	9.8		6	0.6	0.86	7	46
Clay-lime	6%	4	16.00	0.59	19.1	19.1	2.7	1.03	2	0.5	0.43	19	42
		5	16.31	0.56	19.1	18.4	2.8		2	0.6	0.39	20	37
		6	16.38	0.55	19.1	18.5	2.0		2	0.5	0.36	24	35

UCS[1] Unconfined compressive strength can be found in Appendix A; DUW= Dry Unit Weight; CMC= Compaction Moisture Content; MC= Moisture Content; Cycles Of F-T test: to loss of specimen integrity; D=constrained modulus; $Normalized\ D = \frac{Residual\ D}{D} \times 100\%$*;* $Normalized\ UCS = \frac{Residual\ UCS}{UCS} \times 100$

Table 4.4. Wet-dry cycling test results (cement-stabilized soils)

Status			Before W-D cycling (0 Cycle) (End of Curing)						End of W-D cycling				
Mixtures	Binder Content (%)	Specimen No.	DUW (kN/m^3)	Void Ratio	CMC (%)	MC (%)	D (GPa)	Initial UCS[1] (MPa)	Cycles	Residual D (GPa)	Residual UCS (MPa)	Normalized D (%)	Normalized UCS (%)
Grave-cement	3%	13	21.69	0.20	6.2	6.9	25.5	4.40	12	12.2	3.98	48	90
		14	22.14	0.14	6.2	7.4	30.2		12	8.0	6.55	27	149
		15	23.72	0.21	6.2	6.9	29.2		12	8.4	3.64	29	83
Sand-cement	6%	10	19.19	0.35	7.5	8.3	20.8	4.70	12	12.6	2.77	61	59
		11	19.59	0.36	7.5	4.7	19.1		12	13.0	1.94	68	41
		12	19.02	0.40	7.5	11.1	21.2		12	16.7	2.88	79	61
Silt-cement	8%	9	18.54	0.44	12.2	15.3	17.3	4.49	12	9.3	8.65	54	193
		10	18.53	0.44	12.2	22.6	17.4		12	8.3	7.29	48	162
		11	18.57	0.44	12.2	15.0	18.0		12	9.1	5.39	50	120
Clay-cement	12%	13	18.78	0.51	18.0	18.8	8.8	3.68	12	4.9	6.25	56	170
		14	18.98	0.53	18.0	19.0	8.4		12	2.4	5.54	29	151
		15	19.32	0.53	18.0	19.3	9.1		12	2.6	4.39	28	119

UCS[1] Unconfined compressive strength can be found in Appendix A; DUW= Dry Unit Weight; CMC= Compaction Moisture Content; MC= Moisture Content; Cycles Of F-T test: to loss of specimen integrity; D=constrained modulus; $Normalized\ D = \frac{Residual\ D}{D} \times 100\%$*;* $Normalized\ UCS = \frac{Residual\ UCS}{UCS} \times 100$

Table 4.5. Wet-dry cycling test results (fly ash-stabilized soils)

Status			Before W-D cycling (0 Cycle) (End of Curing)						End of W-D cycling				
Mixtures	Binder Content (%)	Specimen No.	DUW (kN/m^3)	Void Ratio	CMC (%)	MC (%)	D (GPa)	Initial UCS[1] (MPa)	Cycles	Residual D (GPa)	Residual UCS (MPa)	Normalized D (%)	Normalized UCS (%)
Gravel-fly ash	13%	1	20.14	0.19	6.5	5.6	10.2	1.98	12	7.6	3.81	75	192
		2	20.40	0.18	6.5	5.4	8.8		12	8.4	3.70	96	187
		3	22.19	0.20	6.5	5.4	11.3		12	7.2	2.73	64	138
Silt -fly ash	13%	13	20.02	0.33	8.3	9.6	3.9	0.63	7	3.3	1.01	86	160
		14	19.87	0.34	8.3	10.3	2.7		7	2.2	0.74	82	117
		15	19.77	0.35	8.3	11.0	2.9		7	1.9	0.56	64	88
Sand - fly ash	13%	10	20.6	0.28	7.3	7.4	9.2	2.65	12	4.6	1.73	50	65
		11	20.3	0.30	7.3	7.6	9.8		12	5.4	1.44	55	55
		12	20.6	0.28	7.3	7.7	8.7		12	5.3	1.41	61	53

UCS^1 Unconfined compressive strength can be found in Appendix A; DUW= Dry Unit Weight; CMC= Compaction Moisture Content; MC= Moisture Content; Cycles Of F-T test: to loss of specimen integrity; D=constrained modulus; $Normalized\ D = \frac{Residual\ D}{D} \times 100\%$*;* $Normalized\ UCS = \frac{Residual\ UCS}{UCS} \times 100$*.*

Table 4.6. Wet-dry cycling test results (lime-stabilized soils)

Status			Before W-D cycling (0 Cycle) (End of Curing)						End of W-D cycling				
Mixtures	Binder Content (%)	Specimen No.	DUW (kN/m^3)	Void Ratio	CMC (%)	MC (%)	D (GPa)	Initial UCS[1] (MPa)	Cycles	Residual D (GPa)	Residual UCS (MPa)	Normalized D (%)	Normalized UCS (%)
Silt-lime-fly ash* (Class F)	4%, 12%*	1	18.01	0.48	12.7	11.0	5.2	1.87	12	2.5	1.50	49	80
		2	18.08	0.48	12.7	11.2	6.1		12	3.3	1.75	54	94
		3	18.34	0.45	12.7	11.1	5.2		12	3.2	1.64	62	88
Clay-lime	6%	1	16.28	0.56	19.2	19	2.3	1.03	10	0.8	1.42	34	138
		2	16.77	0.52	19.2	18.4	2.2		10	0.7	1.57	31	152
		3	16.54	0.54	19.2	18.9	2.5		10	0.6	1.46	25	142

UCS[1] Unconfined compressive strength can be found in Appendix A; DUW= Dry Unit Weight; CMC= Compaction Moisture Content; MC= Moisture Content; Cycles Of F-T test: to loss of specimen integrity; D=constrained modulus; $Normalized\ D = \frac{Residual\ D}{D} \times 100\%$*;* $Normalized\ UCS = \frac{Residual\ UCS}{UCS} \times 100$.

Table 4.7. Physical properties of specimens tested in vacuum saturation

Mixtures	Binder Content (%)	Specimen NO.	DUW (kN/M^3)	Void Ratio	CMC (%)	MC (%)	MC (%) (After Vacuum saturation)	MC Increase (%)
Grave-Cement	3%	1	21.65	0.20	6.2	6.9	9.2	2.3
		2	22.09	0.20	6.2	6.7	9.2	2.5
		3	21.53	0.20	6.2	7.1	9.5	2.4
		4	22.23	0.18	6.2	7.0	8.7	1.7
Gravel-fly ash	13%	1	22.13	0.20	8.2	7.6	8.9	1.3
		2	21.69	0.22	8.2	7.5	9.2	1.7
		4	22.82	0.23	8.2	7.4	9.3	1.9
Sand-cement	6%	1	20.05	0.36	8.2	8.7	22.4	13.7
		4	19.84	0.36	8.2	8.7	20.0	11.3
		6	19.45	0.37	8.6	9.0	22.7	13.7
Sand -fly ash	13%	3	20.46	0.32	6.4	6.0	19.8	13.8
		4	19.62	0.35	7.3	6.1	21.0	14.9
		5	19.71	0.34	7.3	6.9	20.0	13.1
Silt-cement	8%	1	19.52	0.41	11.1	13.4	23.2	9.8
		3	18.88	0.41	11.1	14.0	24.4	10.4
		14	18.68	0.43	12.4	16.0	26.5	10.5
		15	19.26	0.39	12.4	15.8	23.9	8.1
Silt -fly ash	13%	8	19.13	0.40	9.5	9.6	21.5	11.9
		11	19.14	0.39	10.5	10.5	21.6	11.1
		12	19.15	0.39	10.5	10.5	21.0	10.5
Silt-lime-fly ash* (Class F)	4%, 12%*	7	18.08	0.48	12.7	12.2	26.3	14.1
		8	18.26	0.46	12.7	12.3	26.4	14.1
		9	20.21	0.49	12.7	12.4	26.2	13.8
Clay-cement	12%	1	16.92	0.54	19.4	19.5	34.5	15.0
		3	16.71	0.54	19.4	19.4	34.5	15.1
		4	16.37	0.55	19.4	19.9	34.4	14.5
Clay-lime	6%	1	15.17	0.60	20.1	19.50	37.2	17.7
		3	15.71	0.61	20.1	19.60	37.5	17.9
		6	15.27	0.59	20.5	21.00	37.0	16.0

DUW= Dry Unit Weight; CMC= Compaction Moisture Content; MC= Moisture Content;

Table 4.8. UCS and normalized UCS

Status		UCS (MPa)				Normalized UCS			
Mixtures	Binder Content (%)	Standard	Unsaturated	Vacuum saturated	UCS after F-T cycling	Standard UCS	Unsaturated UCS	Vacuum saturation UCS	Normalized UCS of F-T cycling
Gravel-cement	3%	4.40	5.25	4.40	3.05	100%	119%	100%	69%
Silt-cement	8%	4.49	4.72	4.47	1.99	100%	105%	100%	44%
Sand-cement	6%	4.70	4.02	2.34	3.01	100%	86%	50%	64%
Clay-cement	12%	3.68	3.77	2.98	1.98	100%	102%	81%	54%
Gravel-fly ash	13%	1.98	2.90	1.81	1.17	100%	146%	91%	59%
Silt -fly ash	13%	0.63	0.86	0.63	0.37	100%	136%	100%	59%
Sand -fly ash	13%	2.65	2.48	2.35	0.82	100%	94%	89%	31%
Silt-lime-fly ash* (Class F)	4%, 12%*	1.87	1.78	1.08	0.84	100%	95%	58%	45%
Clay-lime	6%	1.03	1.96	0.66	0.39	100%	190%	64%	38%

Table 5.1. Freeze-thaw cycling model development

Mixtures	Binder content (%)	Specimen No.	DUW (kN/M^3)	Void Ratio	Initial UCS[1] (MPa)	k	R^2	Average k
Gravel-cement	3%	5	21.71	0.22	4.40	0.595	0.98	0.621
		6	22.30	0.18		0.616	0.99	
		7	21.54	0.22		0.694	0.99	
		8	21.72	0.21		0.580	1.00	
Gravel-cement	4%	A	21.71	0.22	5.8	0.022	0.81	0.029
		B	22.30	0.18		0.035	0.60	
Silt-cement	8%	5	19.23	0.39	4.49	0.193	0.87	0.138
		6	18.93	0.41		0.208	0.94	
		7	19.15	0.39		0.103	0.84	
		8	19.05	0.40		0.047	0.70	
Sand-cement *	8%	5	19.35	0.36	6.5	0.002	-0.41	0.004
		6	19.36	0.36		0.004	-0.48	
		7	19.84	0.33		0.005	0.26	
		8	19.86	0.33		0.005	0.50	
Sand-cement	6%	4	19.30	0.37	4.70	0.006	0.05	0.009
		5	20.60	0.40		0.013	0.50	
		6	22.20	0.37		0.007	-0.26	
Clay-cement	12%	5	16.48	0.54	3.68	0.035	-1.75	0.049
		6	16.55	0.55		0.071	0.57	
		8	17.25	0.52		0.041	-1.32	
Gravel-fly ash	13%	4	22.88	0.15	1.98	0.141	0.87	0.229
		5	22.00	0.20		0.217	0.84	
		6	21.80	0.22		0.329	0.83	
Silt-fly ash	13%	5	19.40	0.38	0.63	0.459	1.00	0.528
		6	19.68	0.36		0.742	1.00	
		7	19.05	0.40		0.384	1.00	
Sand -fly ash	13%	10	19.99	0.31	2.65	0.101	0.86	0.070
		11	20.66	0.27		0.041	0.87	
		12	20.24	0.30		0.067	0.88	
Silt-lime-fly ash* (Class F)	4%, 12%*	4	18.26	0.46	1.87	0.566	0.91	0.478
		5	19.99	0.50		0.427	0.88	
		6	20.21	0.49		0.442	0.90	
Clay-lime	6%	4	16.00	0.59	1.03	0.941	0.87	0.850
		5	16.31	0.56		0.857	0.97	
		6	16.38	0.55		0.752	0.97	

DUW= Dry Unit Weight

FIGURES

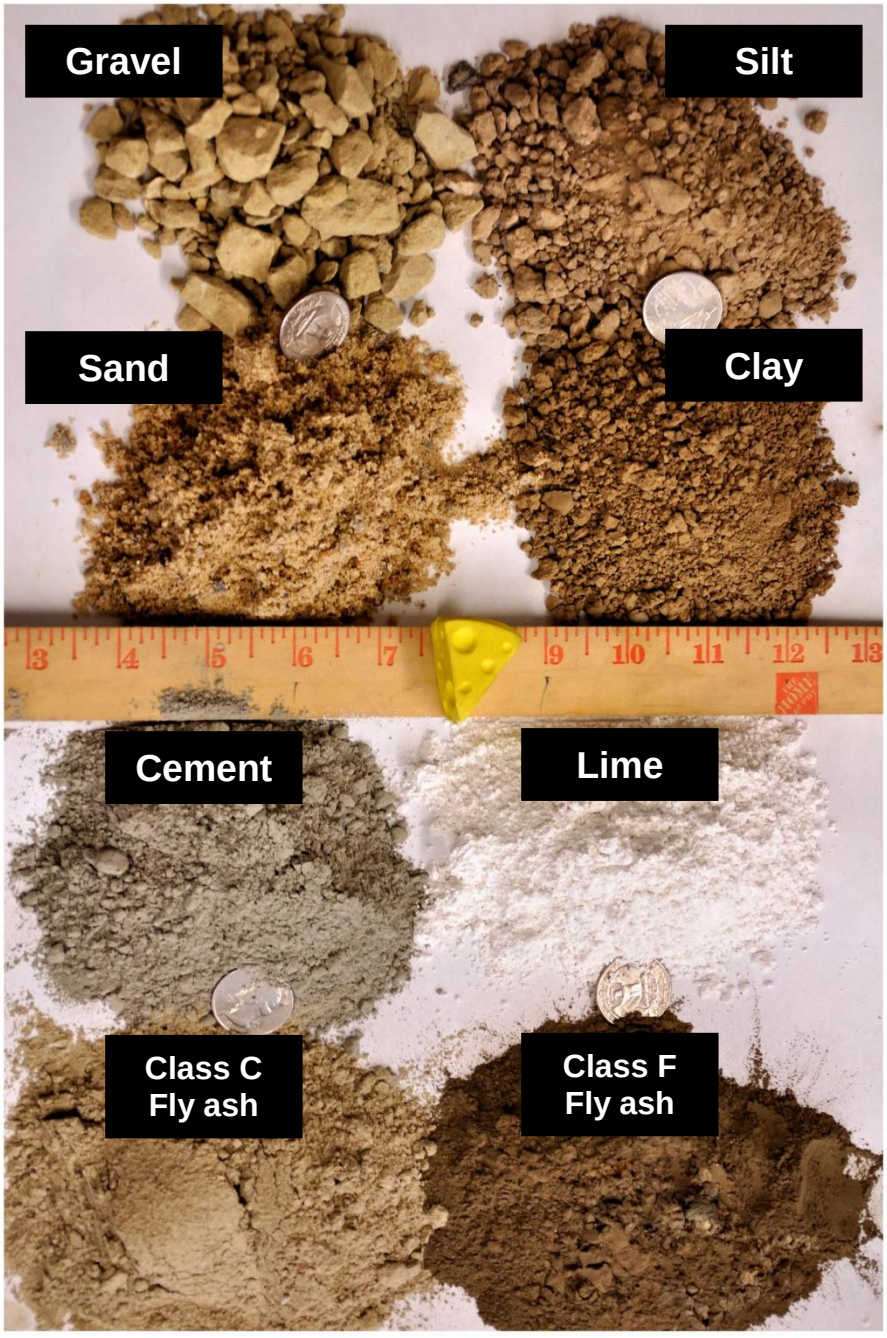

Figure 3.1 Host soils and binders

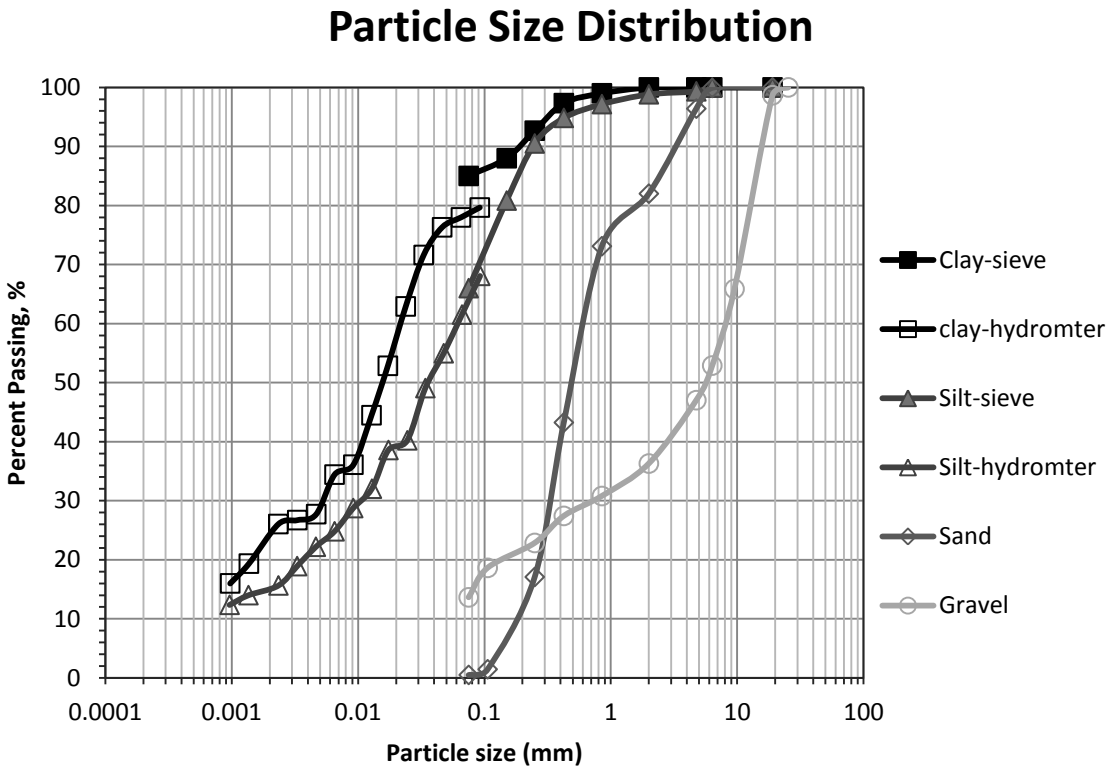

Figure 3.2. Particle size distributions for gravel, sand, silt, and clay.

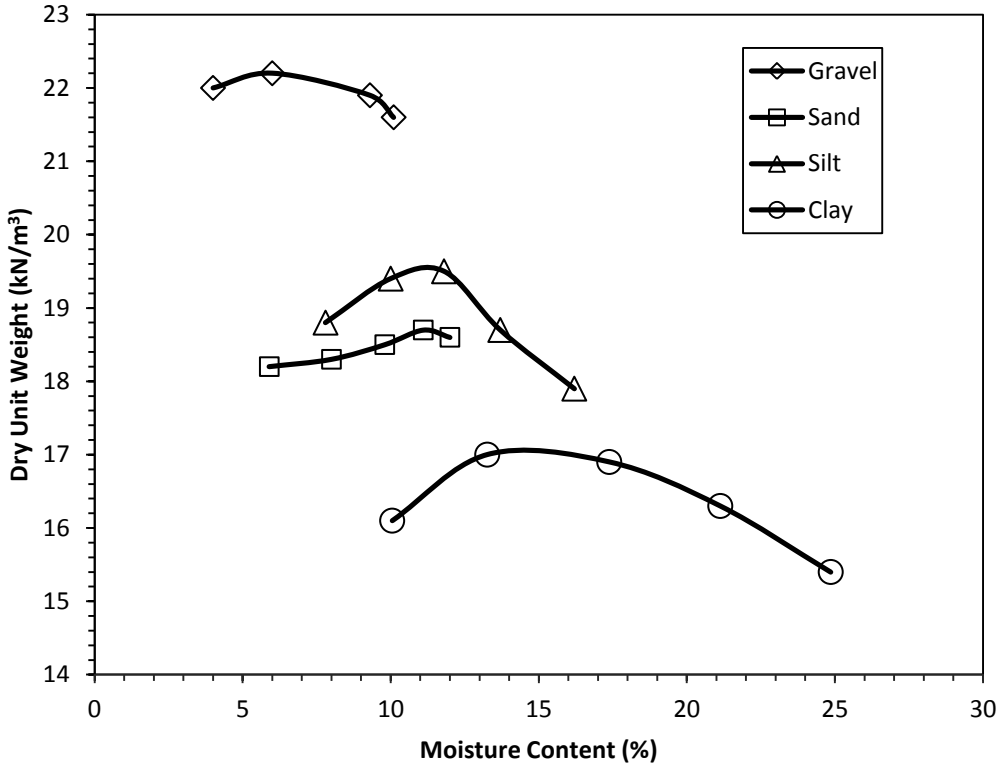

Figure 3.3. Compaction curves for gravel, sand, silt, and clay.

Figure 3.4. Specimens subject to wet-dry cycling

Figure 3.5. Specimens subject to freeze-thaw cycling

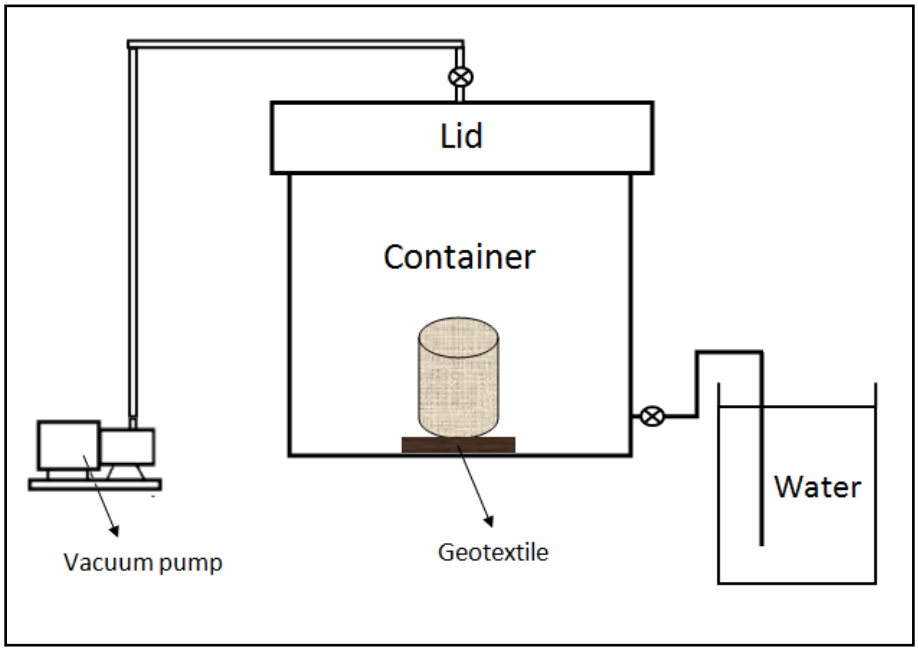

(a)

(b)

Figure 3.6. (a) A schematic of vacuum saturation test setup. (b) A vacuum saturation test system developed at University of Wisconsin-Madison.

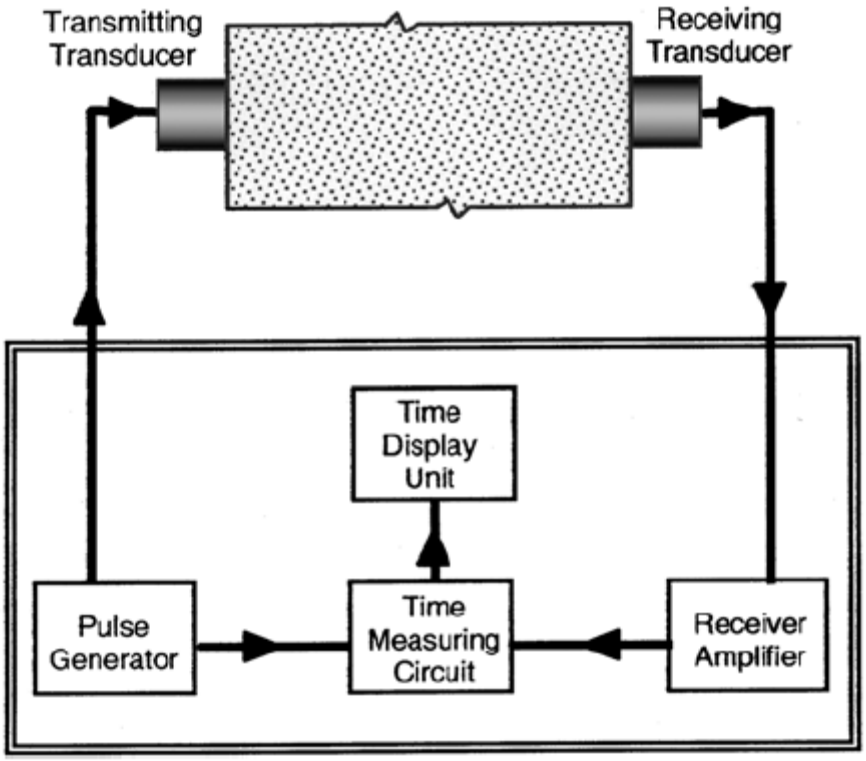

Figure 3.7. Schematic of Pulse Velocity Apparatus (ASTM C 597)

Figure 3.8. Test Equipment: PUNDIT-PLUS

Figure 4.1. Problems with adhesion of coupling agent and soil particles after 2 cycles of freeze-thaw cycling (clay-lime specimens)

Figure 4.2. Cracks develop around the clay-lime specimens during F-T cycling

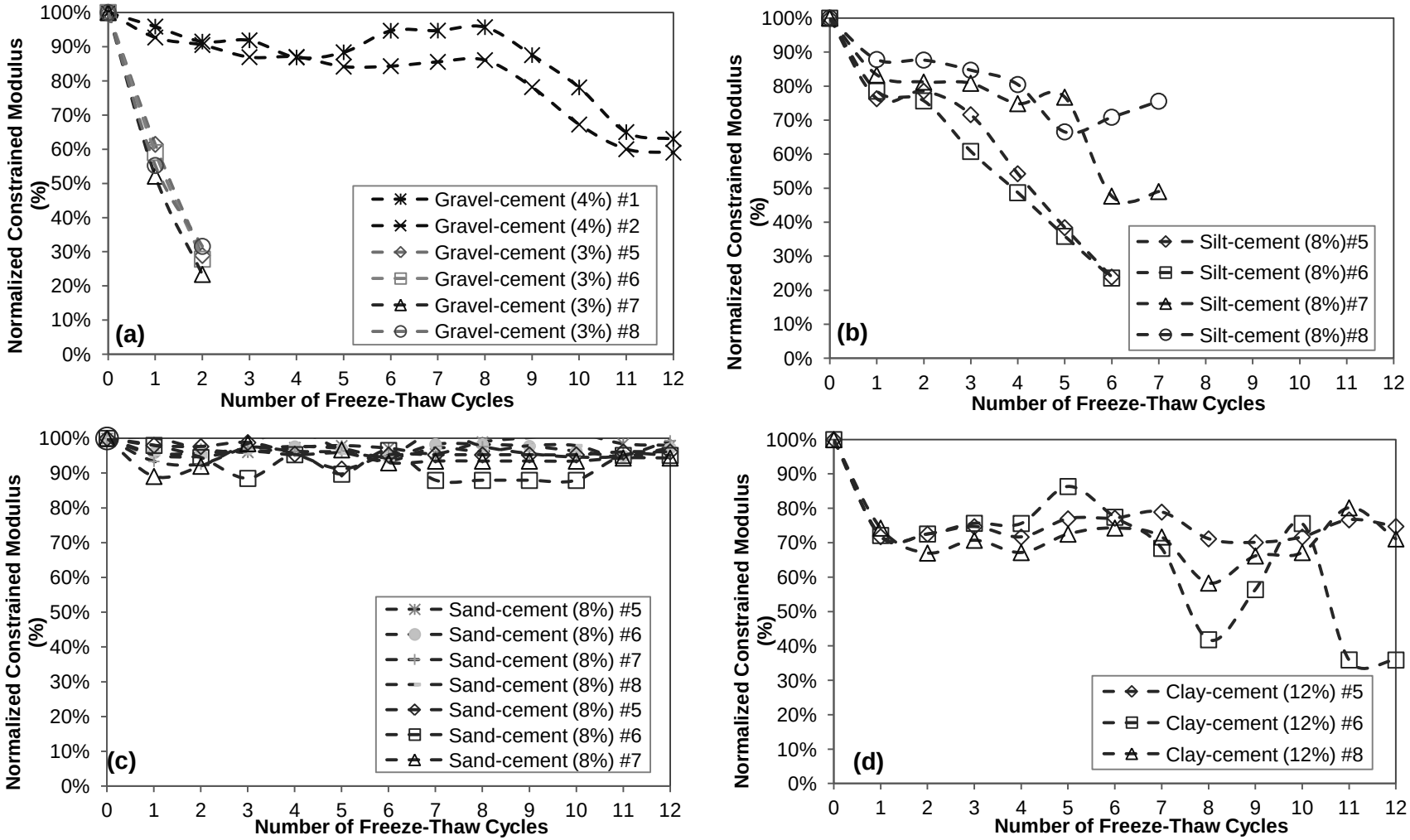

Figure 4.3. Normalized constrained modulus vs. number of Freeze-Thaw cycles of (a) gravel-cement with cement content 3% and 4% (b) silt-cement with cement content 8% (c) sand-cement with cement content 8% and 6% (d) clay-cement with cement content 12%

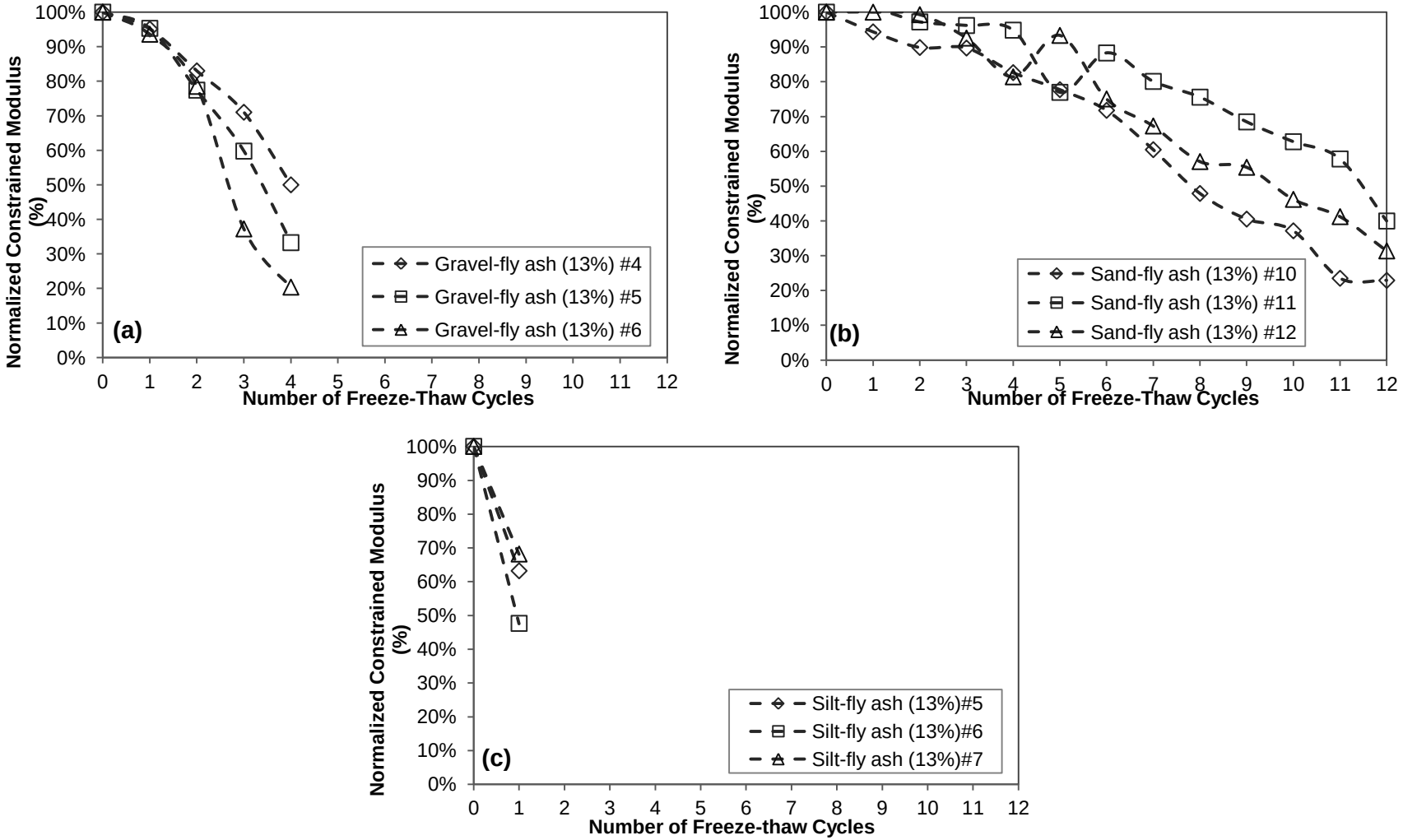

Figure 4.4. Normalized constrained modulus change vs. number of freeze-thaw cycles of (a) gravel-fly ash with fly ash content 13% (b) sand-fly ash with fly ash content 13% (c) silt-fly ash with fly ash content 13%

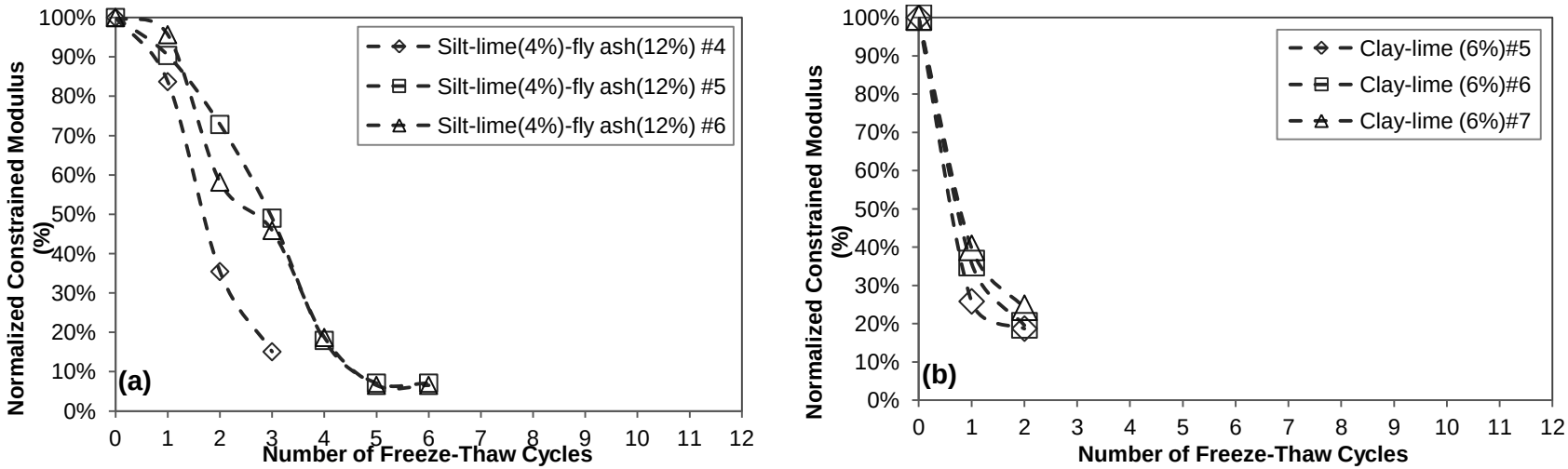

Figure 4.5. Normalized constrained modulus change vs. number of freeze-thaw cycles of (a) silt-lime-fly ash with lime content 4% and fly ash content 13% (b) clay-lime with lime content 6%

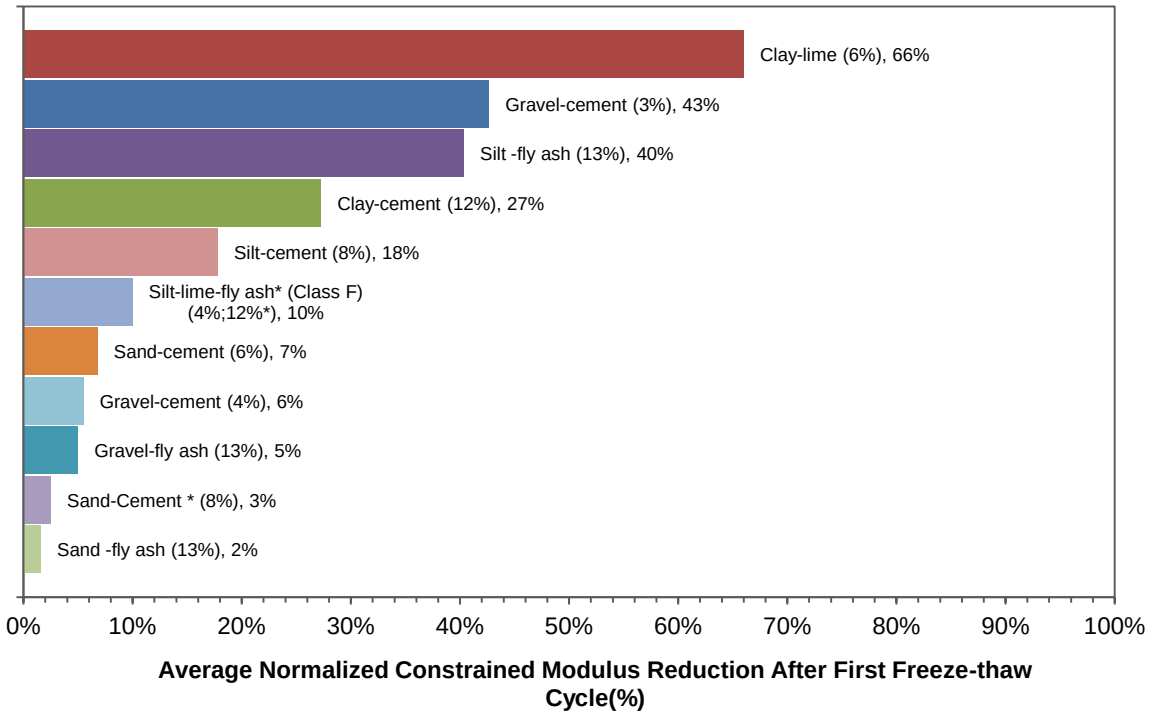

(a)

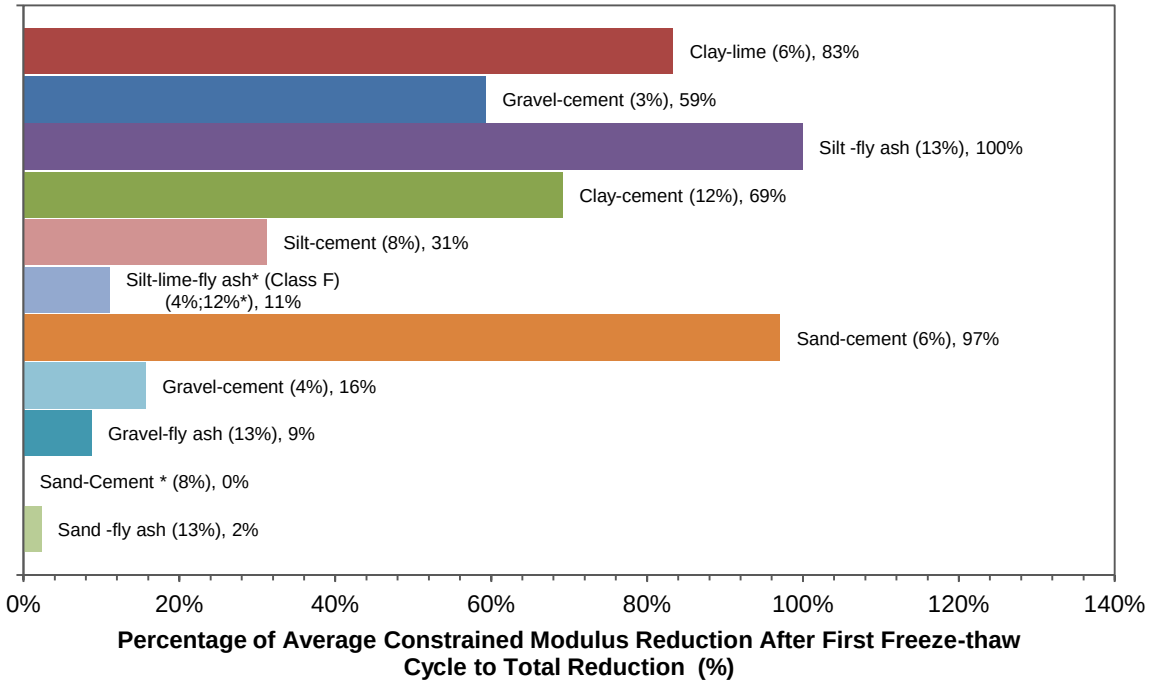

(b)

Figure 4.6. (a) Constrained modulus reduction after first freeze-thaw cycle (b) percentage of constrained modulus reduction to total reduction after first freeze-thaw cycle

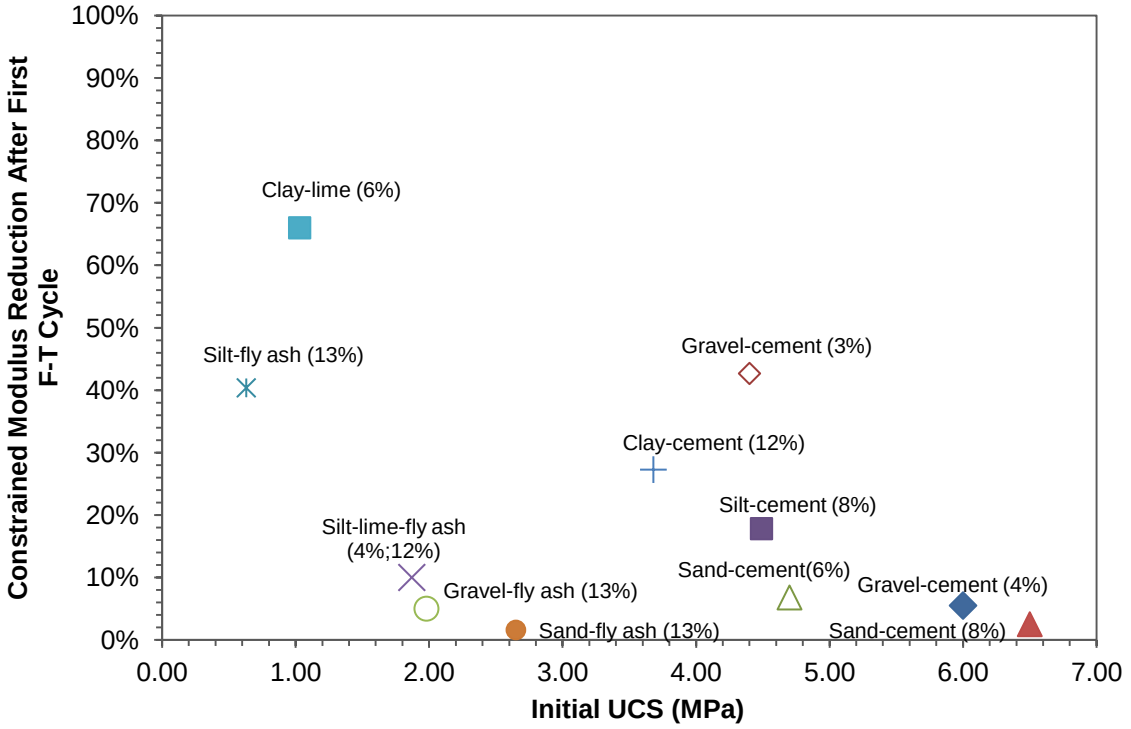

(a)

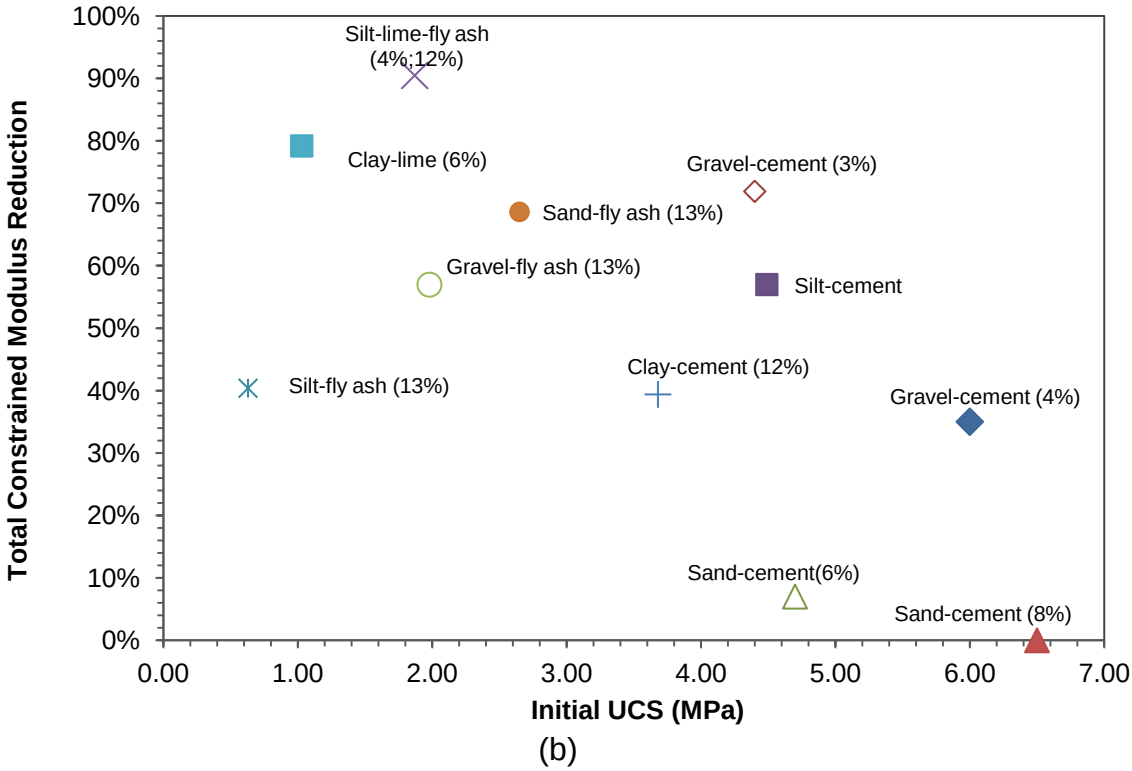

(b)

Figure 4.7. (a) First freeze-thaw cycle's and (b) total constrained modulus reduction vs. initial UCS

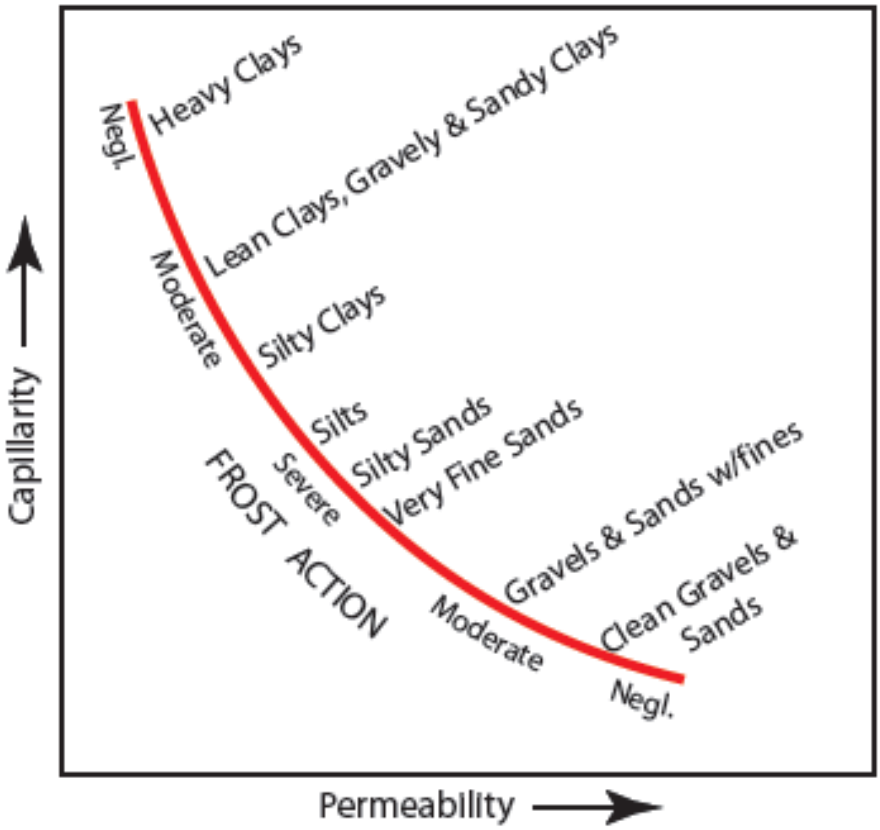

Figure 4.8. Frost susceptibility of subgrade soil (ACPA)

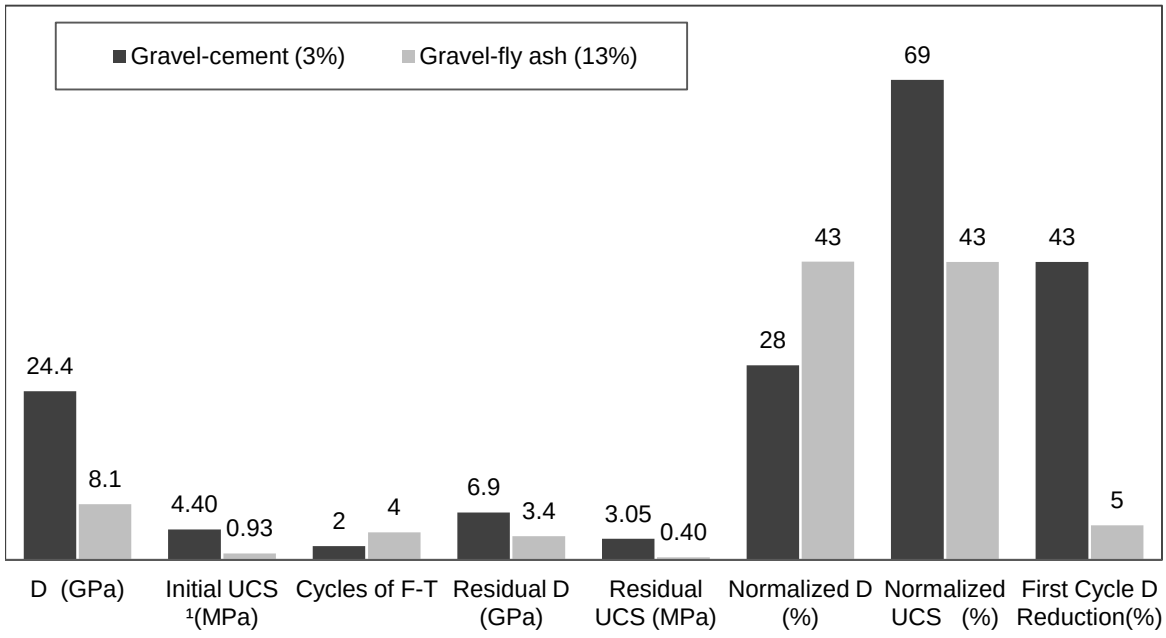

(a)

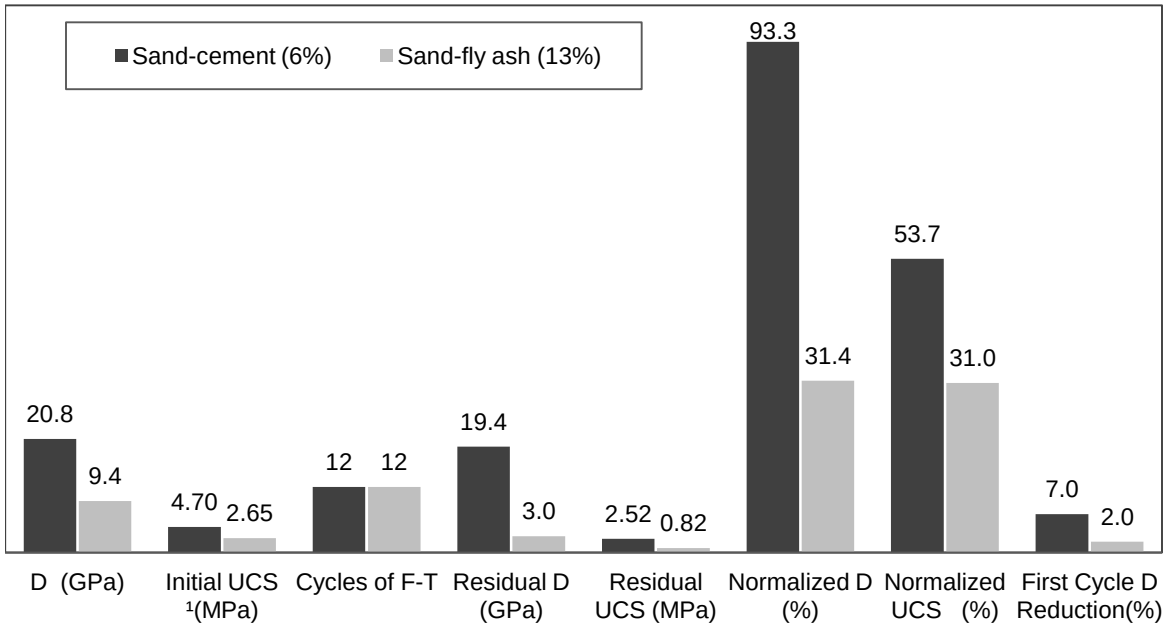

(b)

Figure 4.9. Comparison of constrained modulus, number of cycles to failure, residual UCS, constrained modulus reduction and UCS for (a) gravel-cement (3%) and gravel-fly ash (13%) (b) sand-cement (6%) and sand- fly ash (13%) (freeze-thaw cycling)

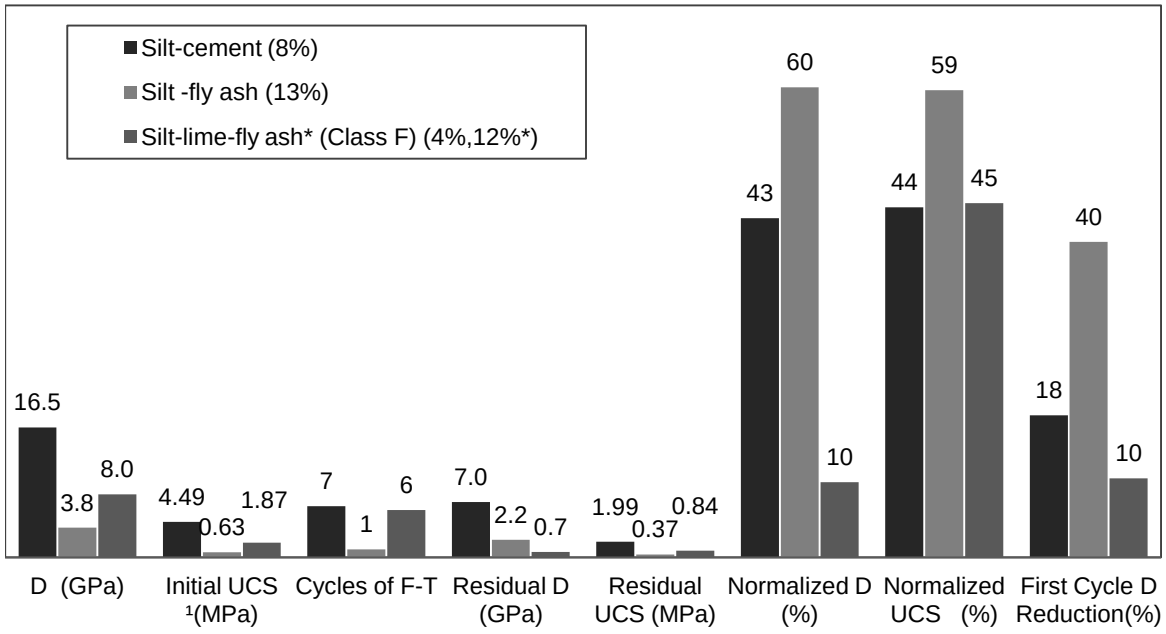

(a)

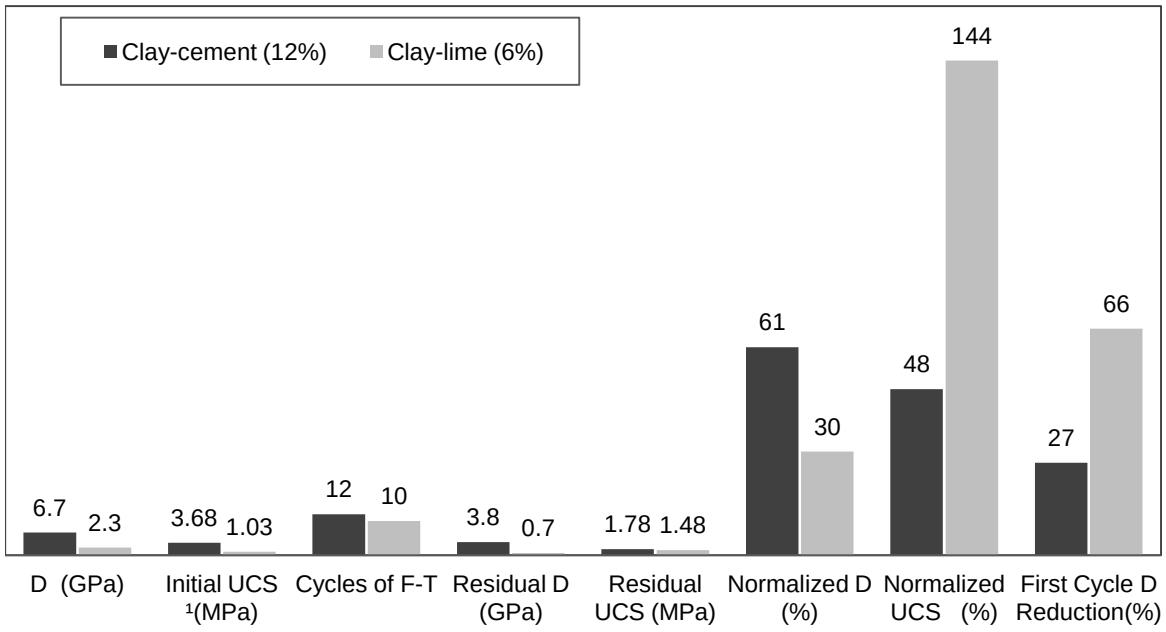

(b)

Figure 4.10. Comparison of constrained modulus, number of cycles to failure, residual UCS, constrained modulus reduction and UCS for (a) silt-cement (3%), silt-fly ash (13%) and silt-lime-fly ash* (4%,12%*) (b) clay-cement (12%) and clay-lime (6%) (freeze-thaw cycling)

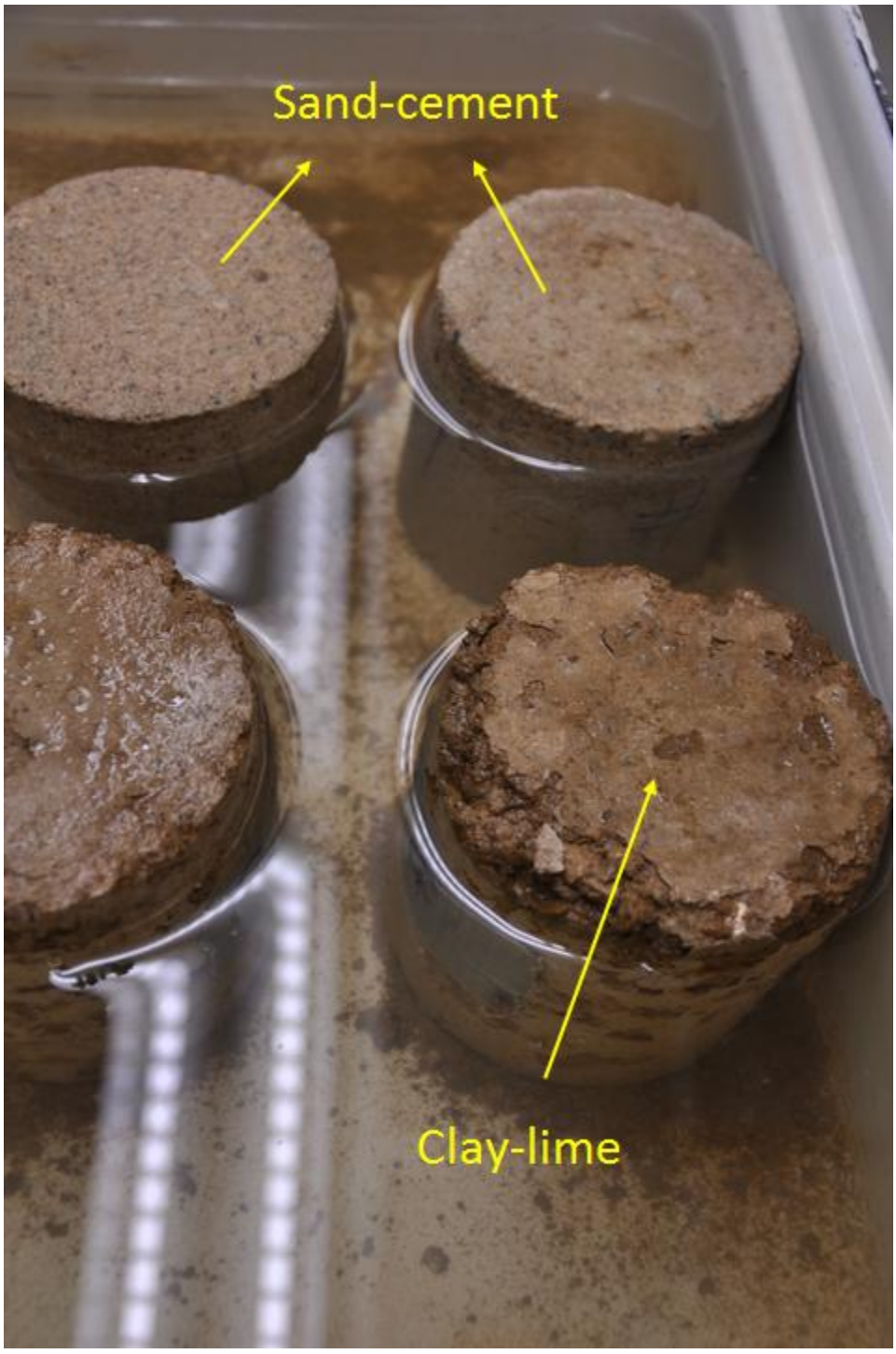

Figure 4.11. Sand-cement and clay-lime specimens subject to wet-dry cycling

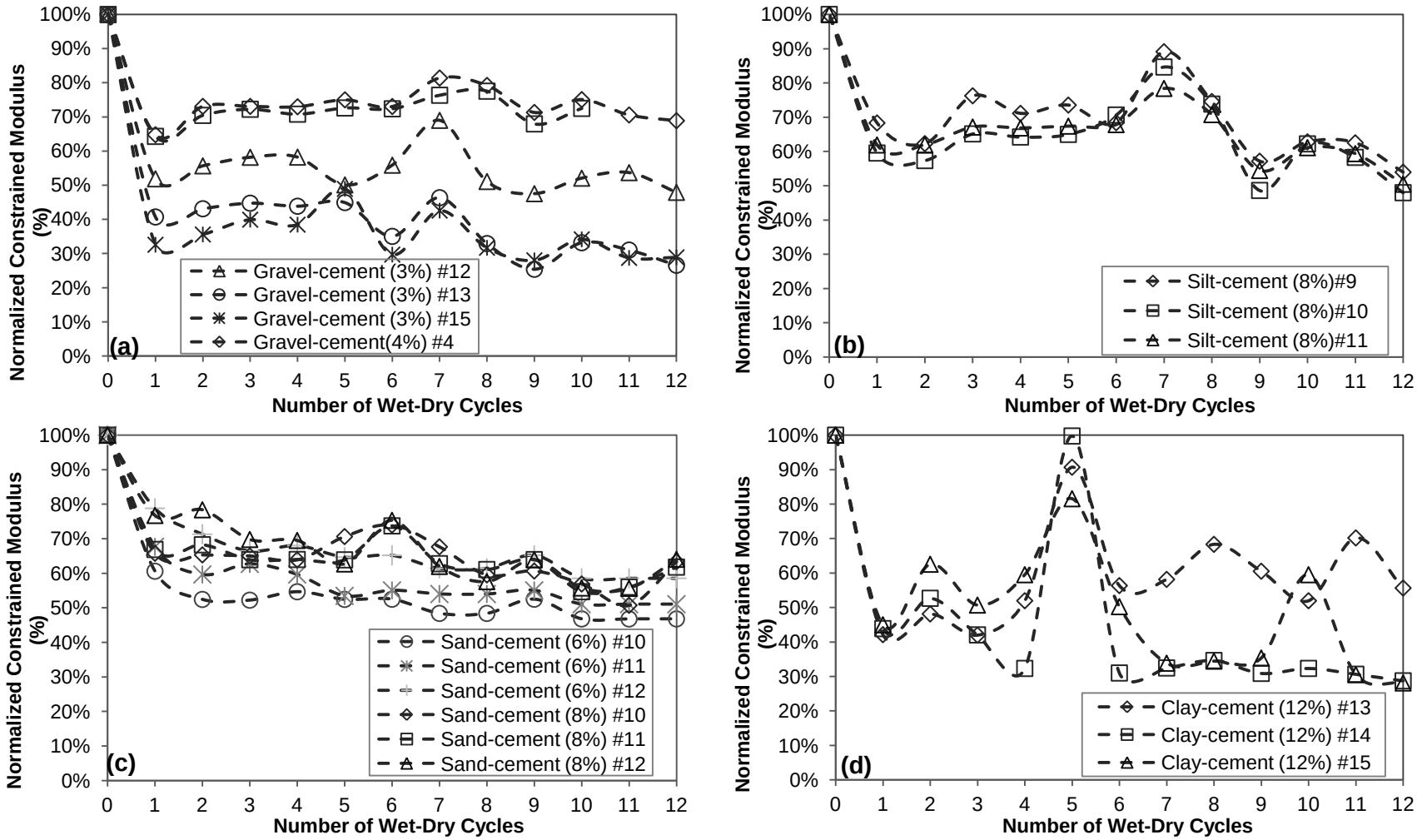

Figure 4.12. Normalized constrained modulus vs. number of wet-dry cycles of (a) gravel-cement with cement content 3% and 4% (b) silt-cement with cement content 8% (c) sand-cement with cement content 8% and 6% (d) clay-cement with cement content 12%

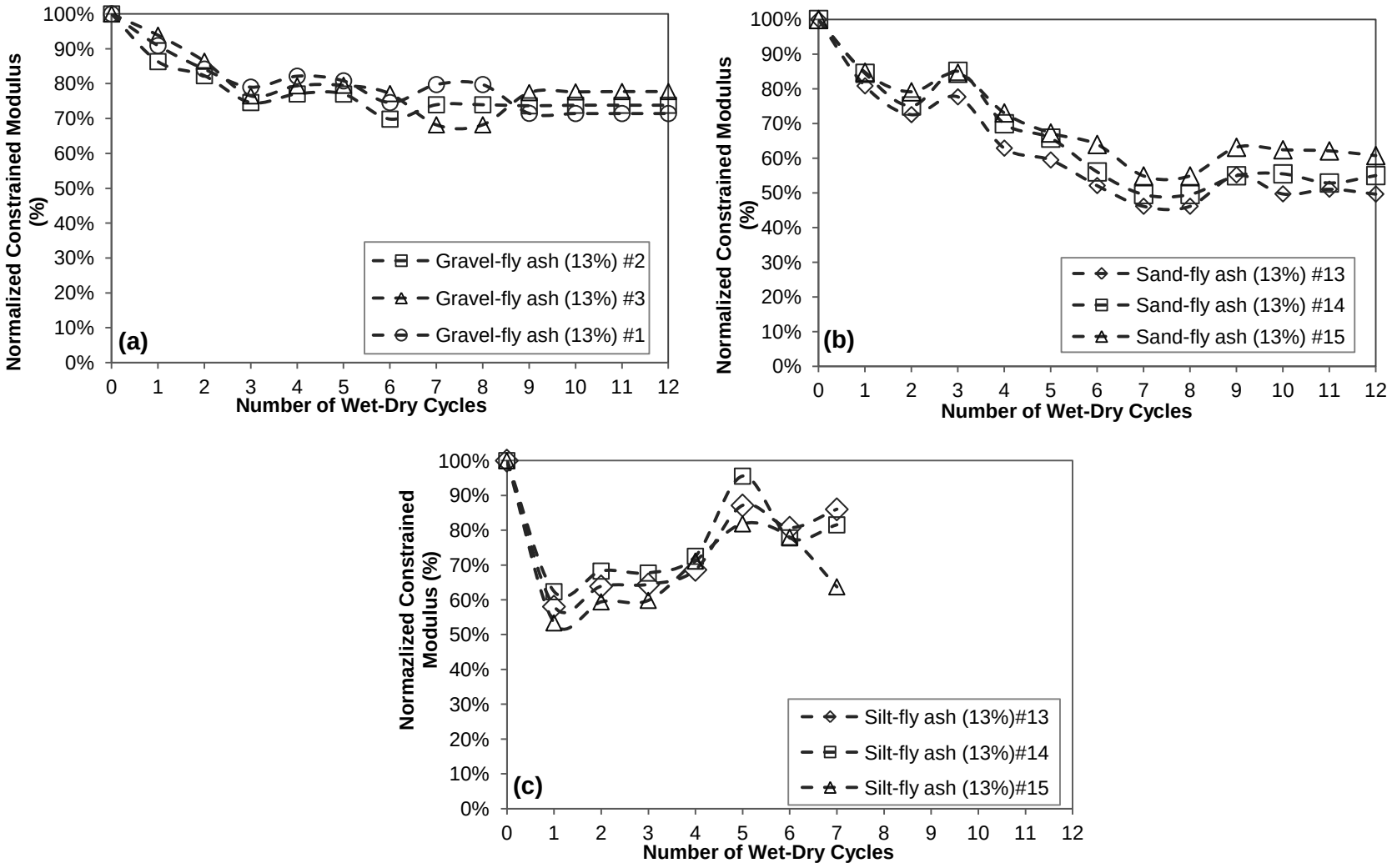

Figure 4.13. Normalized constrained modulus vs. number of wet-dry cycles of (a) gravel-fly ash with fly ash content 13% (b) sand-fly ash with fly ash content 13% (c) silt-fly ash with fly ash content 13%

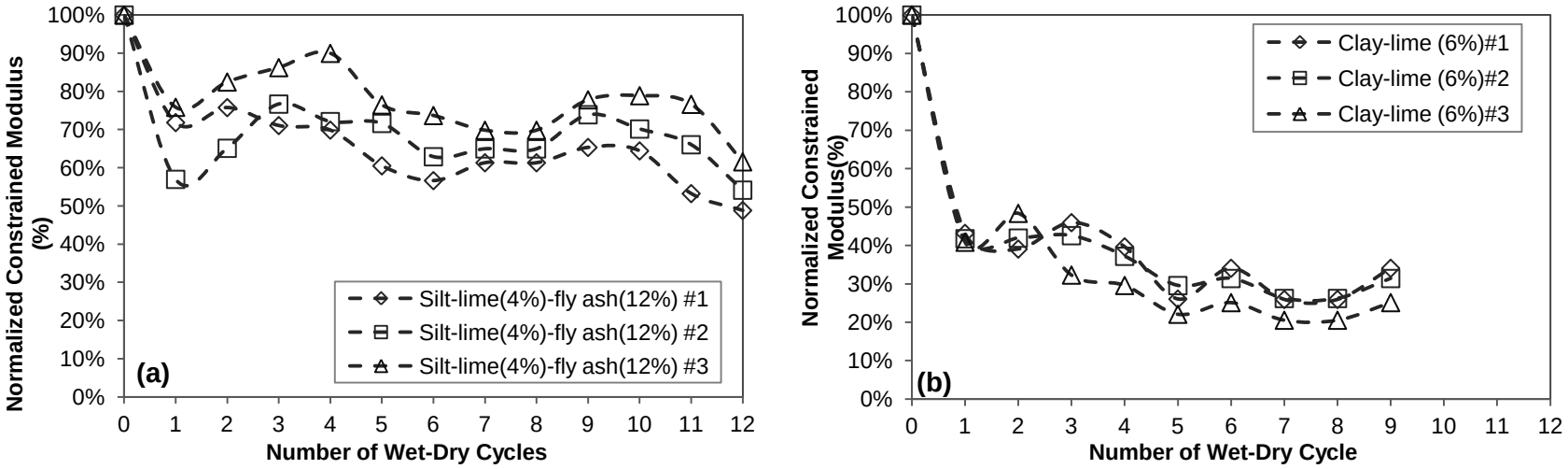

Figure 4.14. Normalized constrained modulus vs. number of wet-dry cycles of (a) silt-lime-fly ash with lime content 4% and fly ash content 13% (b) clay-lime with lime content 6%

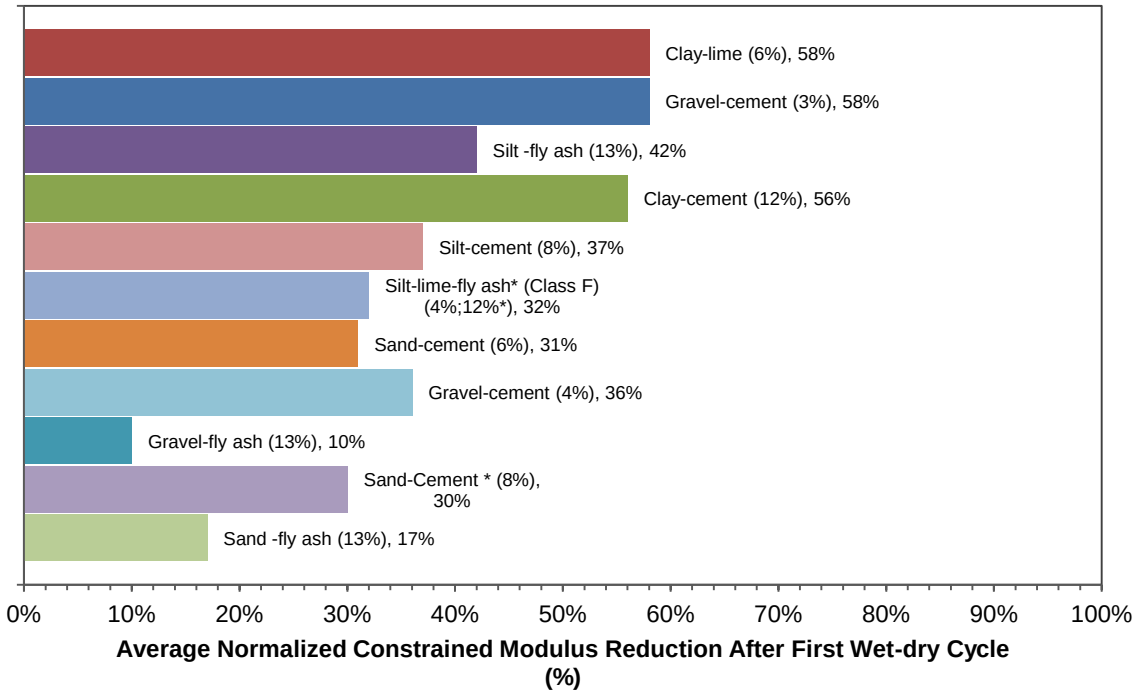

(a)

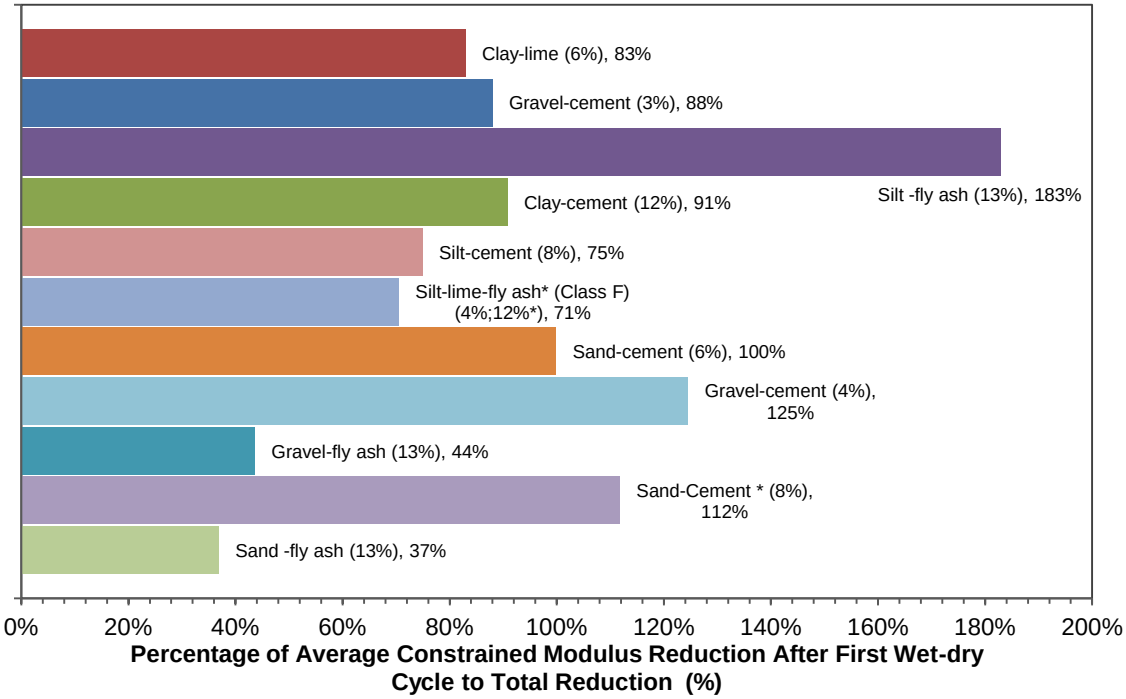

(b)

Figure 4.15. (a) Constrained modulus reduction after first wet-dry cycle (b) percentage of constrained modulus reduction to total reduction after first wet-dry cycle

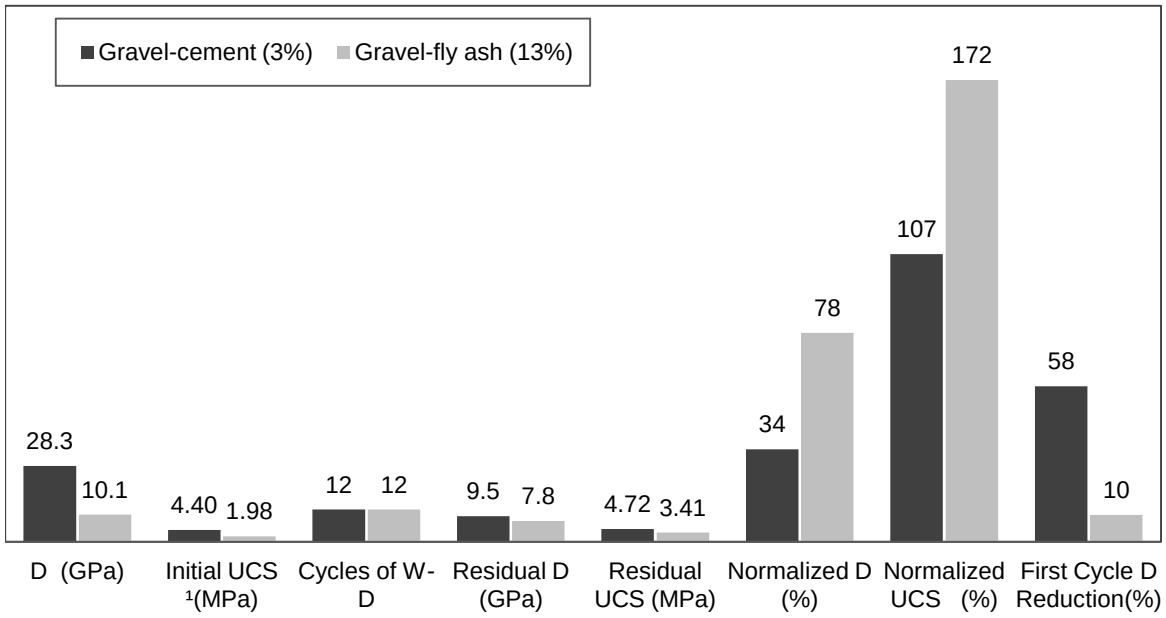

(a)

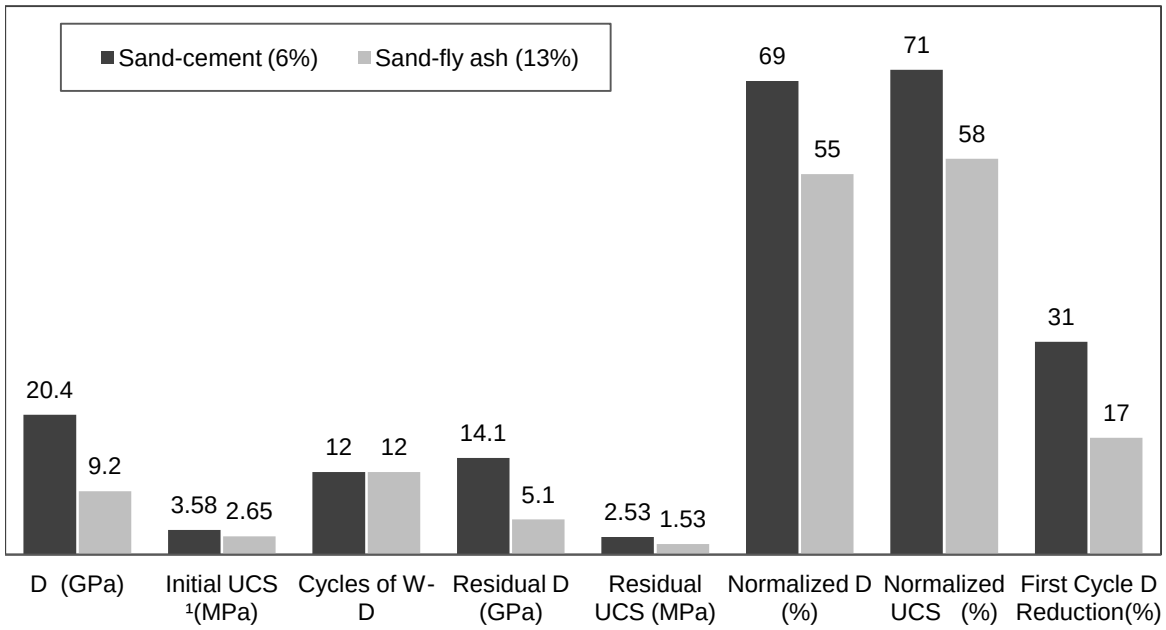

(b)

Figure 4.16. Comparison of constrained modulus, number of cycles to failure, residual UCS, constrained modulus reduction and UCS for (a) gravel-cement (3%) and gravel-fly ash (13%) (b) sand-cement (6%) and sand- fly ash (13%) (wet-dry cycling)

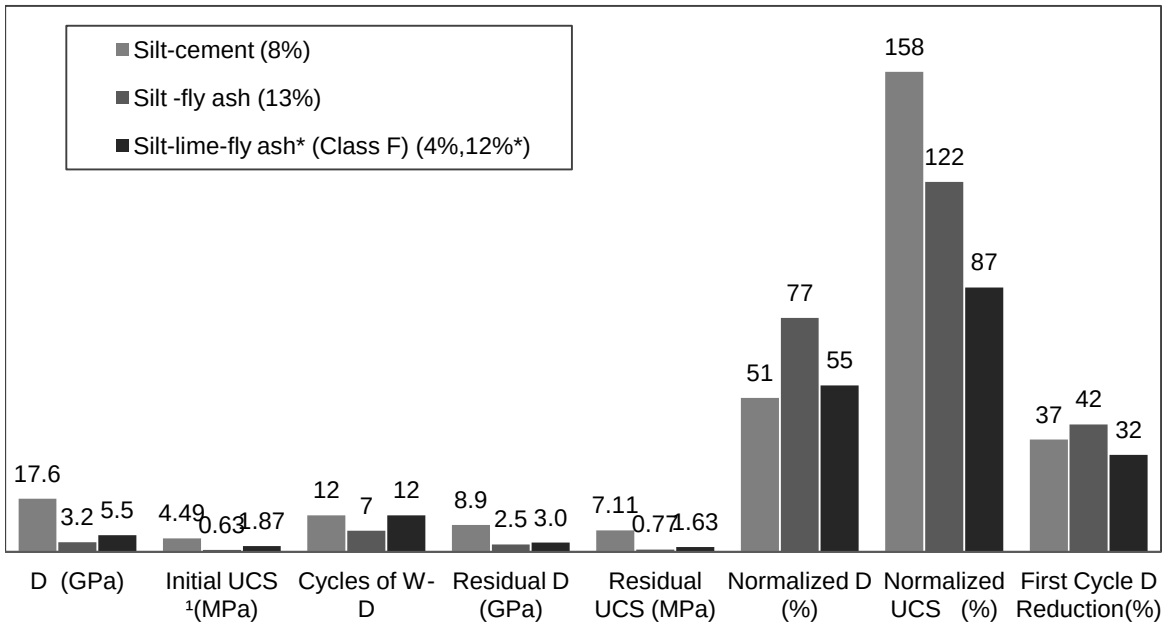

(a)

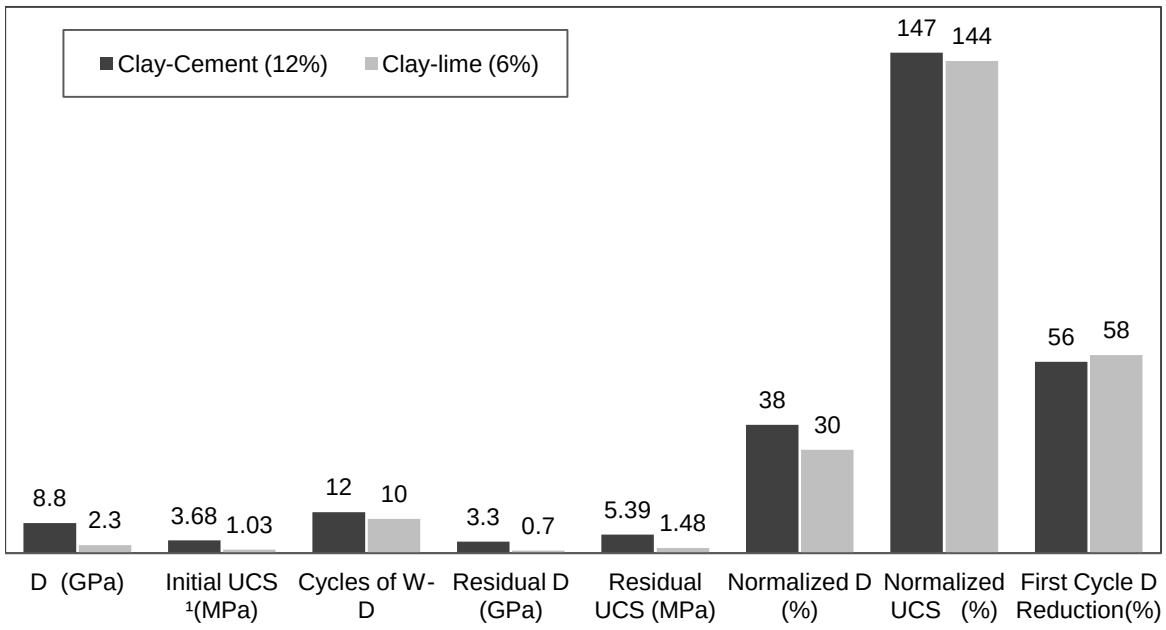

(b)

Figure 4.17. Comparison of constrained modulus, number of cycles to failure, residual UCS, constrained modulus reduction and UCS for (a)silt-cement (3%), silt-fly ash (13%) and silt-lime-fly ash* (4%,12%*) (b) clay-cement (12%) and clay-lime (6%) (wet-dry cycling)

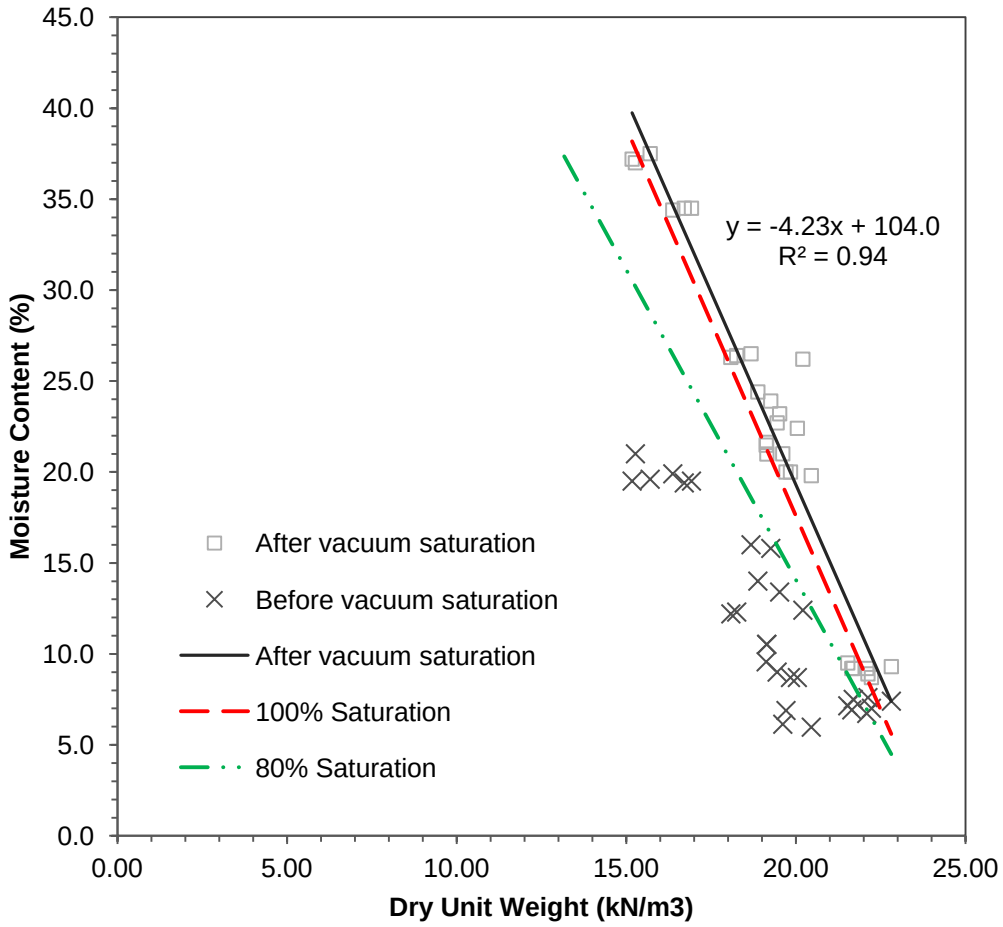

Figure 4.18. Relationship between dry unit weight and moisture content for specimens tested in vacuum saturation

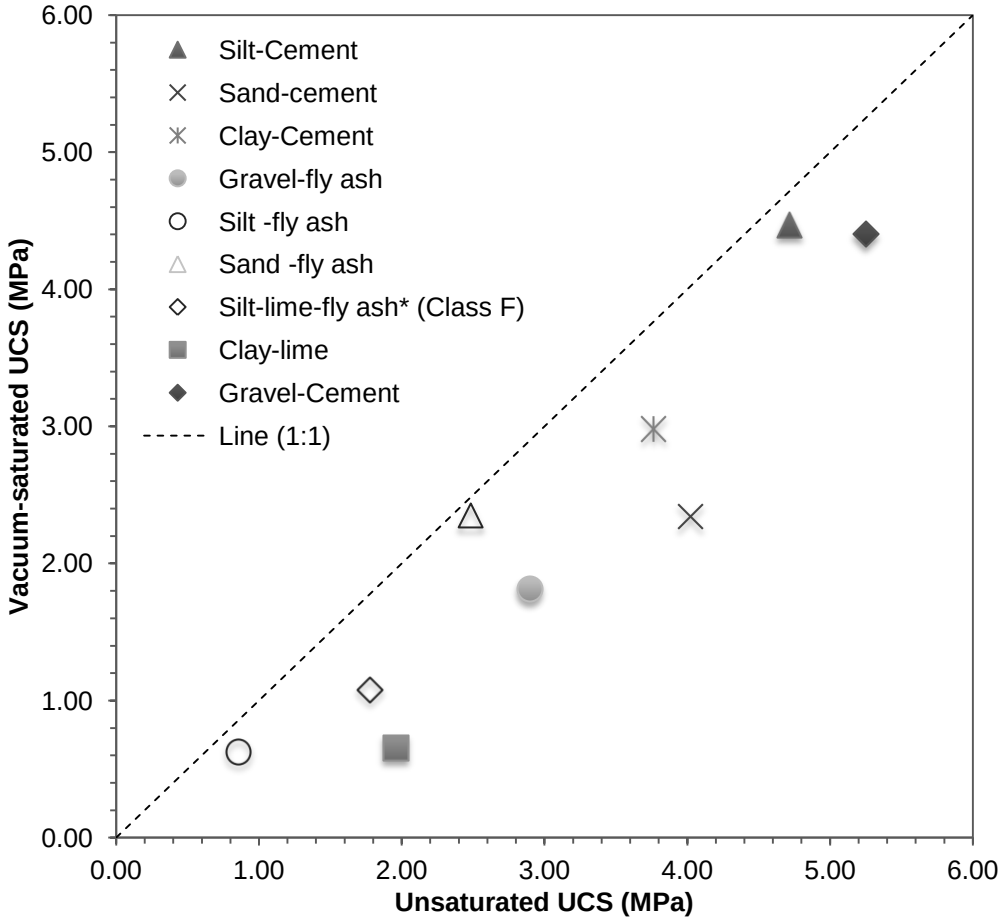

Figure 4.19. Unsaturated UCS vs. vacuum saturated UCS

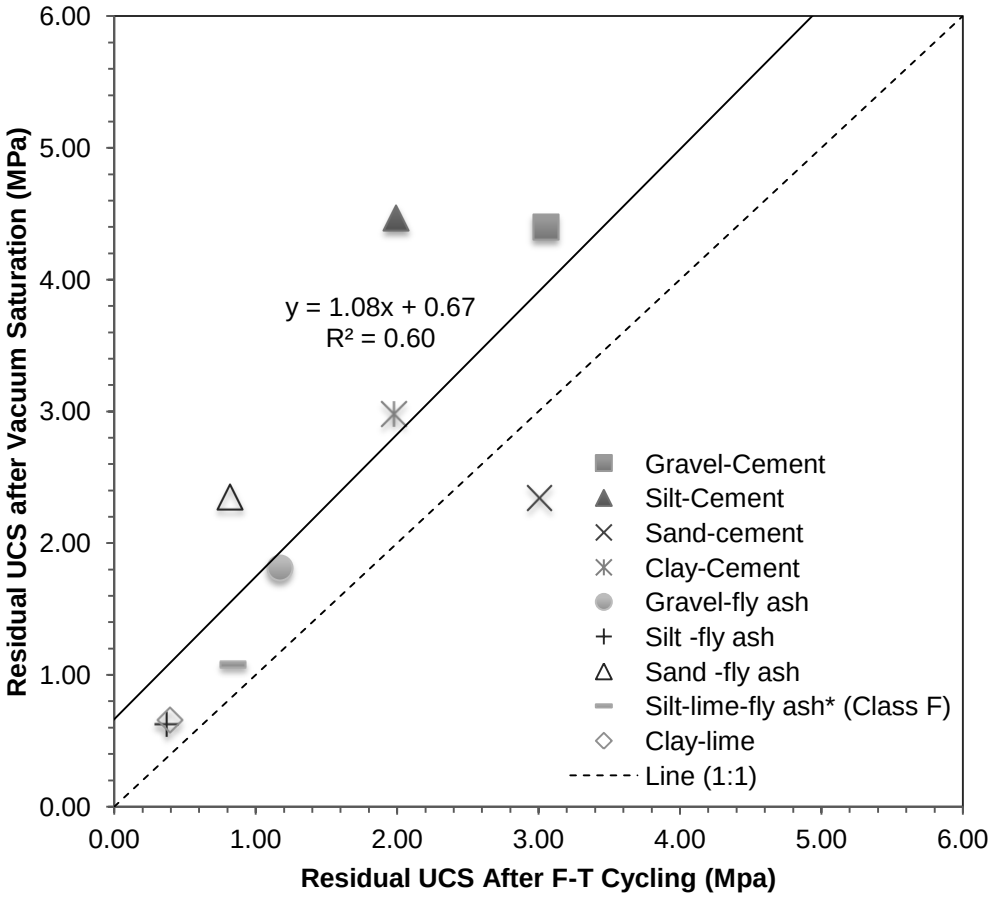

Figure 4.20. Residual UCS after freeze-thaw cycling vs. vacuum saturated UCS

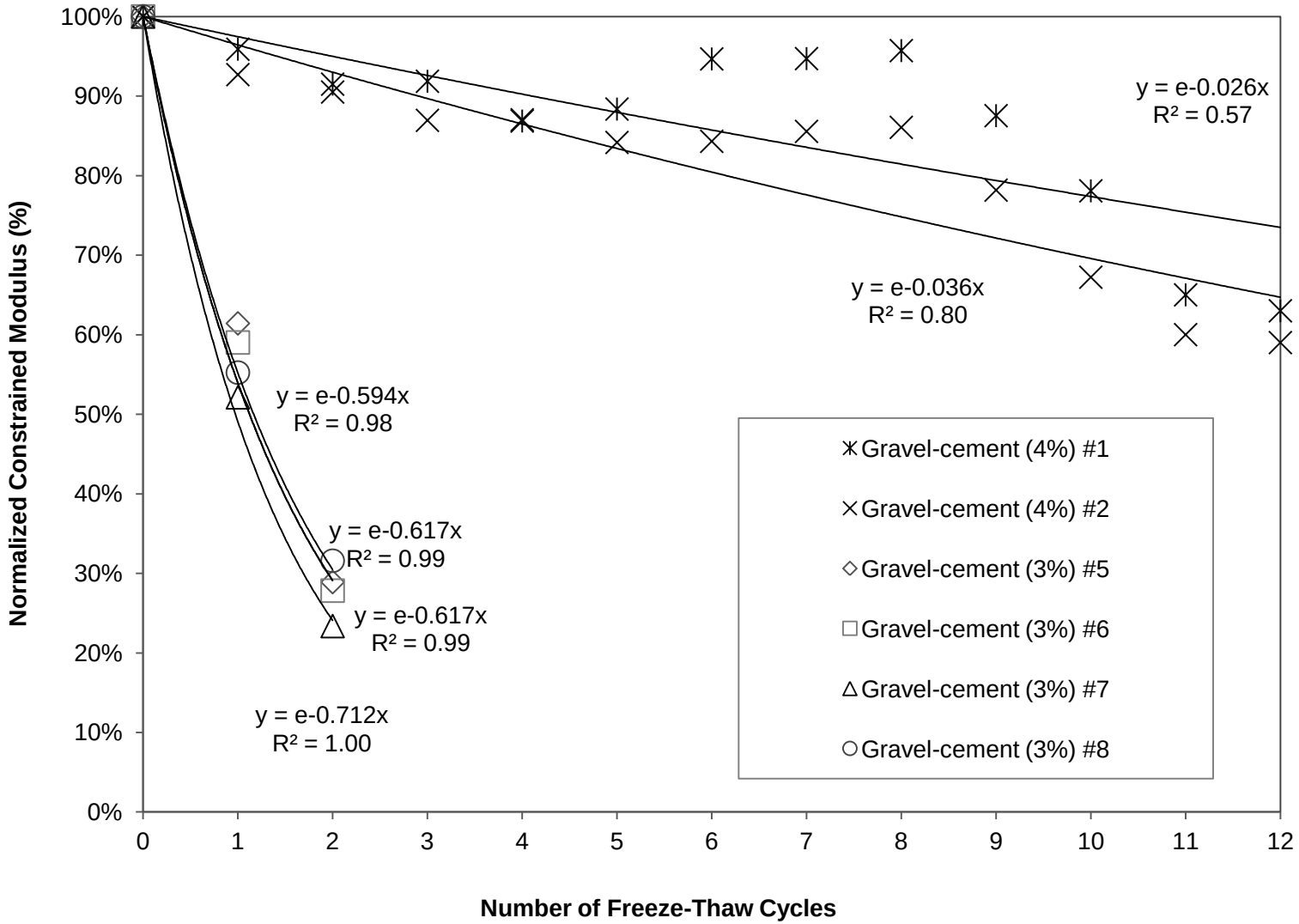

Figure 5.1. Freeze-thaw cycling model development for gravel-cement

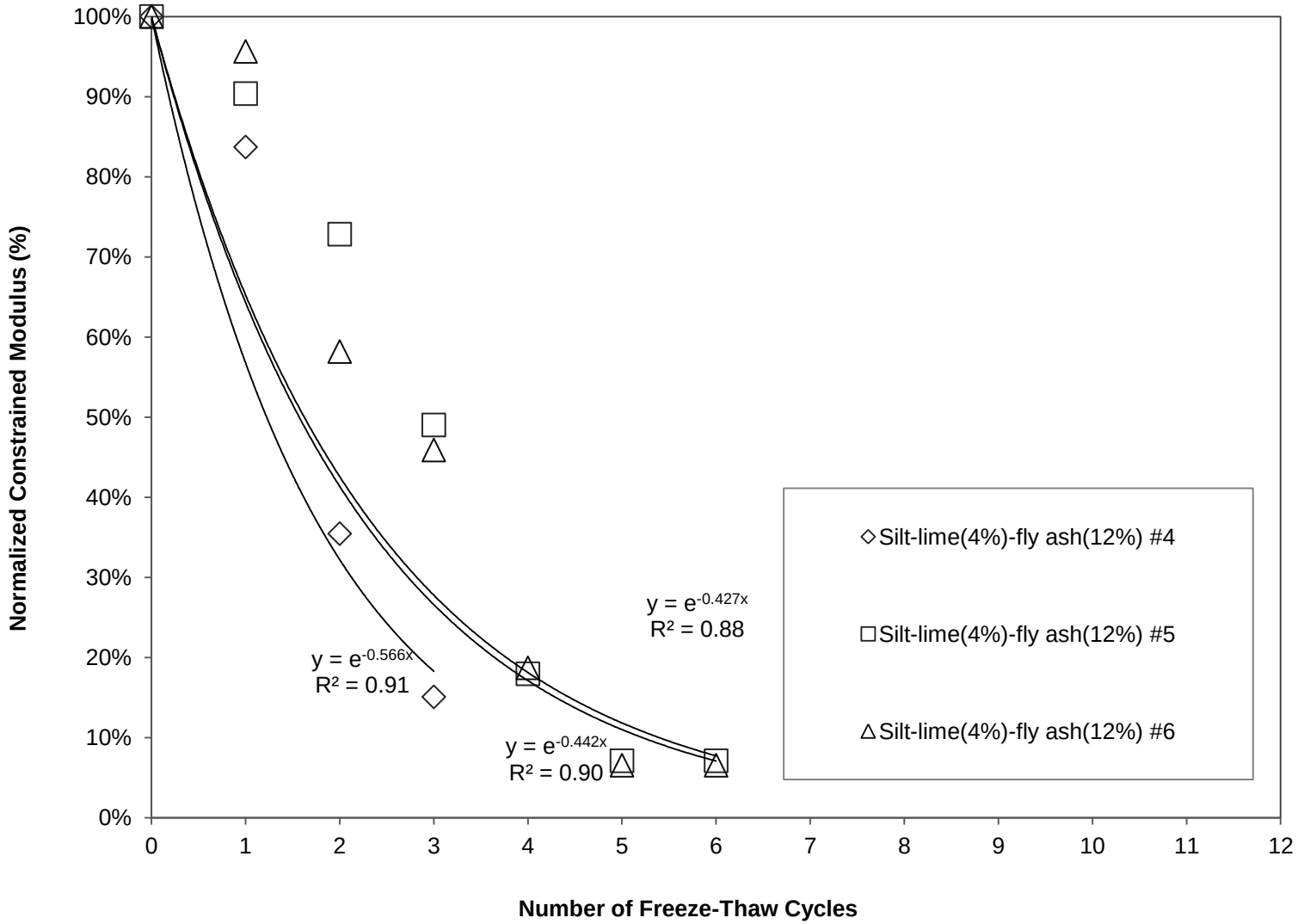

Figure 5.2. Freeze-thaw cycling model development for silt-lime-fly ash

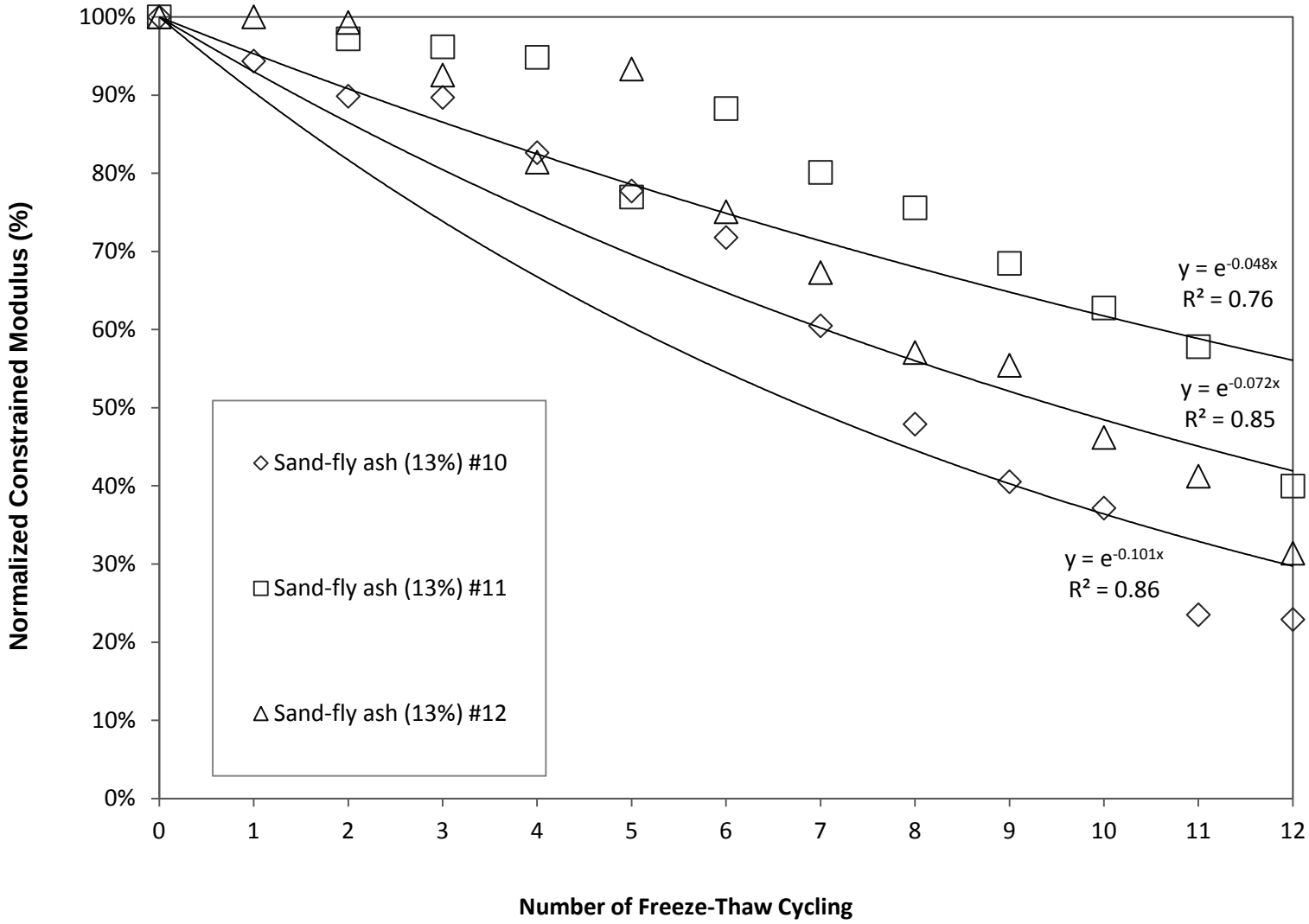

Figure 5.3. Freeze-thaw cycling model development for silt-lime-fly ash

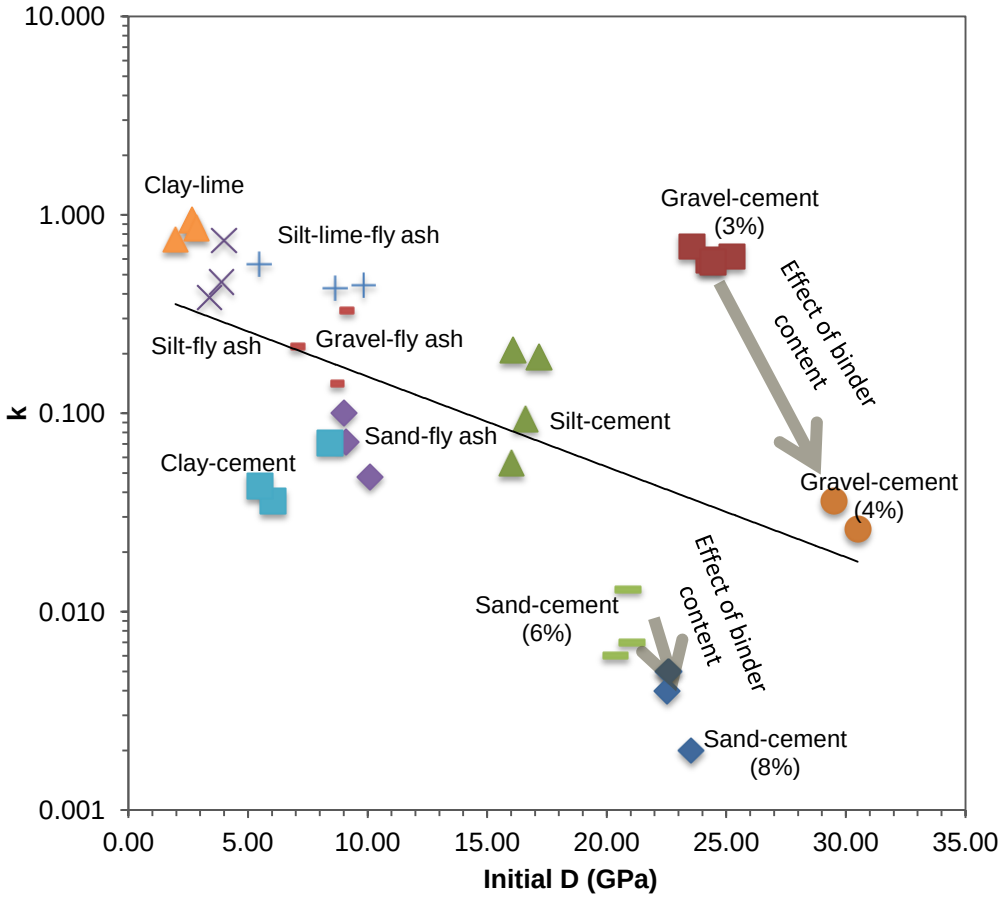

Figure 5.4. Initial Constrained Modulus, D, vs. k

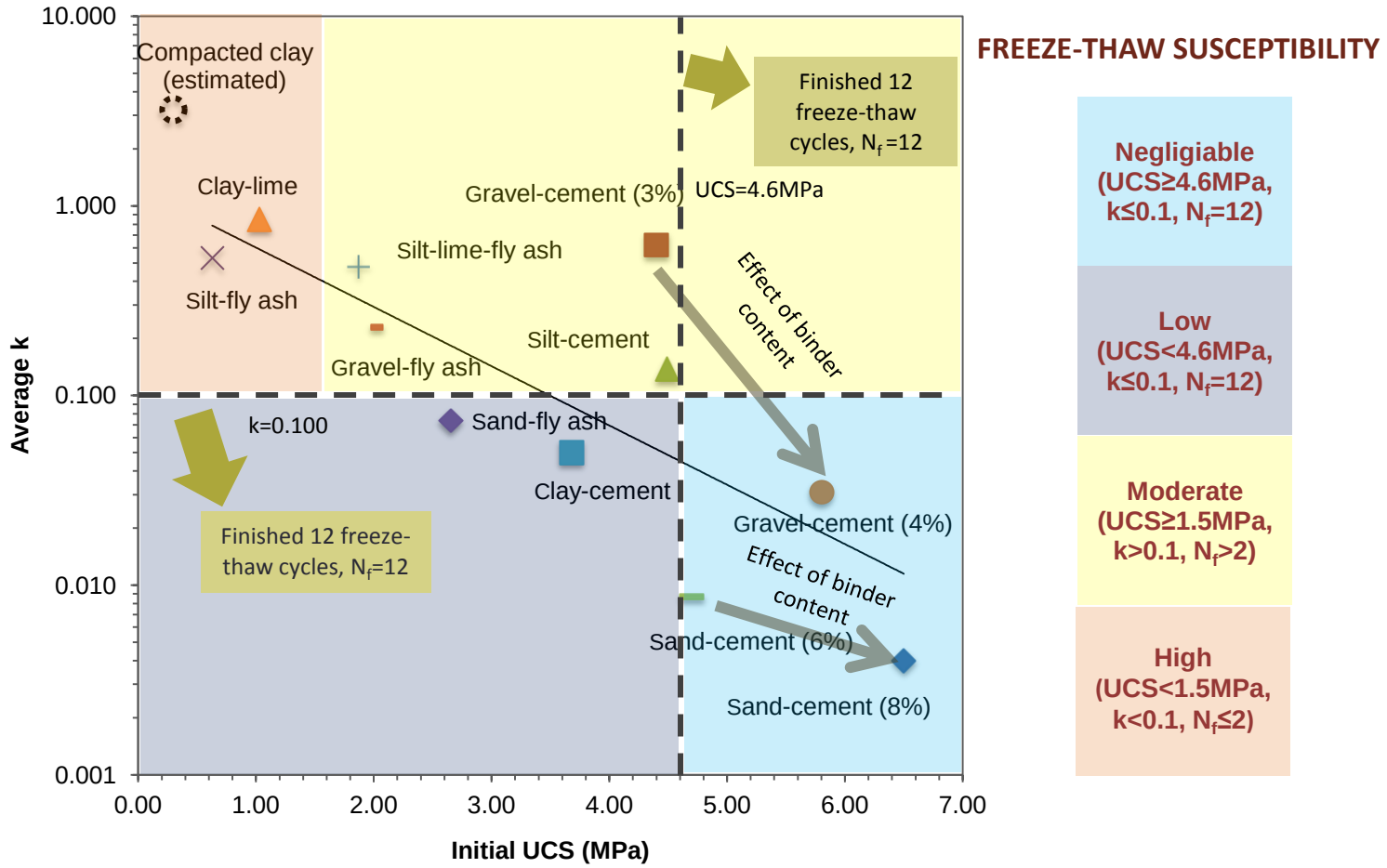

Figure 5.5. Initial UCS vs. k

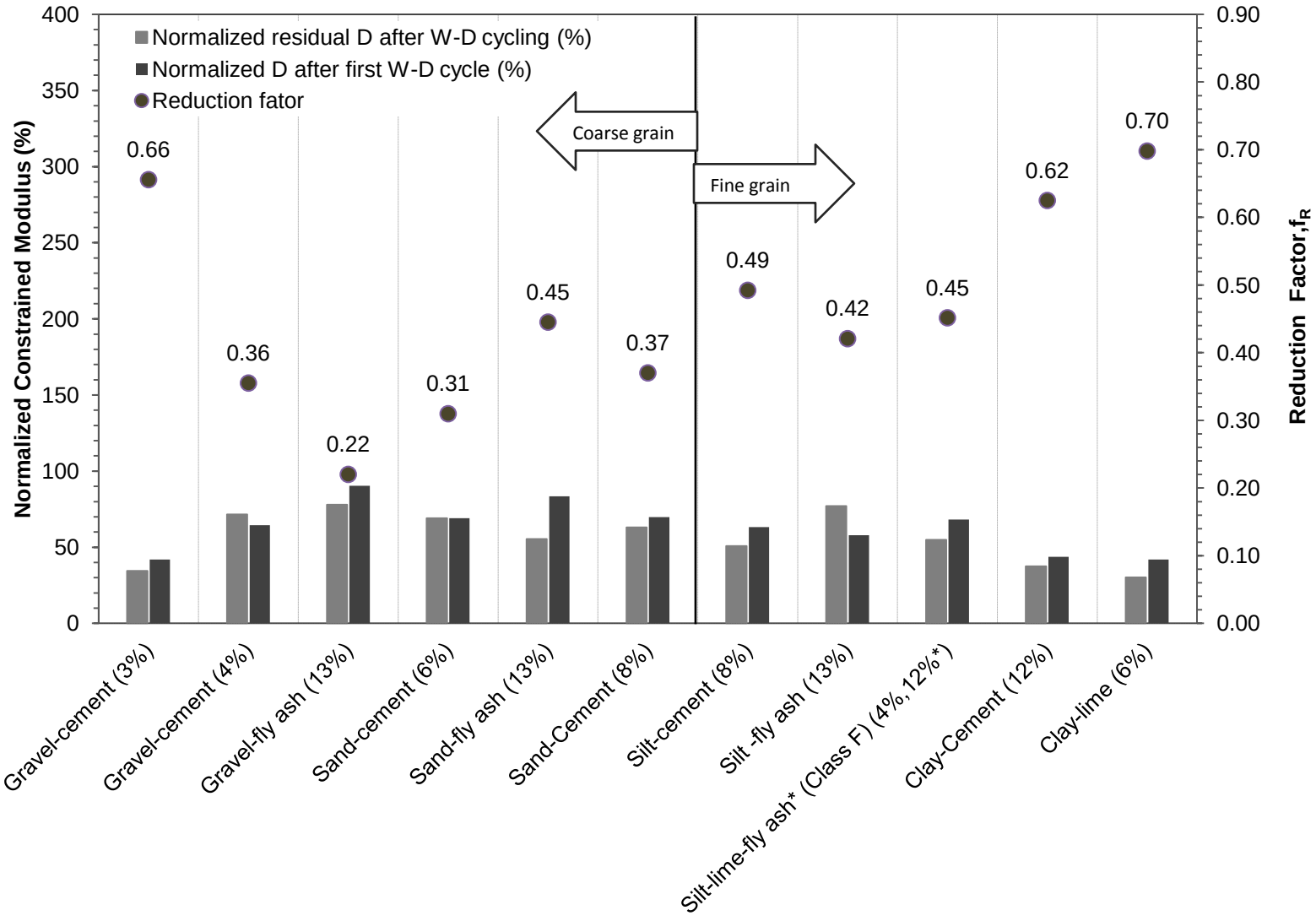

Figure 5.6. Normalized constrained modulus and reduction factor for W-D cycling

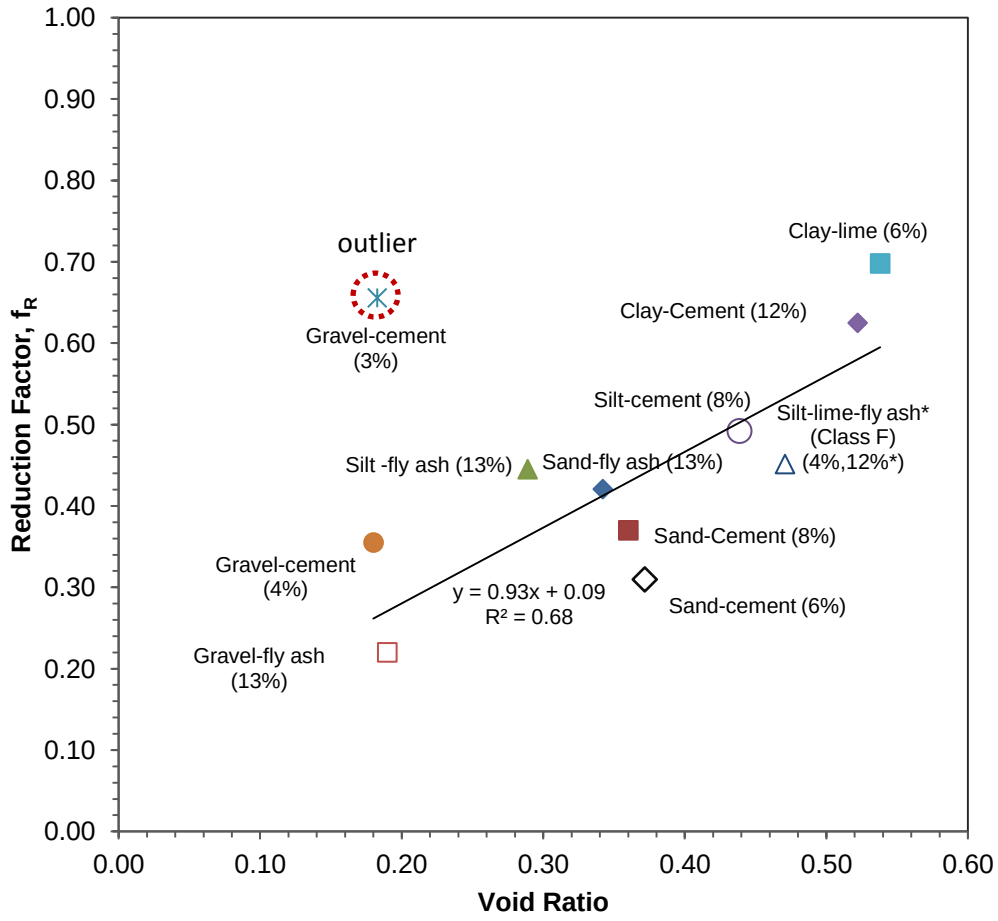

Figure 5.7. Reduction factor, f_R vs. void ratio for wet-dry cycling

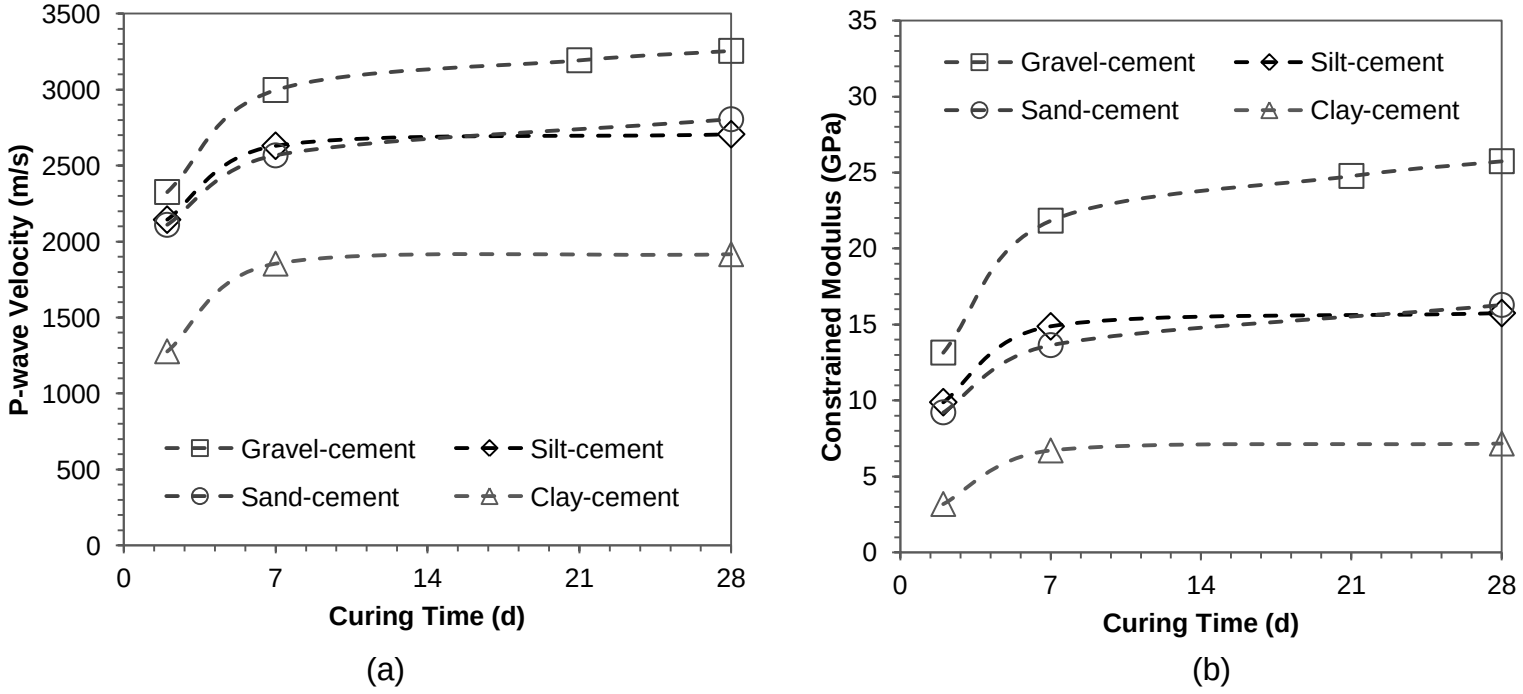

Figure 6.1. (a) P-wave velocity and (b) constrained modulus change vs. curing time for cement-stabilized soils

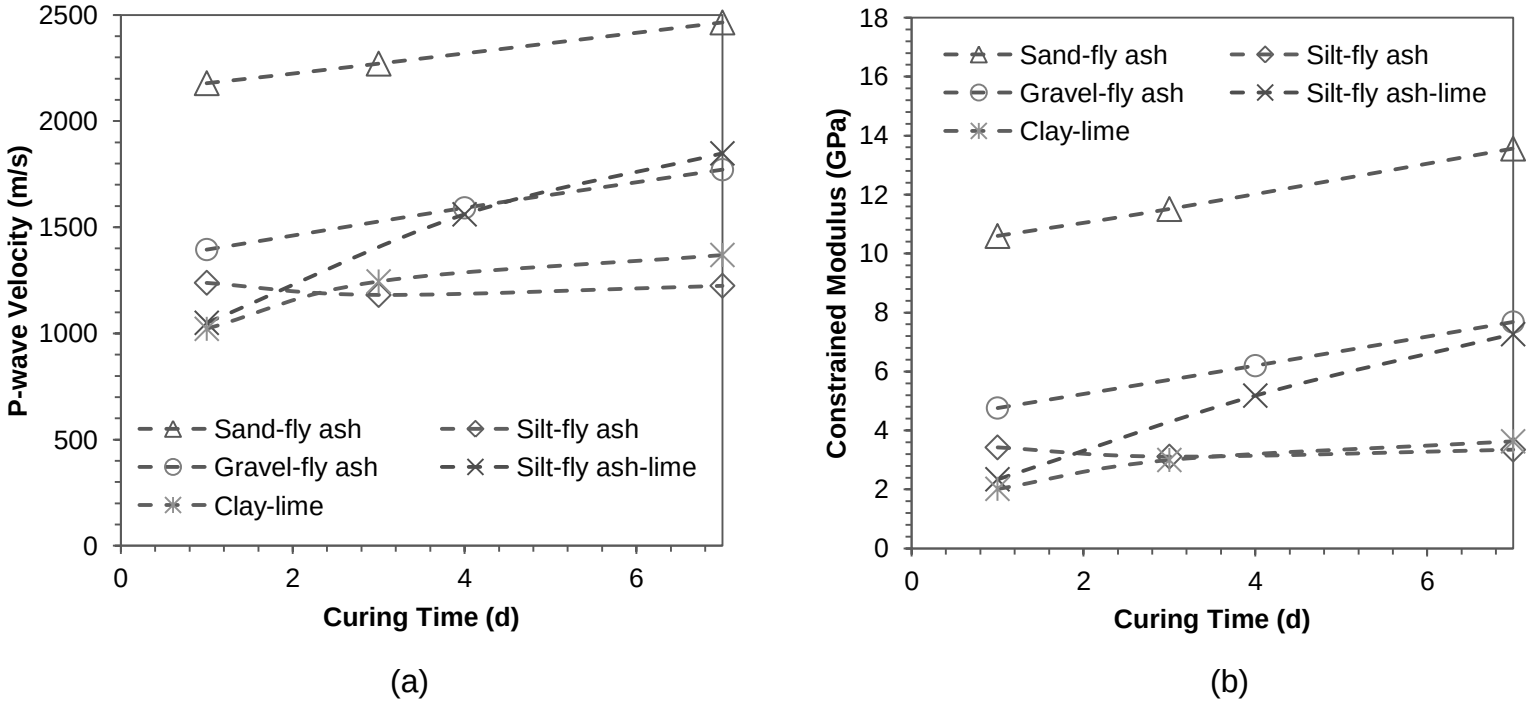

Figure 6.2. (a) P-wave velocity and (b) constrained modulus vs. curing time for fly ash- and lime-stabilized soil

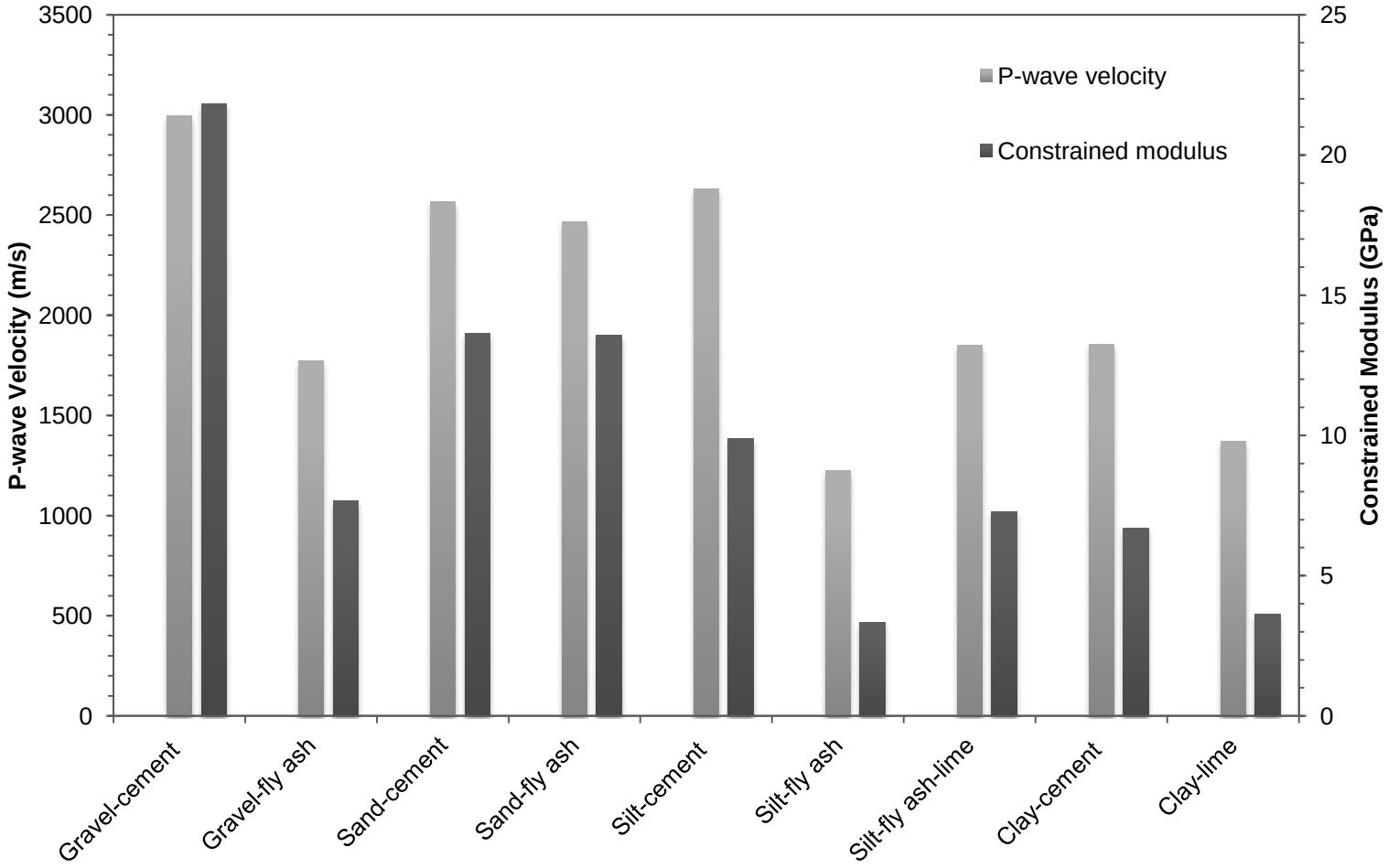

Figure 6.3. Comparison of P-wave velocity and constrained modulus of CSM after 7 days curing

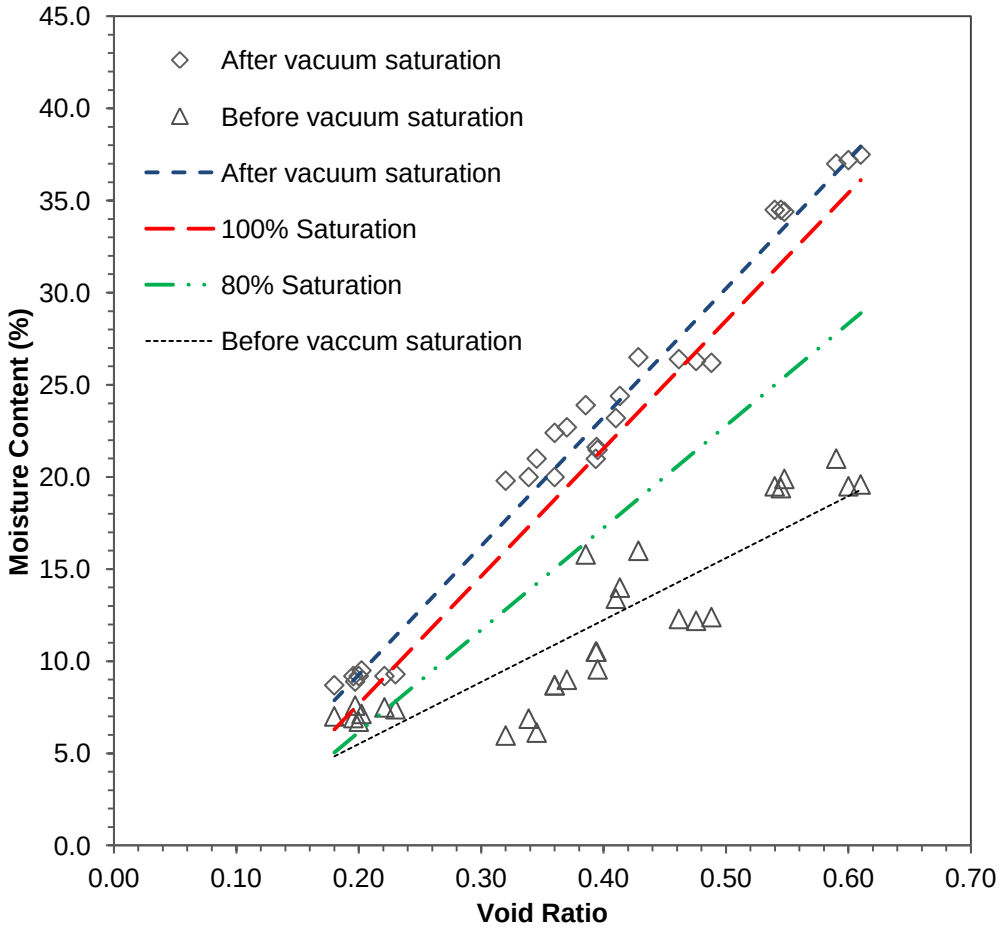

Figure 6.4. Vacuum saturation effect on degree of saturation of all CSMs

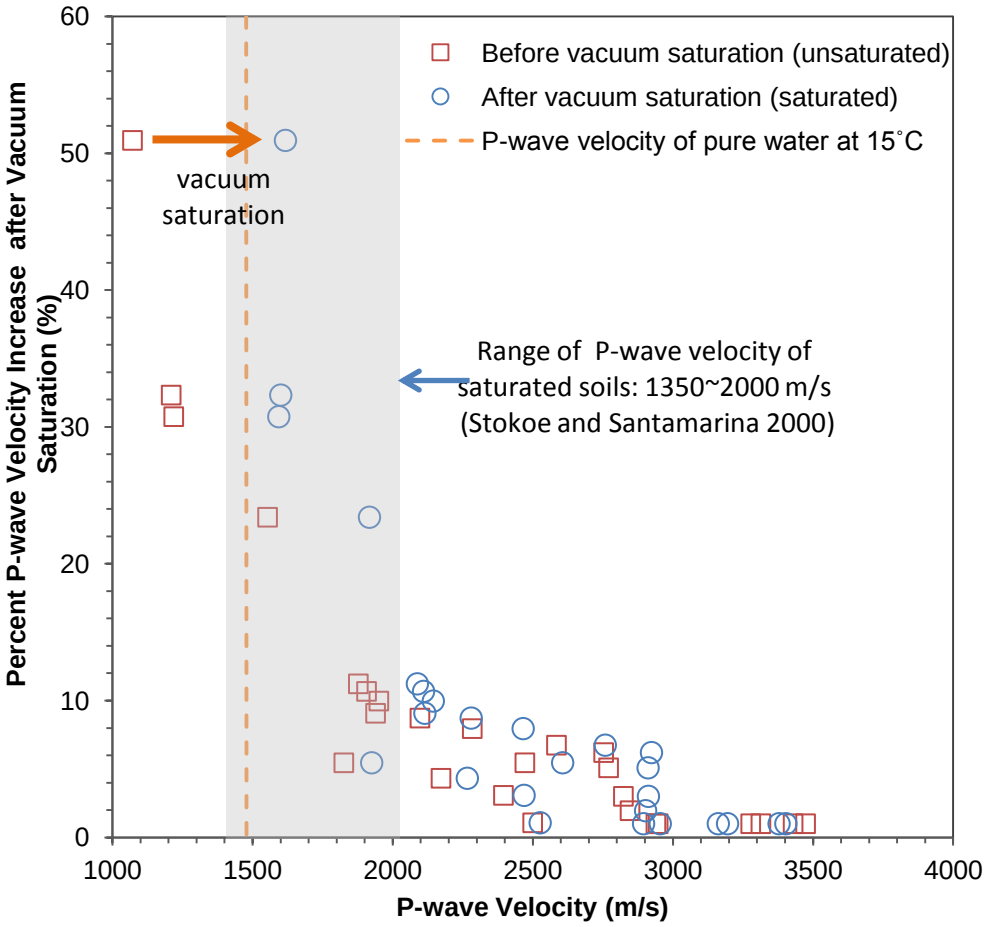

Figure 6.5. Percent increase in P-wave velocity after vacuum saturation vs. P-wave velocity

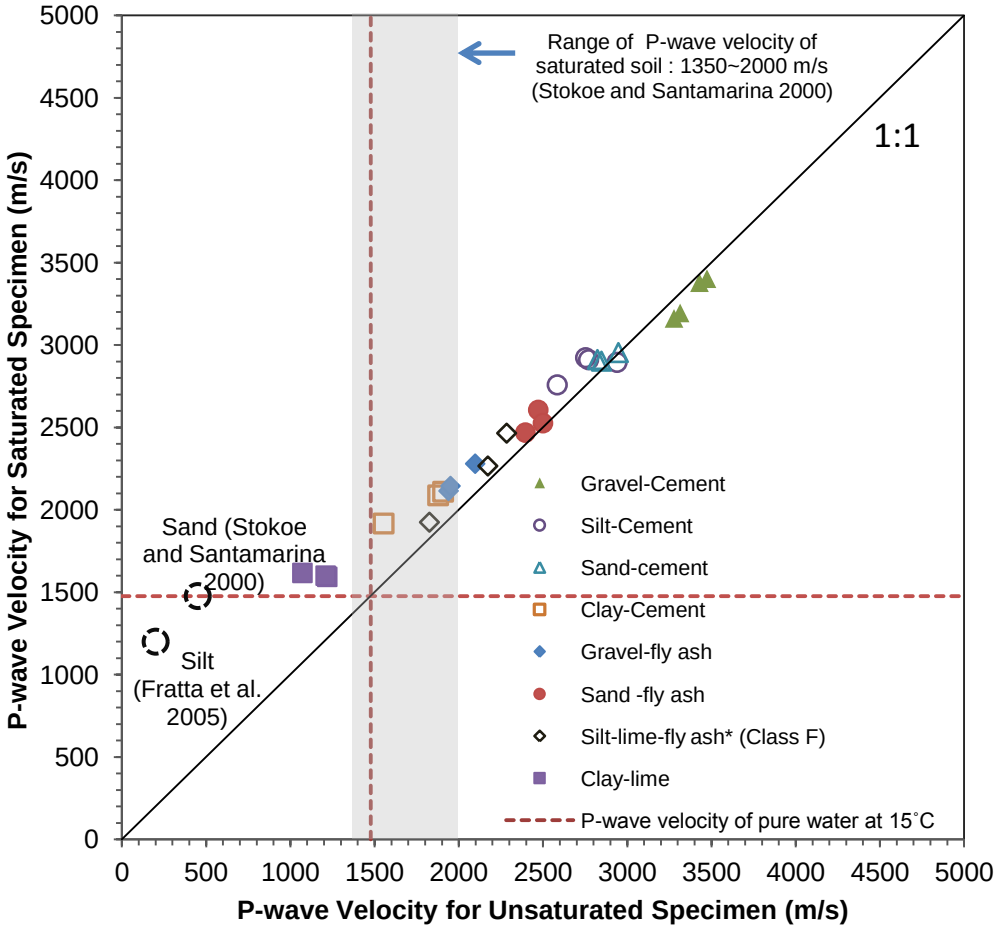

Figure 6.6. P-wave velocity for unsaturated specimen vs. P-wave velocity for saturated specimen

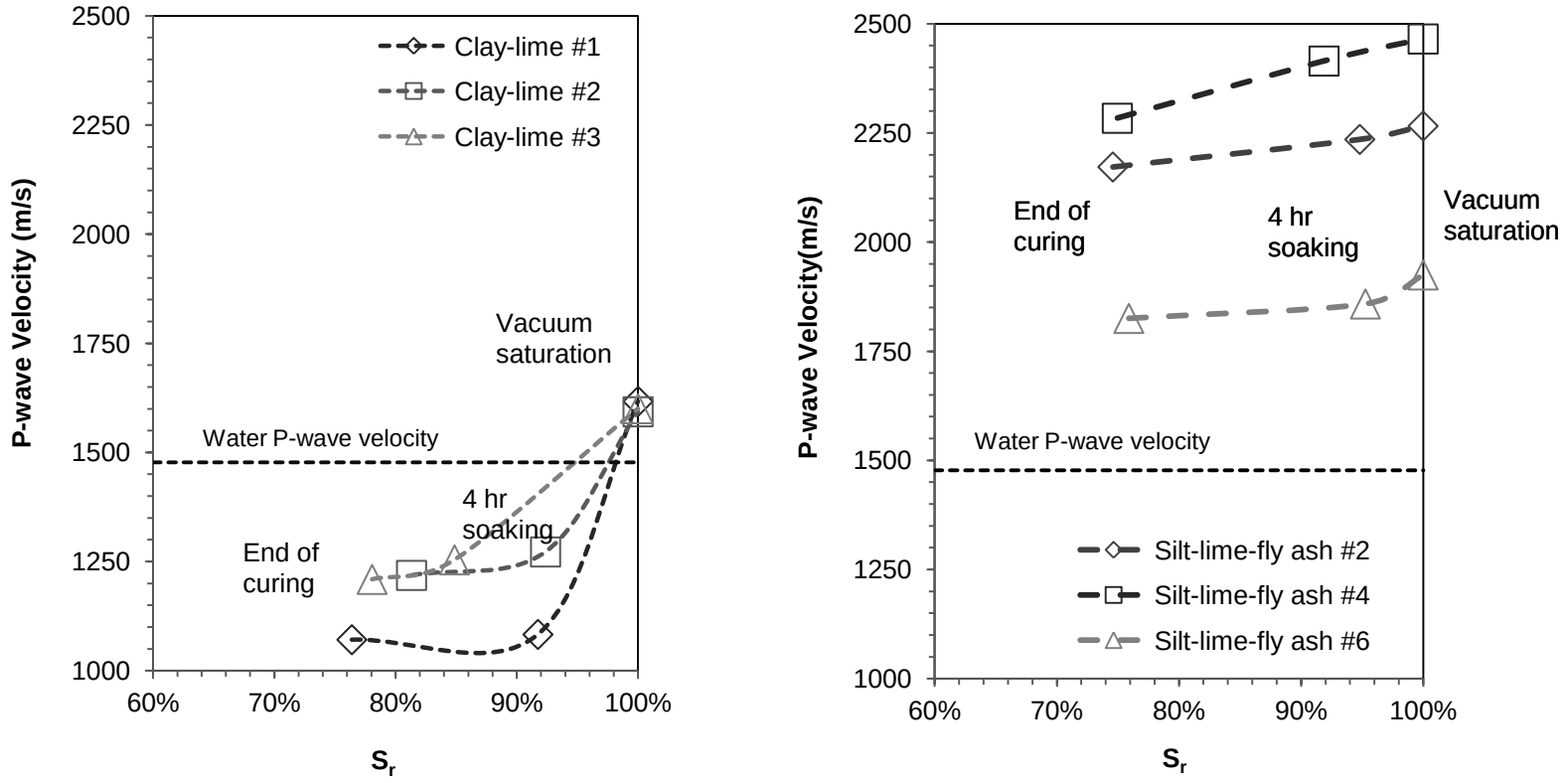

Figure 6.7. Degree of saturation vs. P-wave velocity of (a) Clay-lime (b) Silt-lime fly ash

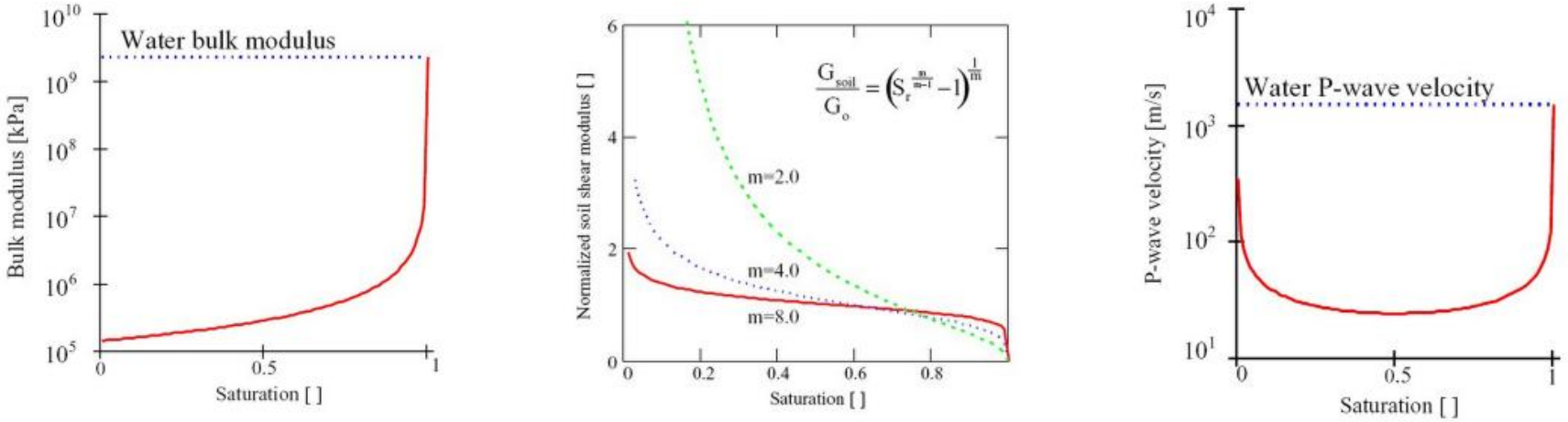

(a) (b) (c)

Figure 6.8. (a) Fluid bulk modulus (b) Normalized soil shear modulus (c) P-wave velocity versus degree of saturation (Curves for temperature 25 ˚C and atmospheric pressure 100 kPa, air stiffness =1.42·10^5 Pa and water stiffness=2.19·10^9 Pa) (Fratta et al. 2005)

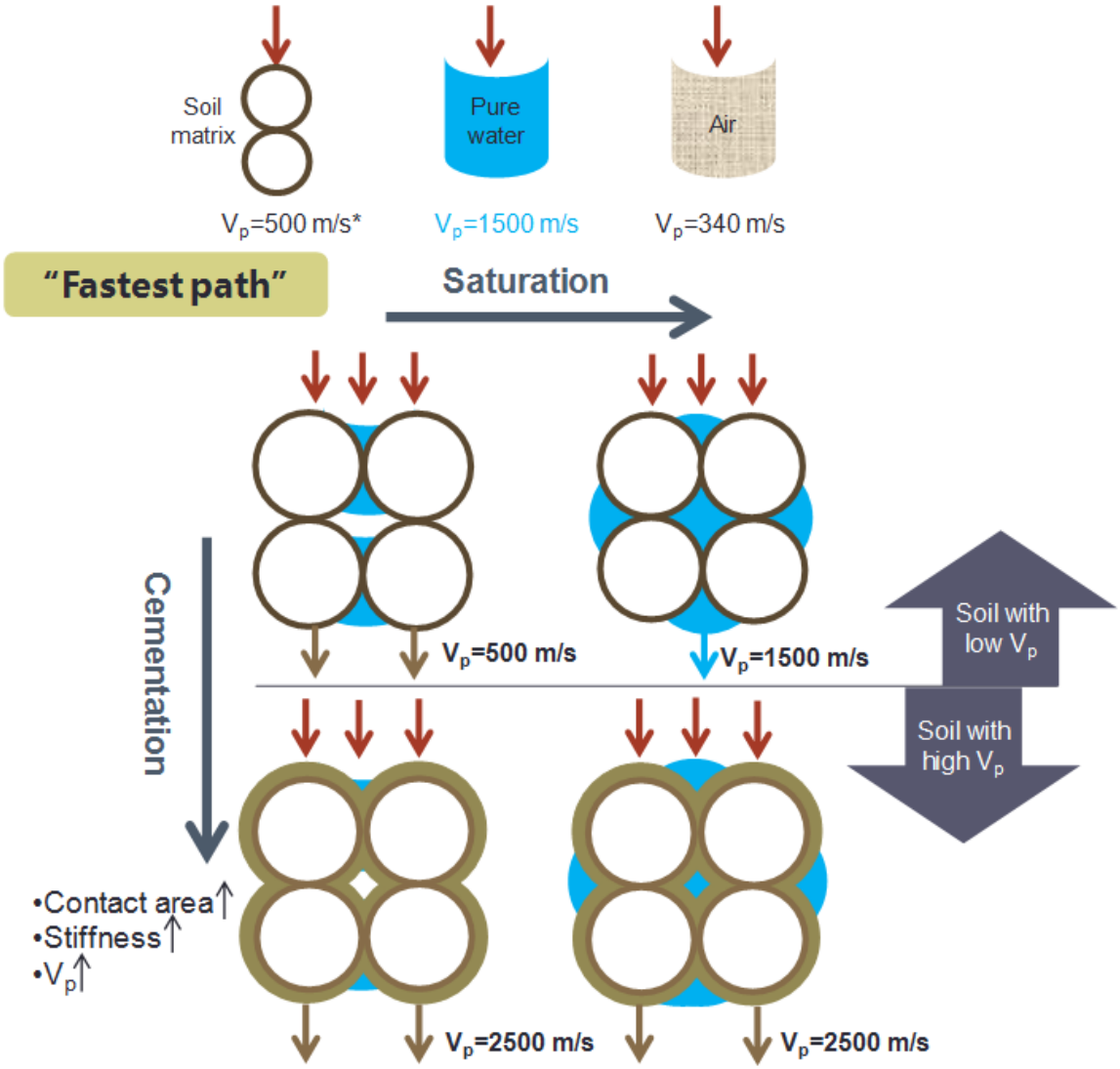

Figure 6.9. Saturation and cementation stiffening effect on granular soil specimens

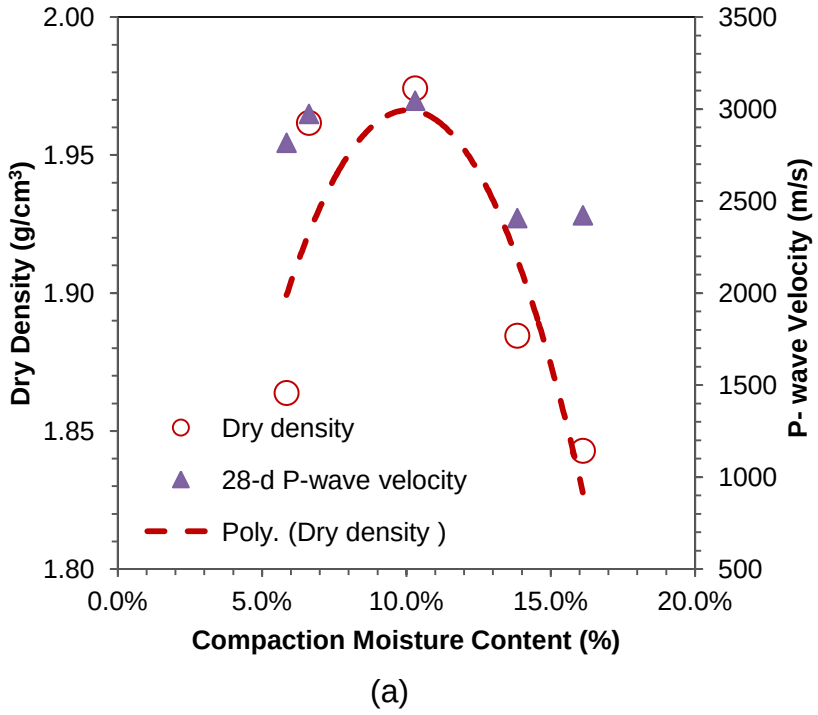

(a)

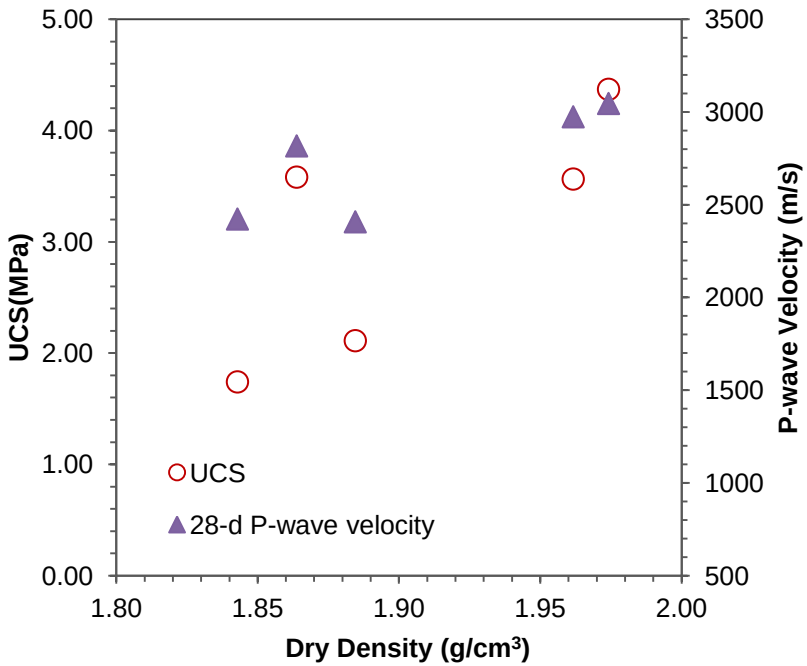

(b)

Figure 6.10. (a) Compaction characteristics of P-wave velocity (b) dry density effect on UCS and P-wave velocity of silt-cement.

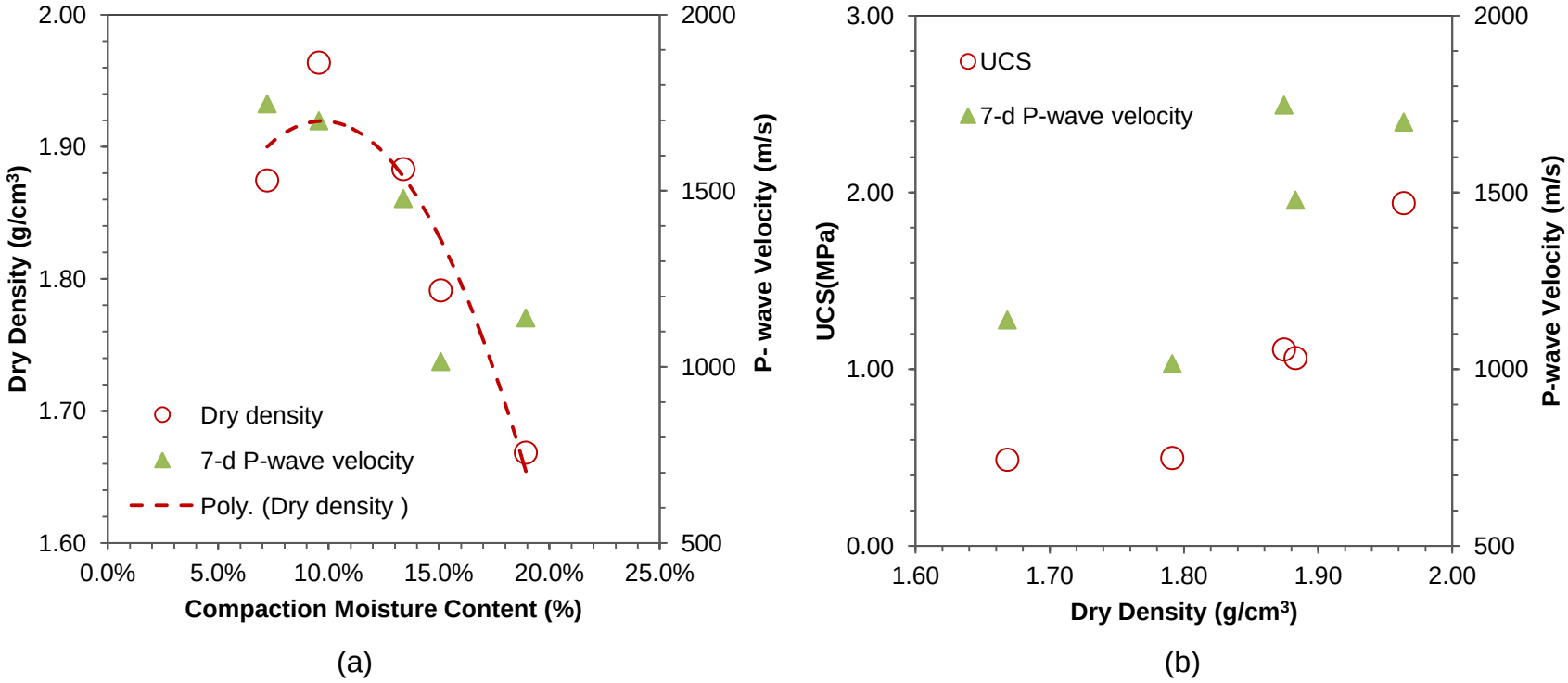

Figure 6.11. (a) Compaction characteristics of P-wave velocity (b) dry density effect on UCS and P-wave velocity of silt-lime-fly ash.

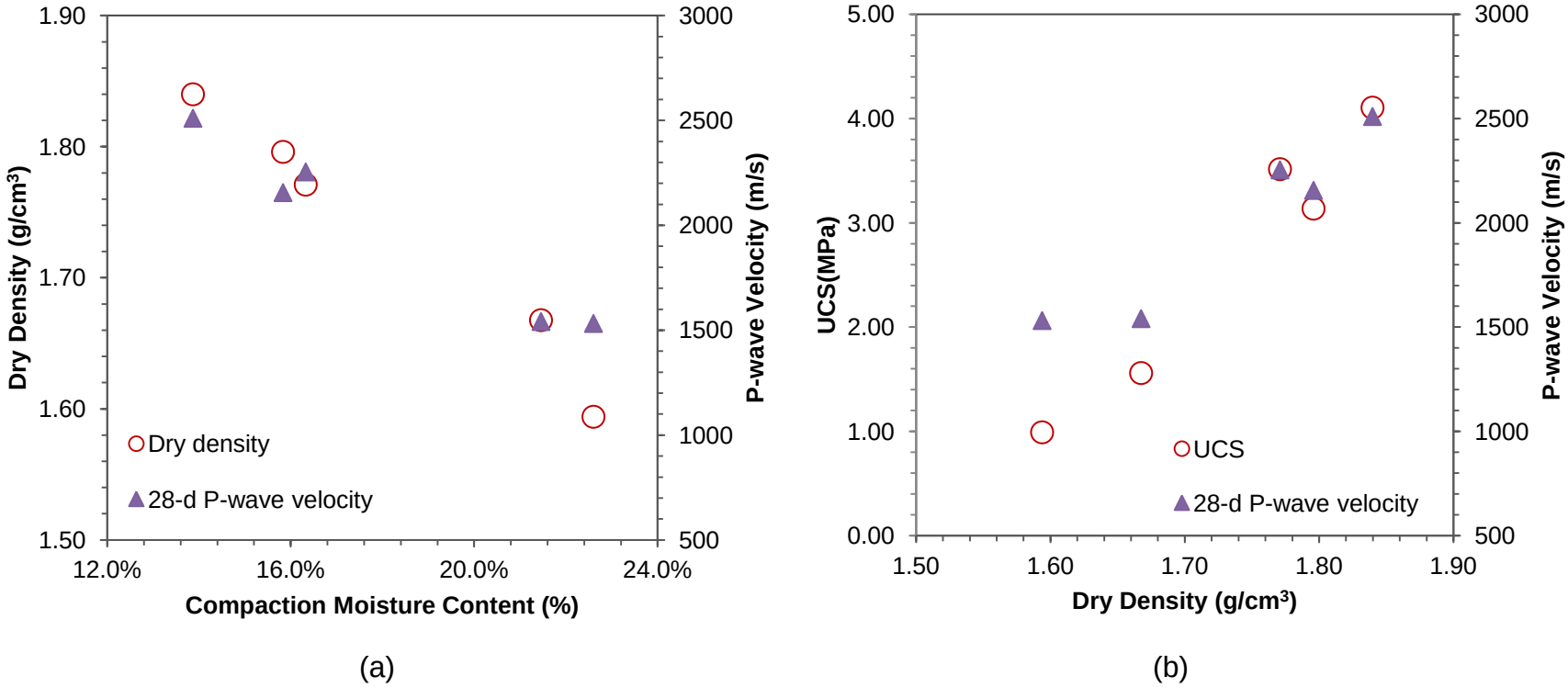

.

Figure 6.12. (a) Compaction characteristics of P-wave velocity (b) dry density effect on UCS and P-wave velocity of clay-cement

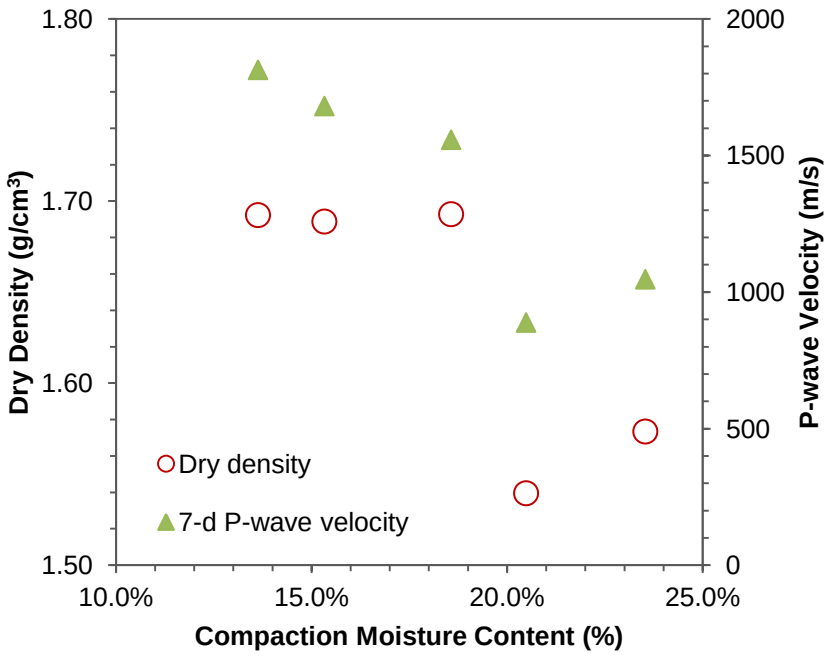

(a)

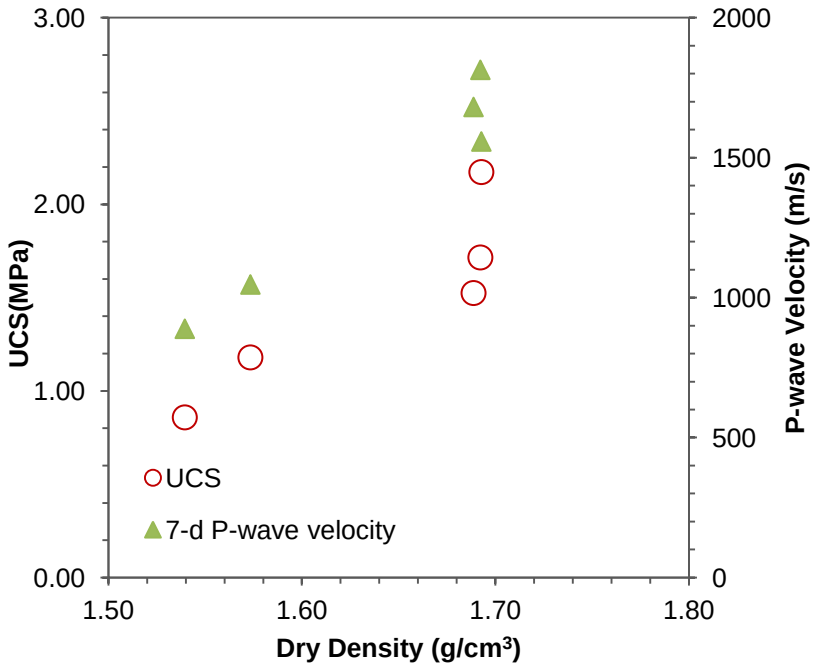

(b)

Figure 6.13. (a) Compaction characteristics of P-wave velocity (b) dry density effect on UCS and P-wave velocity of clay-lime

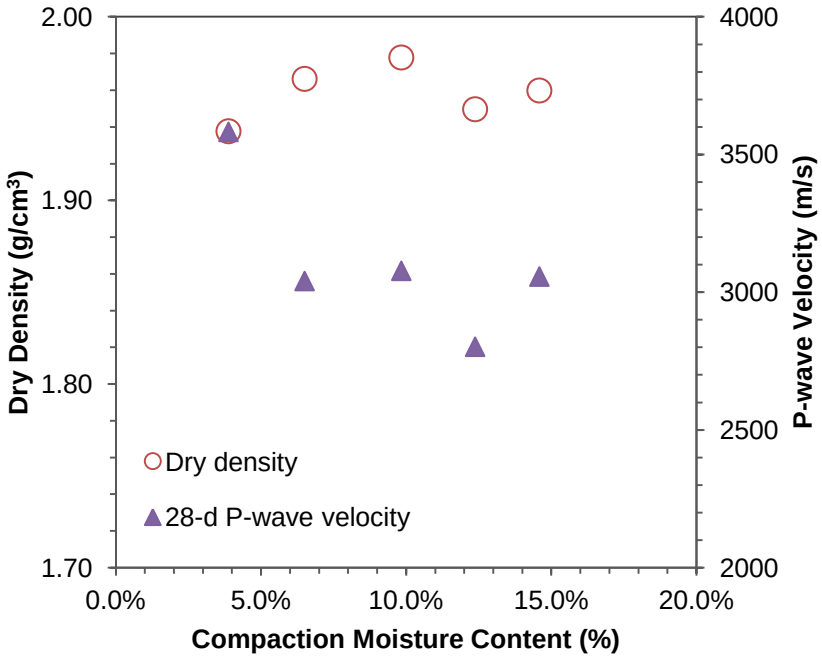

(a)

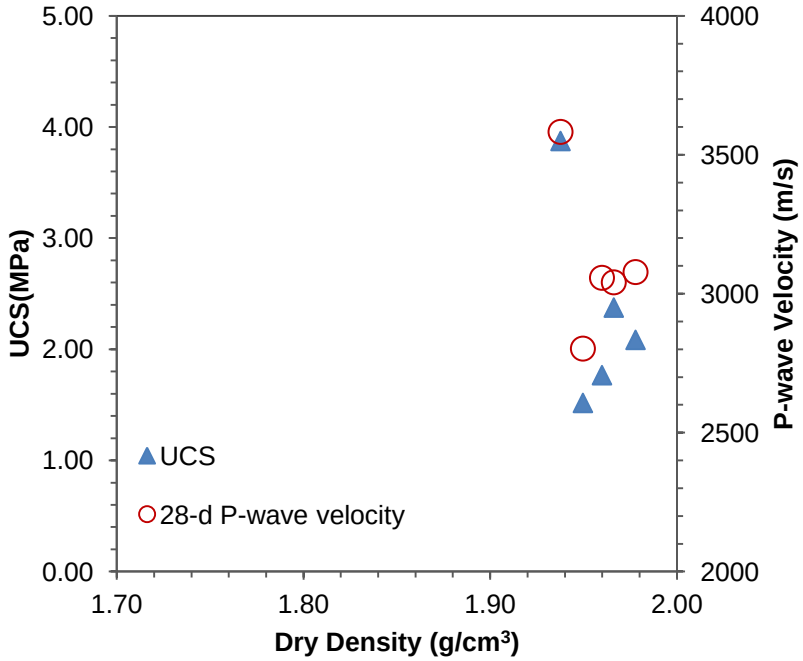

(b)

Figure 6.14. (a) Compaction characteristics of P-wave velocity (b) dry density effect on UCS and P-wave velocity of sand-cement

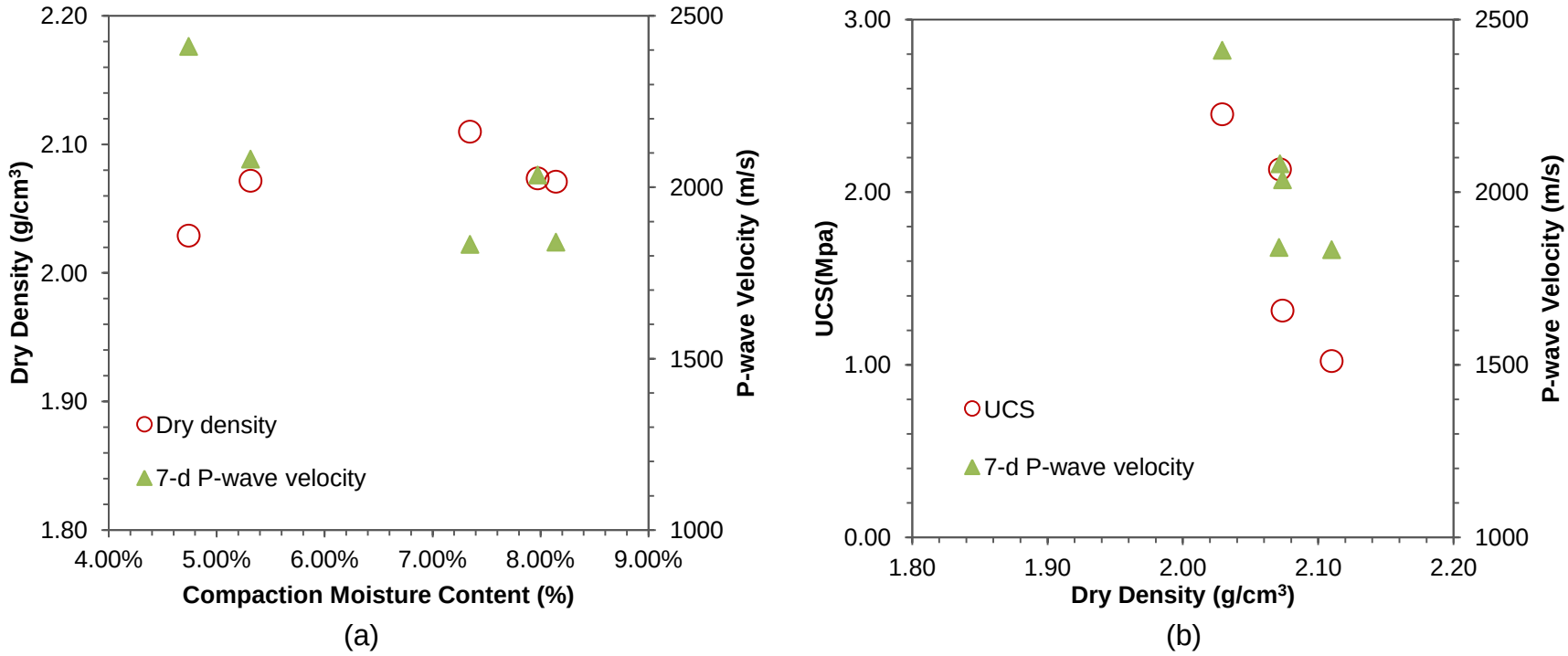

Figure 6.15. (a) Compaction characteristics of P-wave velocity (b) dry density effect on UCS and P-wave velocity of sand-fly ash

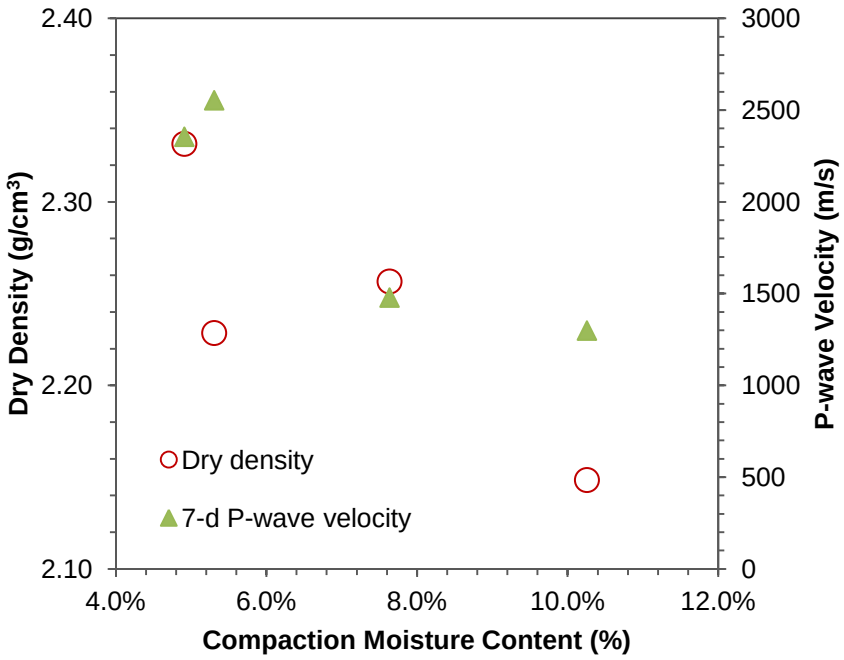

(a)

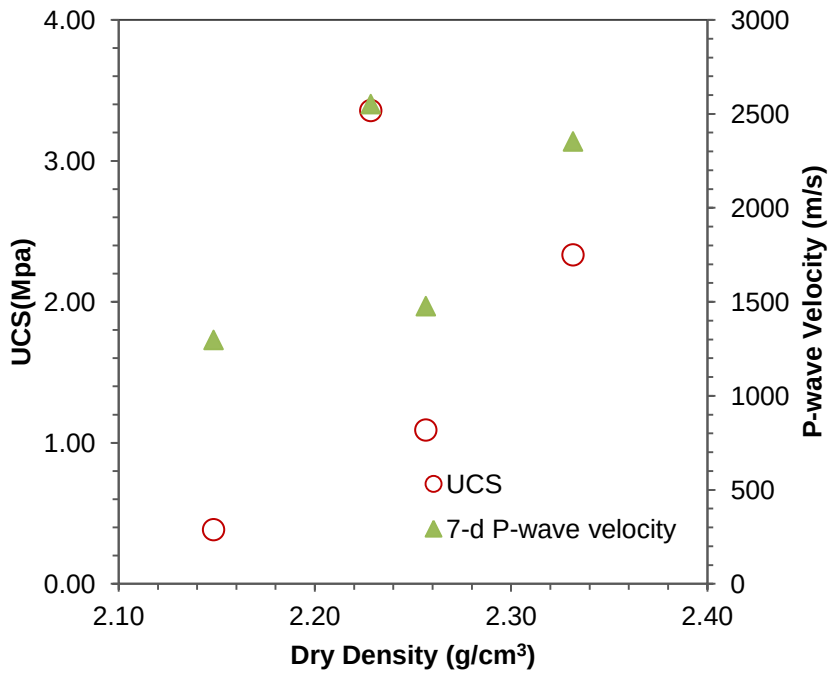

(b)

Figure 6.16. (a) Compaction characteristics of P-wave velocity (b) dry density effect on UCS and P-wave velocity of gravel-fly ash

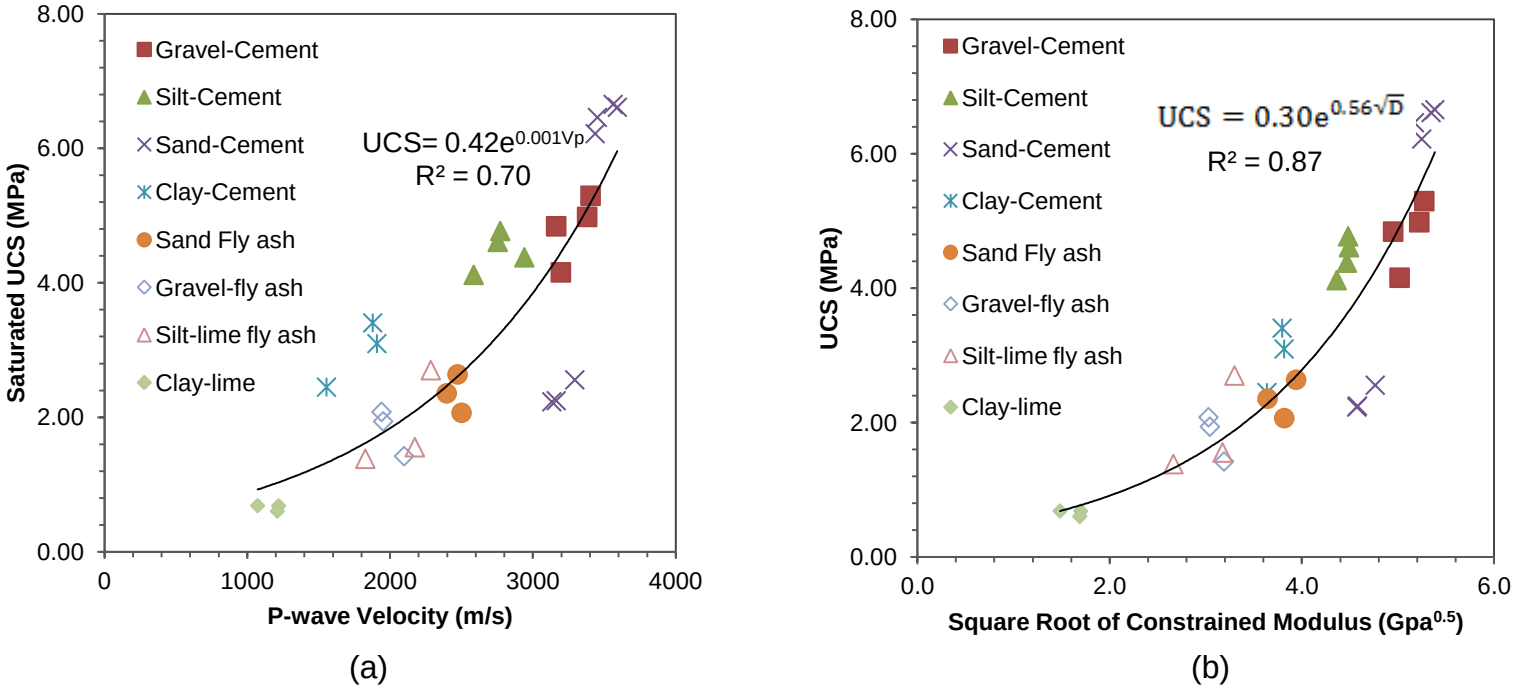

Figure 6.17. Relationship between UCS of CSM with (a) P-wave velocity and (b) square root of constrained modulus

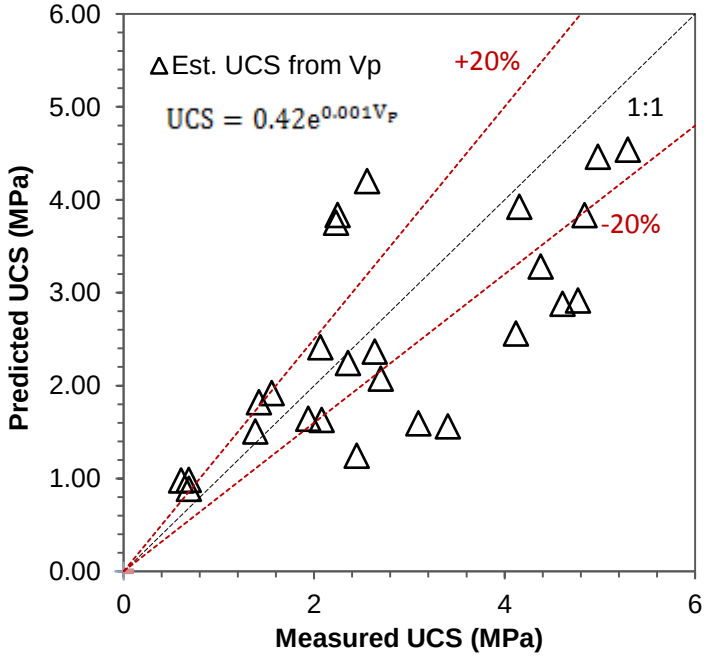

(a)

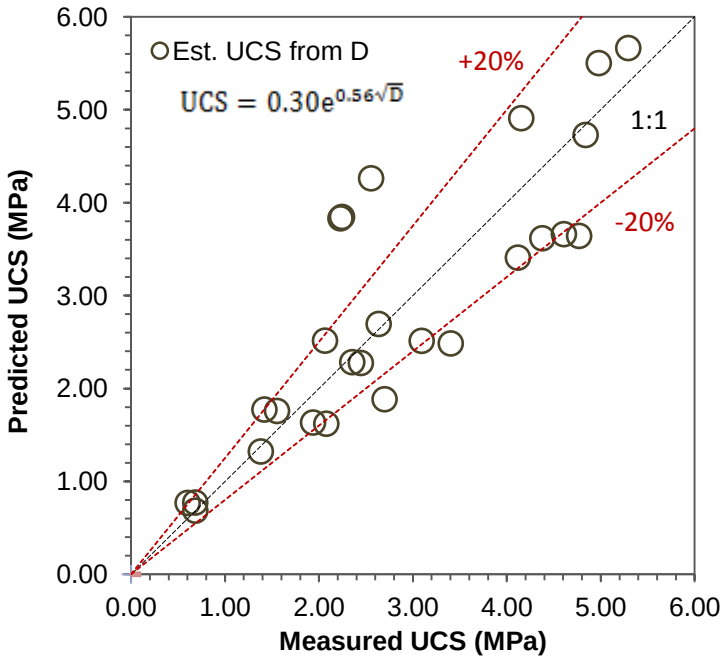

(b)

Figure 6.18. Predicted UCS vs. saturated UCS predicted from (a) P-wave velocity (b) constrained modulus

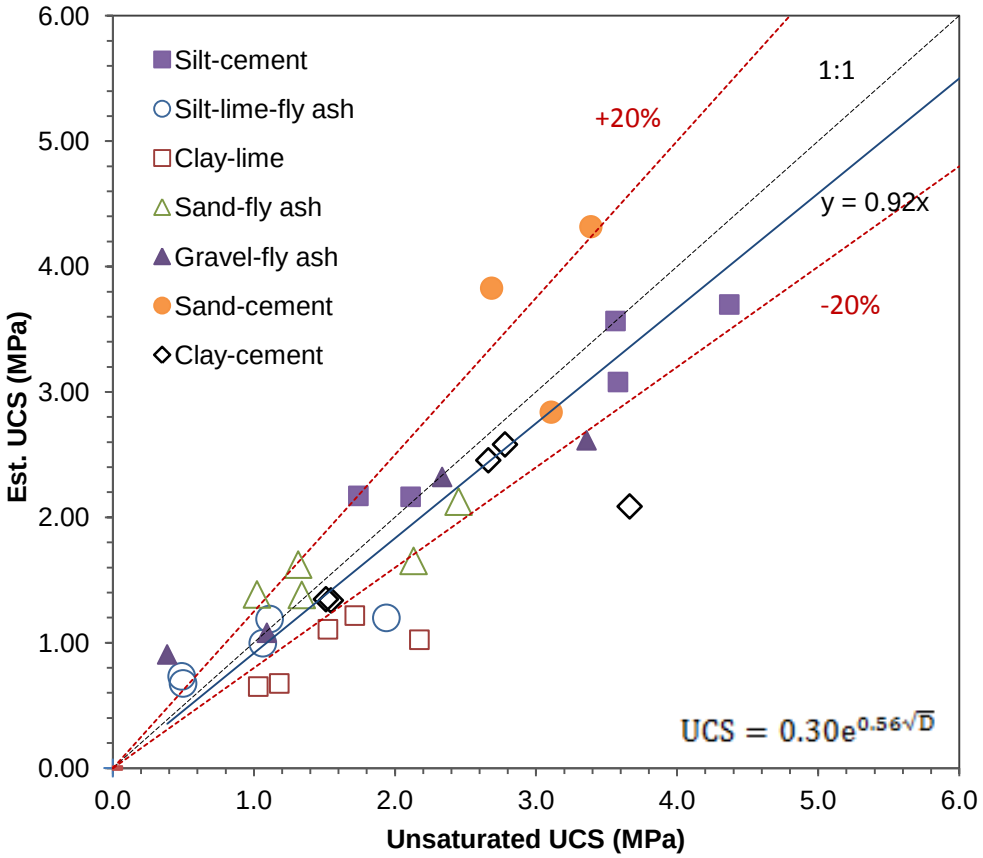

Figure 6.19. Predicted UCS vs. measured UCS (unsaturated)

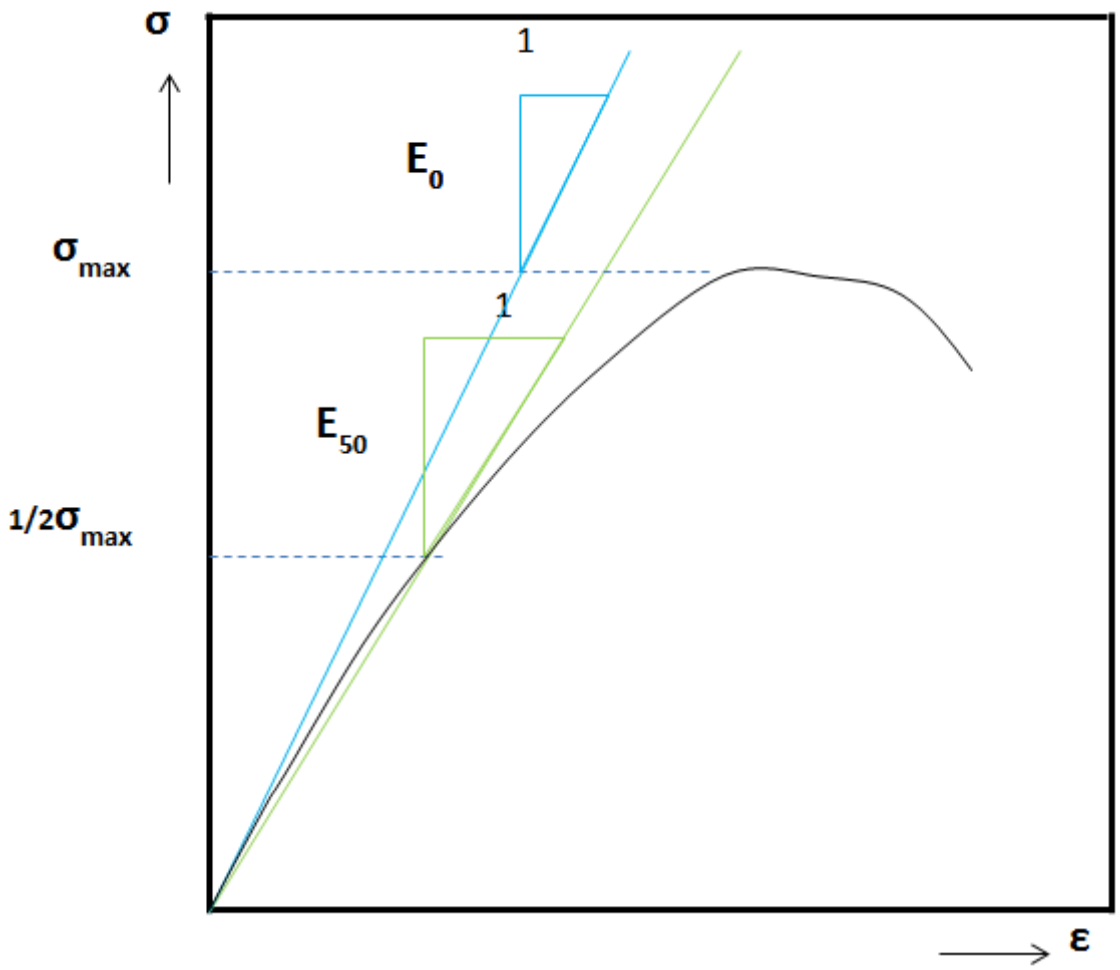

Figure 6.20. Typical stress-strain curve from UCS test for CSM

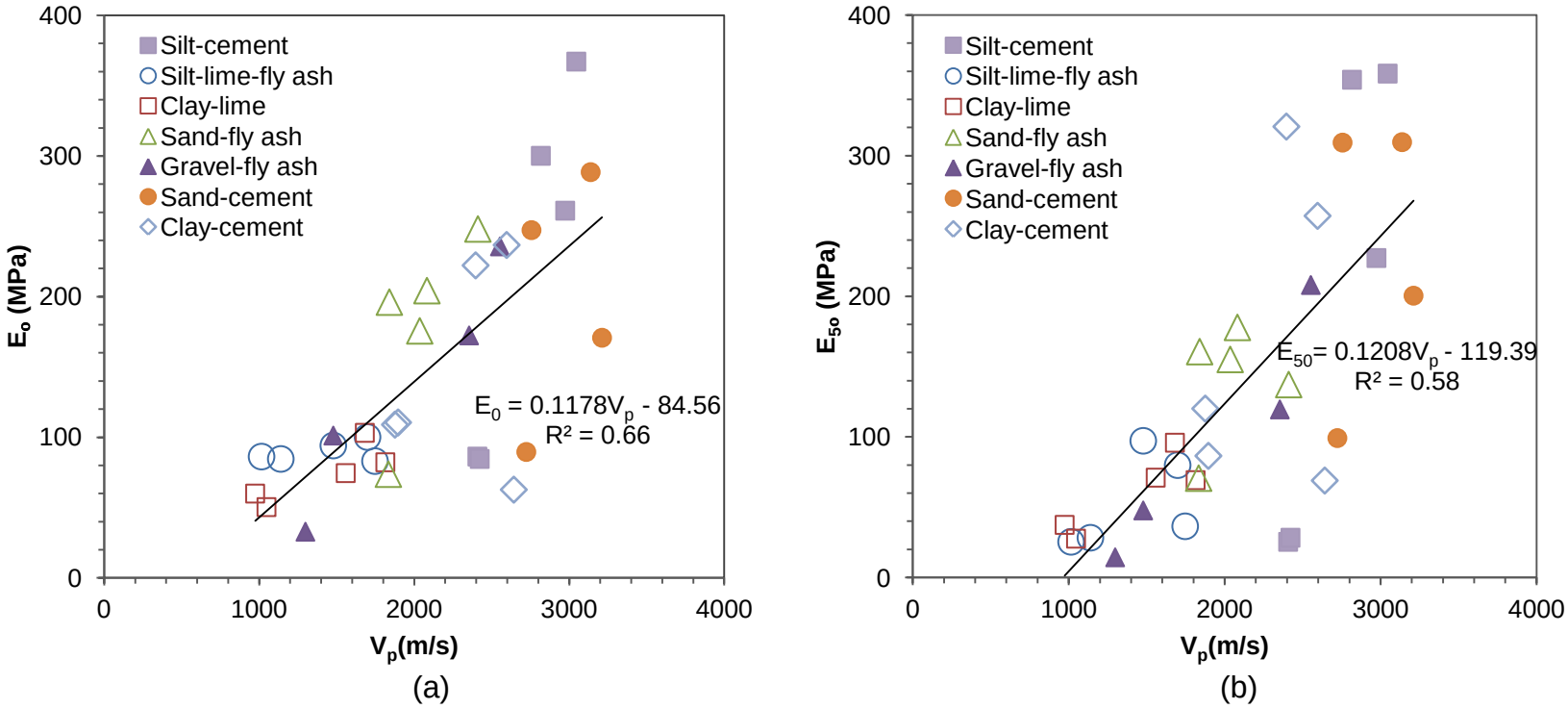

Figure 6.21. P-wave velocity vs. (a) Young's modulus (b) secant modulus

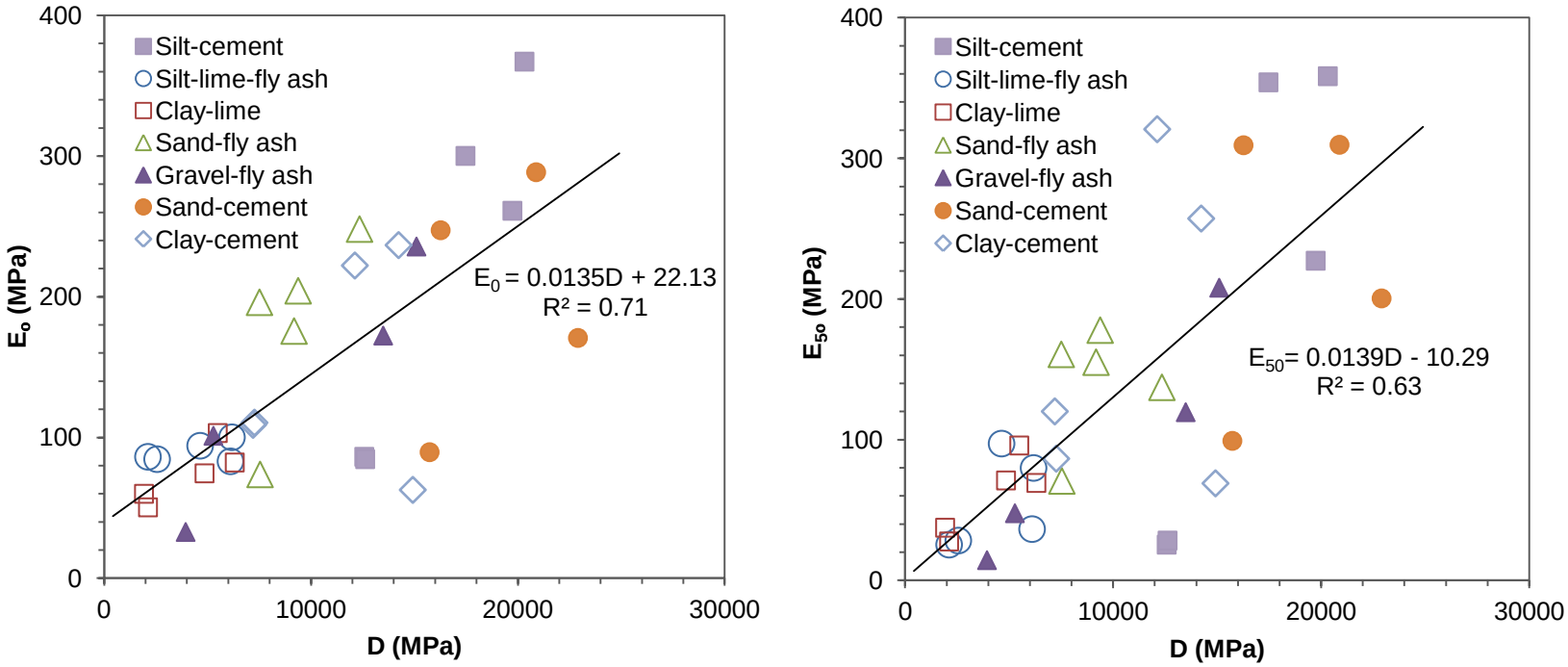

Figure 6.22. Constrained modulus vs. (a) Young's modulus (b) secant modulus

APPENDIX A MIX DESIGN

Mix designs were conducted to determine appropriate binder contents (Wen et al. 2011). For soil-lime, the method developed by the National Lime Association (NLA) (2006) was followed, soil-cement by the Portland Cement Association (PCA) (1992), and soil-fly ash by the Federal Highway Administration (FHWA) guideline. Three replicates were used for each unconfined compressive strength (UCS) test.

1. SOIL-CEMENT MIXTURES

The PCA soil-cement design guide requires the cement addition should result an unconfined compressive strength larger than 2.07 MPa after 7-day curing for soil-cement mixtures. The mix design results indicated that 3% cement content is suitable for stabilizing gravel, 6% for sand, 8% for silt, and 12% for clay, as shown in Figure A.1.

2. SOIL-FLY ASH (CLASS C) MIXTURES

The 7-day unconfined compressive strength of 2.76 MPa specified by the Federal Highway Administration (FHWA) cannot be achieved by the gravel mixes or silt mixes, as shown in Figure A.2. Based on the past studies, 13% Class C fly ash was recommended for stabilizing silt, sand, and gravel.

3. SOIL-LIME MIXTURES

At least 2% lime should be used to stabilize clay based on the minimum pH of 12.49 as shown in Figure A.3. It was found that 6% lime could lead to an UCS of 0.48 MPa specified by the NLA, as seen in Figure A.4.

Lime and Class F fly ash combination was used to stabilize silt. 4% lime and 12% Class F fly ash contents can reach the Mechanistic-Empirical Pavement Design (MEPDG) requirement of 7-day UCS of 1.38 MPa, as shown in Figure A.5.

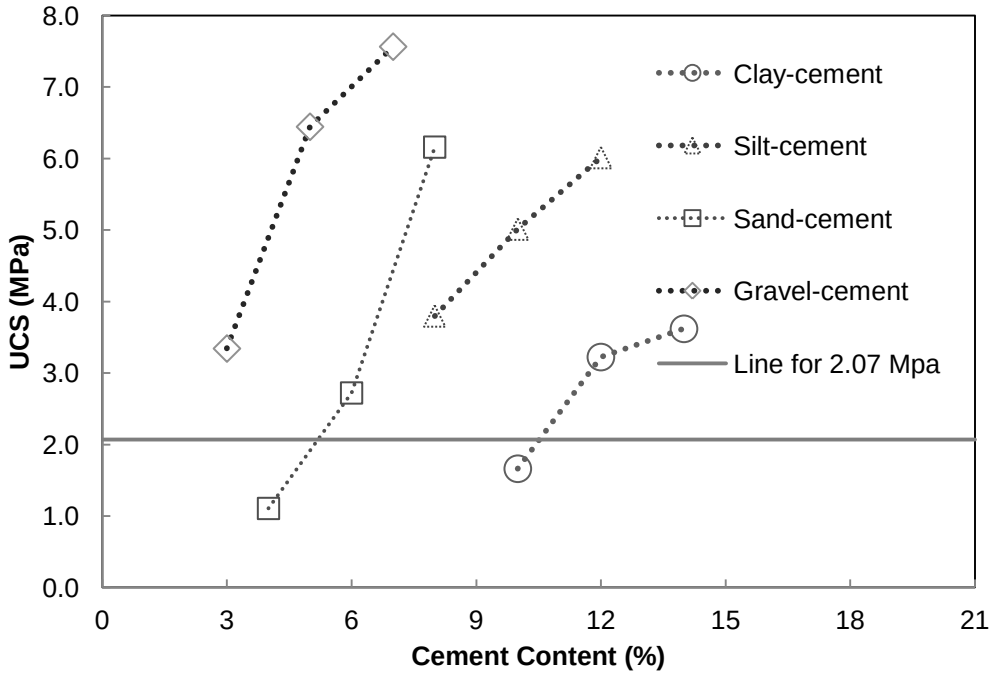

Figure A.1. Results of UCS after 7-day curing for cement-stabilized soils

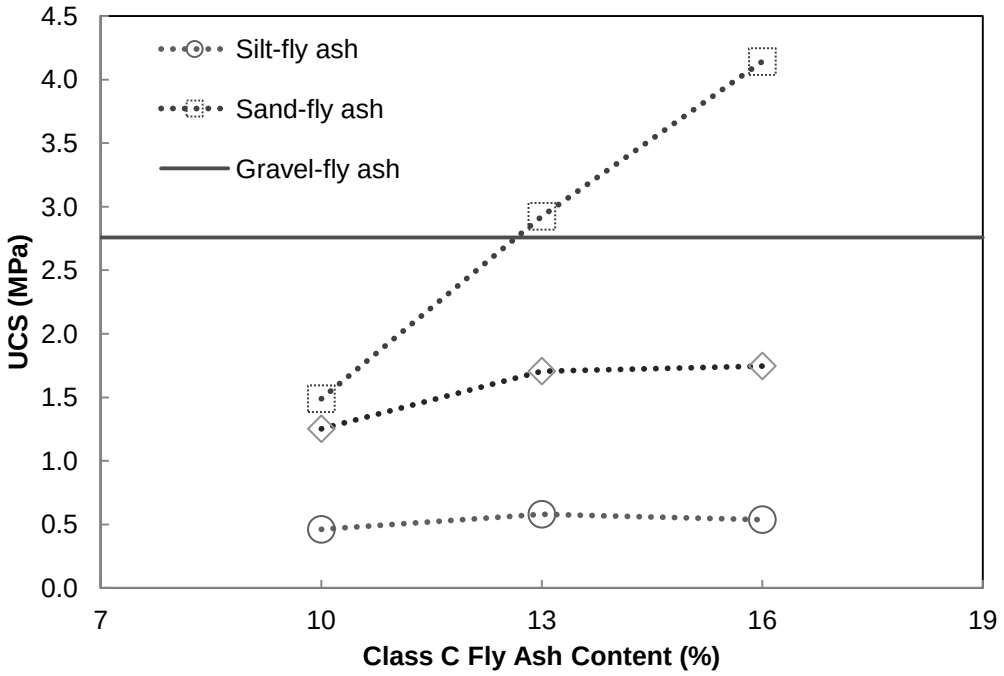

Figure A. 2. Results of UCS after 7-day curing for class C fly ash-stabilized soils

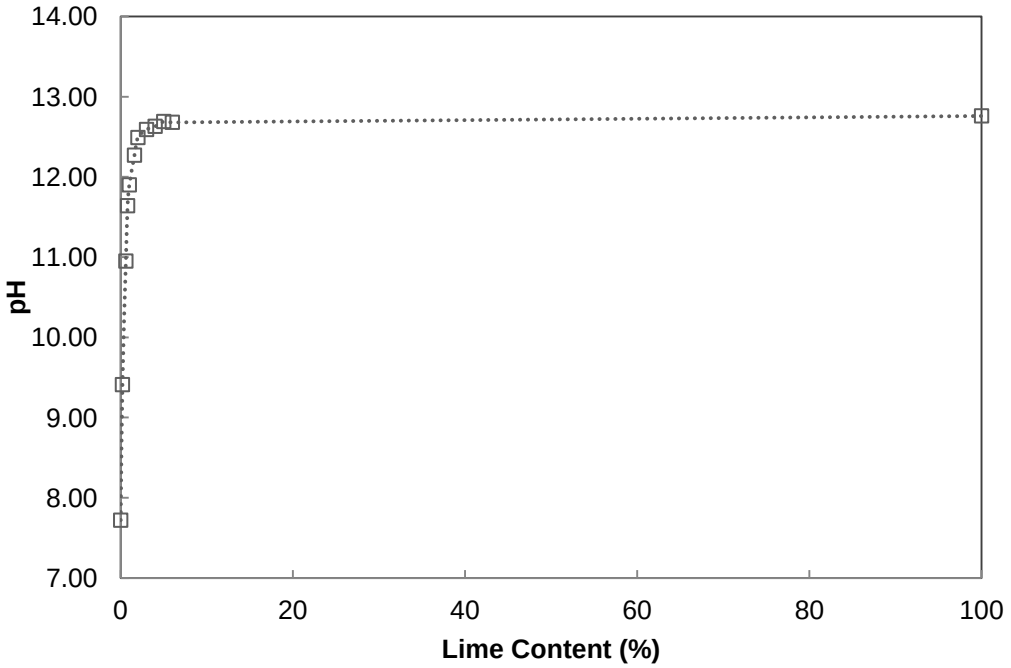

Figure A.3. pH value vs. lime content

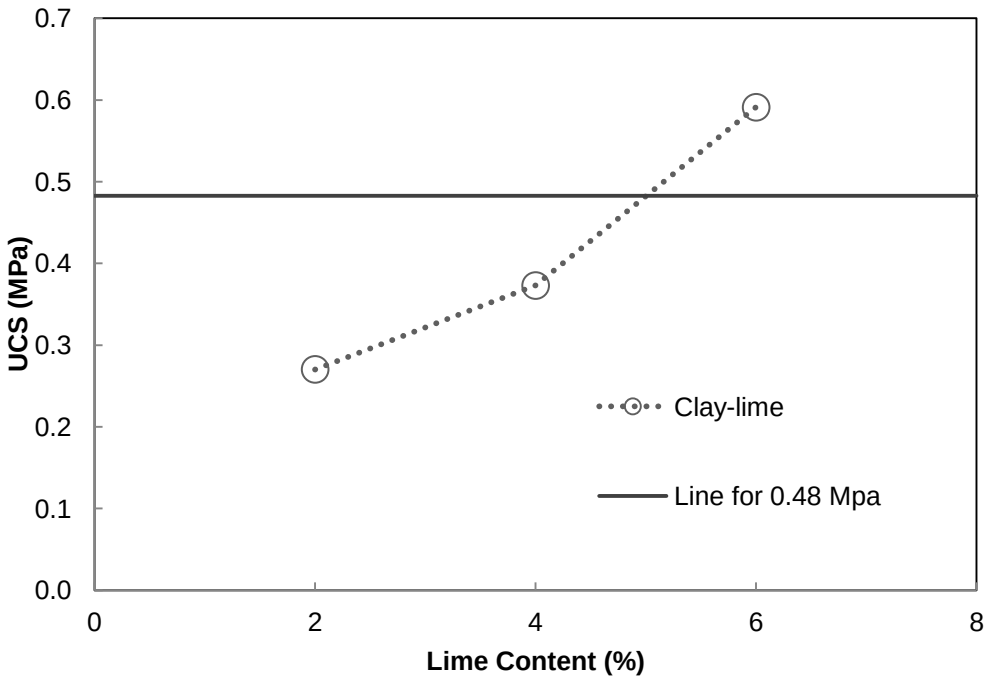

Figure A.4. Results of UCS after 7-day curing for clay-lime mix

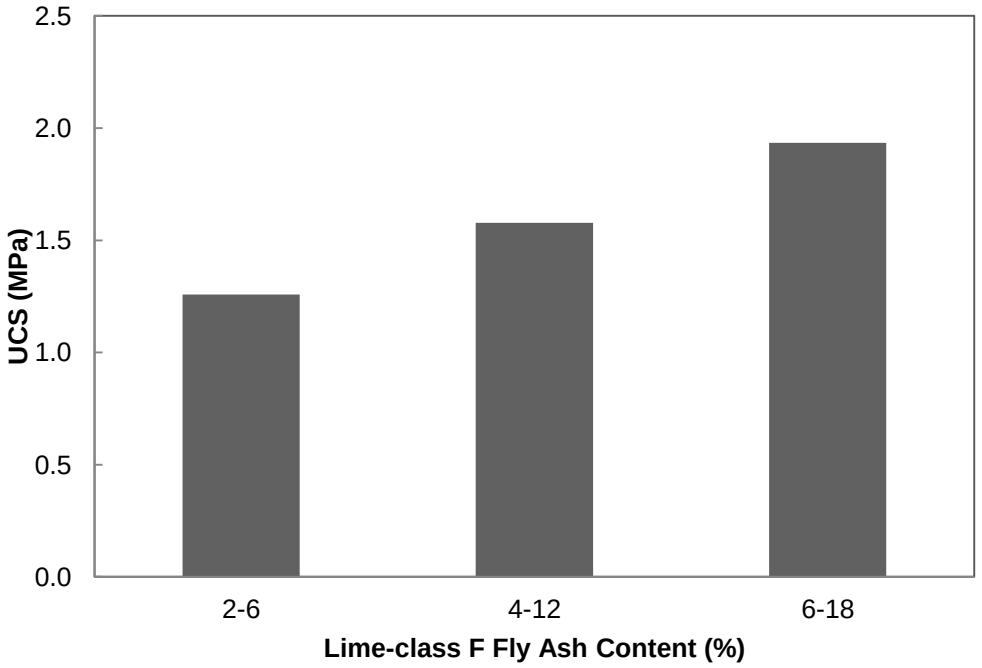

Figure A.5 Results of UCS after 7-day curing for silt-lime-class f fly ash

APPENDIX B INITIAL UCS RESULTS

1. SPECIMENS PREPARATION AND TEST PROCEDURE

Specimens were prepared based on the mix design as shown Table 3.1 to determine the initial UCS at the end of target curing time by Casmer (2011). Specimens were prepared at optimum moisture content and compacted at 95 to 100% maximum density. Cement-stabilized mixtures (gravel, sand, silt, and clay) were tested in accordance with ASTM D 1633: Standard Test Methods for Compressive Strength of Molded Soil-Cement Cylinders (Method A). Fly ash-stabilized mixtures (sand, silt, and gravel) and silt-lime-Class F fly ash were tested in accordance with ASTM C 593: Clay-lime specimens were tested in accordance with ASTM D 5102: Standard Test Methods for Unconfined Compressive Strength of Compacted Soil-Lime Mixtures (Procedure A).

2. UCS RESULTS

The results for UCS on cementitiously stabilized mixtures are presented in Figure A.1. The average UCS were 3.58 MPa, 3.68 MPa, 4.41 MPa and 4.5 MPa for sand-cement, clay-cement, gravel-cement and silt-cement specimens, respectively. Gravel-fly ash exhibited the largest UCS at 1.99 MPa and silt-fly ash the lowest with 0.63 MPa. Sand-fly ash achieved a UCS of 1.42 MPa. Silt with Class C fly ash resulted in the lowest UCS when compared to all mixes tested. However, silt with lime (4% by weight) and Class F fly ash (12% by weight) had a UCS of 1.87 MPa. Clay with 6% lime by weight achieved a UCS of 1.03 MPa.

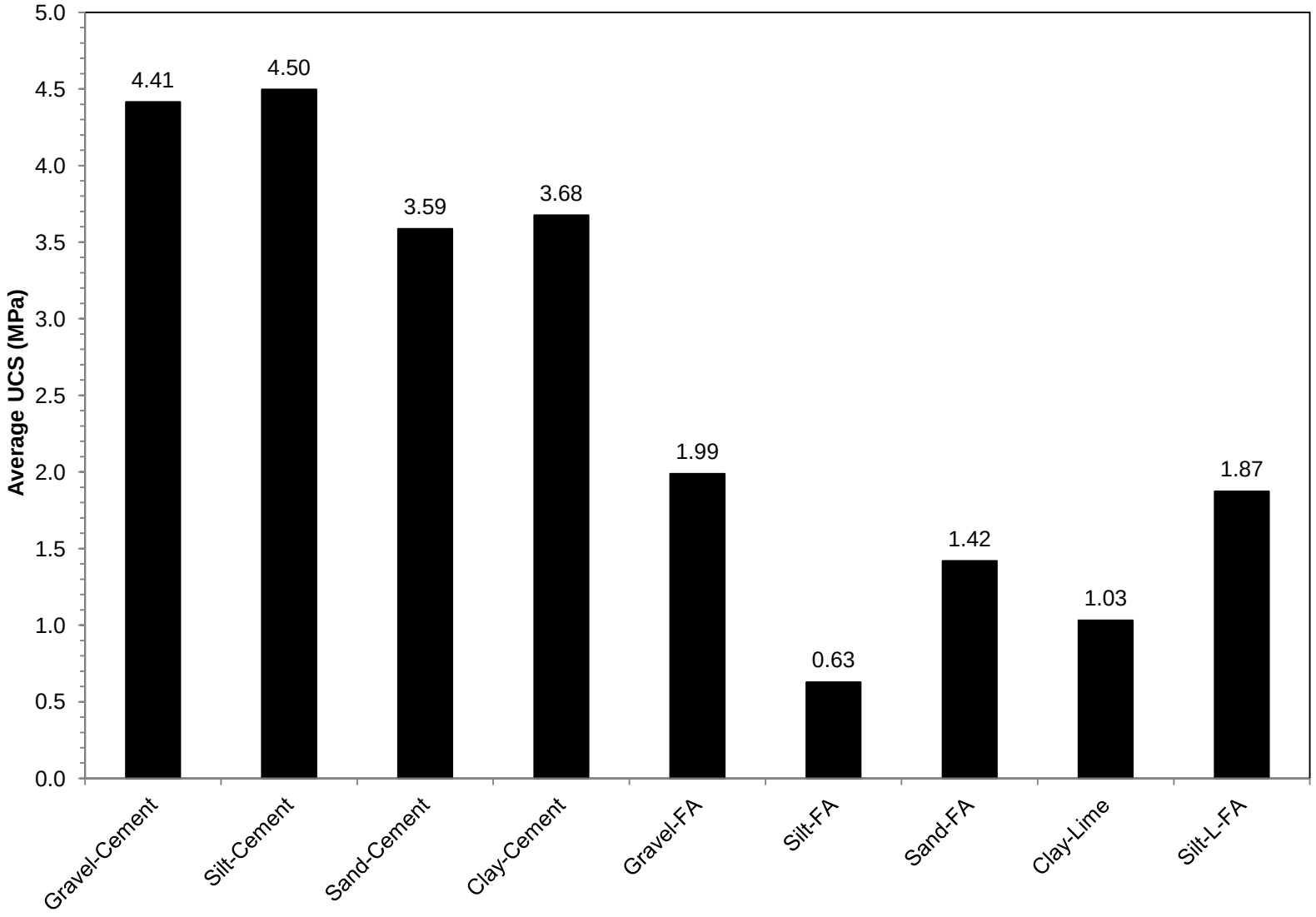

Figure B. 1 Cementitiously stabilized material UCS result